

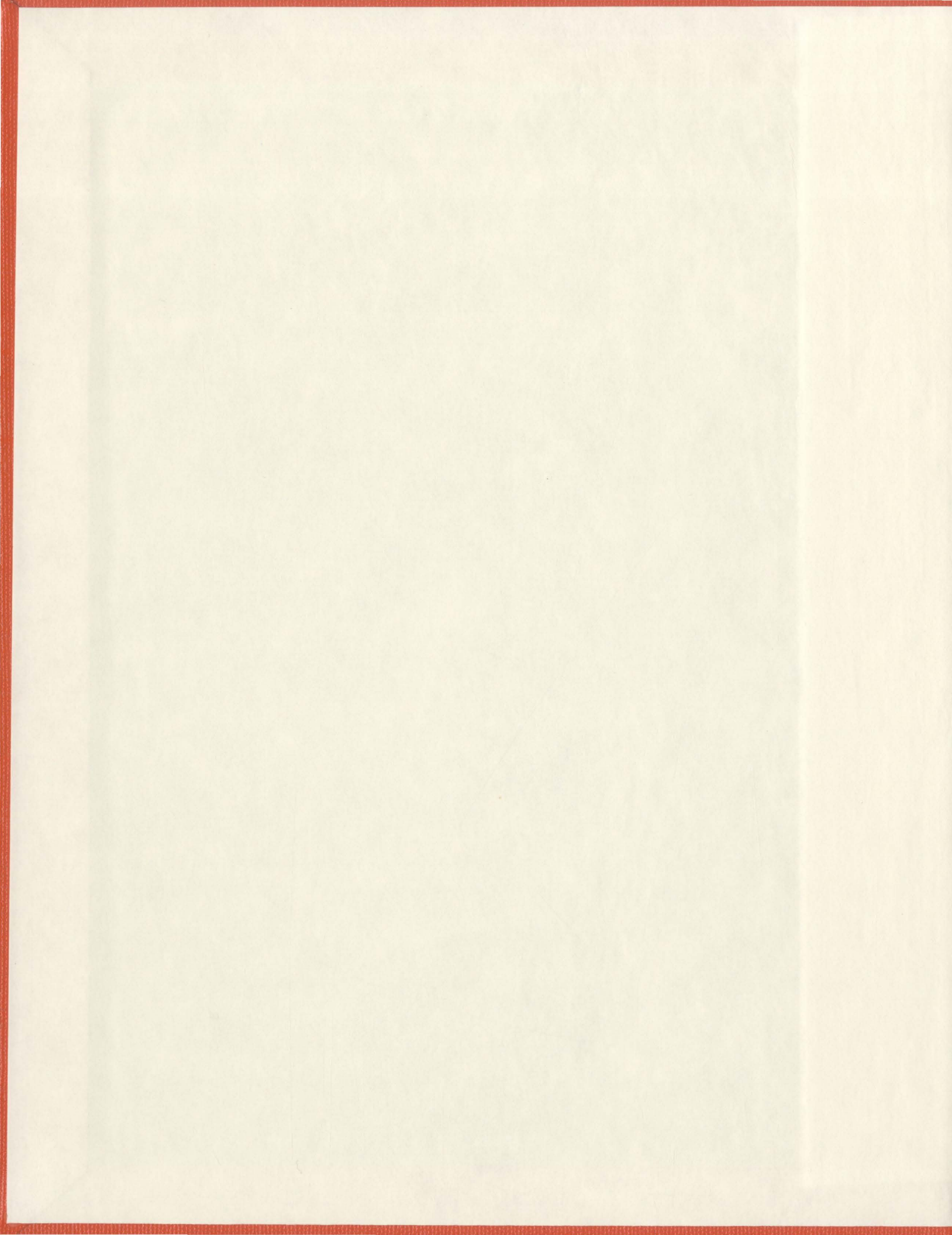
ANALYSES OF STRESS INTENSITY FACTORS FOR
STRUCTURAL INTEGRITY IN MECHANICAL COMPONENTS

CENTRE FOR NEWFOUNDLAND STUDIES

**TOTAL OF 10 PAGES ONLY
MAY BE XEROXED**

(Without Author's Permission)

CHANDRA S. GANTI





Analyses of Stress Intensity factors for Structural Integrity in Mechanical Components

By

Chandra S Ganti

A thesis submitted to the school of graduate studies in partial fulfillment of the
requirements for the degree of Master of Engineering

Faculty of Engineering and Applied Science

Memorial University of Newfoundland

May, 2005

St. John's

Newfoundland

Canada



Library and
Archives Canada

Published Heritage
Branch

395 Wellington Street
Ottawa ON K1A 0N4
Canada

Bibliothèque et
Archives Canada

Direction du
Patrimoine de l'édition

395, rue Wellington
Ottawa ON K1A 0N4
Canada

0-494-06631-8

Your file *Votre référence*

ISBN:

Our file *Notre référence*

ISBN:

NOTICE:

The author has granted a non-exclusive license allowing Library and Archives Canada to reproduce, publish, archive, preserve, conserve, communicate to the public by telecommunication or on the Internet, loan, distribute and sell theses worldwide, for commercial or non-commercial purposes, in microform, paper, electronic and/or any other formats.

The author retains copyright ownership and moral rights in this thesis. Neither the thesis nor substantial extracts from it may be printed or otherwise reproduced without the author's permission.

AVIS:

L'auteur a accordé une licence non exclusive permettant à la Bibliothèque et Archives Canada de reproduire, publier, archiver, sauvegarder, conserver, transmettre au public par télécommunication ou par l'Internet, prêter, distribuer et vendre des thèses partout dans le monde, à des fins commerciales ou autres, sur support microforme, papier, électronique et/ou autres formats.

L'auteur conserve la propriété du droit d'auteur et des droits moraux qui protègent cette thèse. Ni la thèse ni des extraits substantiels de celle-ci ne doivent être imprimés ou autrement reproduits sans son autorisation.

In compliance with the Canadian Privacy Act some supporting forms may have been removed from this thesis.

Conformément à la loi canadienne sur la protection de la vie privée, quelques formulaires secondaires ont été enlevés de cette thèse.

While these forms may be included in the document page count, their removal does not represent any loss of content from the thesis.

Bien que ces formulaires aient inclus dans la pagination, il n'y aura aucun contenu manquant.


Canada

ABSTRACT

Finite element methods offer versatile tools in structural mechanics to analyze various types of structures. The Finite Element Method (FEM) is extended to Linear Elastic Fracture Mechanics (LEFM) for the calculation of stress intensity factors, crack growth etc., with sufficient accuracy. The conventional FEM applied to LEFM is comparatively complicated since the crack tip region involves the singularities. Higher order conventional isoparametric elements are used in the analysis while near the crack tip, where the singularity occurs, enriched crack tip elements are used. Achieving significant accuracy with fewer elements is one of the main criterion in structural analysis. The method developed here has the advantage of fewer elements with minimal re-meshing and ease of modeling with less concern to aspect ratio. The p-version analysis helps in increasing the order of polynomial with out the need to re-mesh and to reuse the same mesh repetitively to get the change in stress intensity factors and eventually the crack growth parameters. Stress intensity factors are a measure of stresses at the crack tip. SIF's are calculated for various crack problems and results are compared, analyzed and presented.

ACKNOWLEDGEMENTS

It gives me great pleasure to acknowledge my supervisor Dr. Munaswamy for the guidance, direction, suggestions, great effort to explain things clearly and financial support during my Masters program. I am indebted to him for giving me an opportunity to work under him and will be remembered for my life as a key factor for my career in Fatigue and fracture mechanics.

I am thankful to Dr.Ray Gosine, Dean, Faculty of Engineering and Applied Science, and Dr.Venkatesan, Associate Dean, Faculty of Engineering and Applied Science for providing assistance and making the stay most pleasant in Memorial University.

I would like to thank Dr.Swamidas and Dr.Adluri for guiding and helping me during course work and at times when needed. I am thankful to the School of Graduate studies and Faculty of Engineering and Applied Science for providing financial assistance for the research work.

My Sincere thanks to my dearest wife, Rama, for her caring, support and understanding and finally I am forever thankful to my Mother, Father and Almighty God for giving me support in all ways.

Contents

Abstract	i
Acknowledgements	ii
Table of Contents	iii
List of figures	vi
List of Tables	ix
Symbols and Abbreviations	xii
1. INTRODUCTION	1
1.1 Finite element method.....	1
1.1.1 h and p-version FEM.....	3
1.1.2 Fracture Mechanics.....	6
1.1.3 Linear Elastic Fracture Mechanics.....	7
1.1.4 Stress Intensity Factors.....	9
1.1.5 Modes of Deformation.....	10
1.1.6 Crack Propagation.....	11
1.2 Scope of Thesis.....	12
1.3 Objectives of Research.....	13
1.4 Outline of Thesis.....	14
2. BACKGROUND AND SCOPE OF WORK	15
2.1 Literature Review.....	15
2.1.1 p-version FEM.....	15
2.1.2 Computational Fracture Mechanics.....	19

3.	FINITE ELEMENT FORMULATION.....	27
3.1	Conventional finite element formulation.....	27
3.1.1	Selection of an element.....	27
3.1.2	Selection of Displacement Functions.....	28
3.1.3	Defining of Stress Strain Relationship.....	30
3.1.4	Derivation of Stiffness matrix and Numerical Integration....	35
3.1.5	Assembly and Solution.....	35
3.2	h and p adaptivity.....	36
3.3	Hierarchical Shape functions.....	36
3.4	Enriched element formulation.....	41
4.	COMPUTER IMPLEMENTATION.....	45
4.1	Java as Programming Language	45
4.1.1	Nodal Connectivity and Nodal Coordinates.....	50
4.1.2	Shape function Derivatives.....	51
4.2	Convergence	52
4.2.1	Iterative techniques used for convergence.....	53
4.2.1.1	Preconditioned Conjugate Gradient Method.....	54
4.3	Numerical Analysis.....	58
5.	NUMERICAL STUDIES AND DISCUSSIONS.....	60
	Example 1.....	62
	Example 2.....	75
	Example 3.....	89

Example 4.....	99
Example 5.....	104
6. CONCLUSIONS AND RECOMMENDATIONS.....	110
6.1 Conclusions.....	110
6.2 Recommendations.....	112
References.....	113
Appendix.....	117

List of Figures

1.1	h type element	4
1.2	p type element	5
1.3	h-p type element	5
1.4	Stress components ahead of the crack tip	8
1.5	Basic Modes of Crack Surface Displacement	10
3.1	Isoparametric Element in Local Coordinates	28
3.2	Nine noded element	38
3.3	Local Coordinate system at the crack tip	42
4.1	Organization flowchart of computer program	49
4.2	Nodal Numbering	51
4.3	Preconditioned Conjugate gradient method	57
5.1.1	Symmetrically loaded center cracked plate in tension	63
5.1.2	K_I vs. p-order comparison for 8 noded and 9 noded 4x4 meshes	71
5.1.3	K_I vs. p-order comparison for 8 noded and 9 noded 6x6 meshes	71
5.1.4	K_I vs. crack length a for element length of 0.2 at the crack tip for 4x4 mesh	72
5.1.5	K_I vs. crack length a for element length of 0.2 at the crack tip for 6x6 mesh	73

5.1.6	Comparison of K_I/K_{ref} vs. p-order and percent change in K_I vs. p-order for 4x4 mesh for 8 noded and 9 noded element.	73
5.1.7	Comparison of K_I/K_{ref} vs. p-order and % change in K_I vs. p-order for 6x6 mesh for 8-noded and 9-noded element.	74
5.2.1	Symmetrically loaded center crack plate in shear	75
5.2.2	Mesh discretization used in the present analysis.	76
5.2.3	Mesh discretization used by Moes et al. [19]	76
5.2.4	K_I, K_{II} vs. p-order for element length 0.2 and 0.25 (4x4 mesh)	83
5.2.5	K_I, K_{II} vs. p-order for element length 0.5 and 0.75 (4x4 mesh)	83
5.2.6	K_I, K_{II} vs. p-order for element length 1 and 1.5 (4x4 mesh)	84
5.2.7	K_I, K_{II} vs. p-order for element length varying from 0.2 to 1.5 (6x6mesh)	85
5.2.8	K_I, K_{II} vs. p-order and degrees of freedom (4x4 mesh)	86
5.2.9	K_I, K_{II} vs. p-order and degrees of freedom (6x6 mesh)	86
5.2.10	K_I, K_{II} vs. crack length (4x4 mesh)	87
5.2.11	K_I, K_{II} vs. crack length (6x6 mesh)	88
5.3.1	Plate with inclined crack in tension.	89
5.3.2	Types of meshes used in the analysis	90
5.3.3	Stress Intensity factors vs. p order for 8 noded elements (16 elements mesh)	94
5.3.4	Stress Intensity factors vs. p order for 9 noded elements(16 elements mesh)	94

5.3.5	K_I, K_{II} vs. p-order for 8 and 9 noded elements(30 elements mesh)	97
5.3.6	K_I, K_{II} vs porder and K_I, K_{II} vs degrees of freedom	98
5.4.1	Plate with center crack at an angle β	100
5.4.2	Discretization mesh used in the analysis	101
5.4.3	Stress Intensity factors vs. angle \hat{C}	103
5.5.1	Circular arc crack subjected to biaxial stress	104
5.5.2	Curved crack discretization	105
5.5.3	Crack mesh used by Huang et al. [26]	106
5.5.4	Stress Intensity factors vs. p-order for 8 and 9 noded elements	109

List of Tables

5.1.1	Degrees of freedom for different meshes and orders	65
5.1.2	SIFs for element length 1.5 in crack plate with tension load.	65
5.1.3	SIFs for element length 1.0 in crack plate with tension load.	66
5.1.4	SIFs for element length 0.75 in crack plate with tension load.	66
5.1.5	SIFs for element length 0.5 in crack plate with tension load.	67
5.1.6	SIFs for element length 0.25 in crack plate with tension load.	67
5.1.7	SIFs for element length 0.2 in crack plate with tension load.	68
5.1.8	SIFs for element length 0.15 in crack plate with tension load.	68
5.1.9	SIFs for element length 0.1 in crack plate with tension load.	69
5.1.10	SIFs for element length 0.05 in crack plate with tension load.	69
5.1.11	SIFs for element length 0.01 in crack plate with tension load.	70
5.1.12	SIFs for element length 0.005 in crack plate with tension load.	70
5.1.13	Stress Intensity factors for varying crack lengths	72
5.2.1	SIF values for 4x4 and 6x6 meshes with element length 0.005	77
5.2.2	SIF values for 4x4 and 6x6 meshes with element length 0.01	78
5.2.3	SIF values for 4x4 and 6x6 meshes with element length 0.05	78
5.2.4	SIF values for 4x4 and 6x6 meshes with element length 0.1	79
5.2.5	SIF values for 4x4 and 6x6 meshes with element length 0.15	79
5.2.6	SIF values for 4x4 and 6x6 meshes with element length 0.2	80
5.2.7	SIF values for 4x4 and 6x6 meshes with element length 0.25	80

5.2.8	SIF values for 4x4 and 6x6 meshes with element length 0.5	81
5.2.9	SIF values for 4x4 and 6x6 meshes with element length 0.75	81
5.2.10	SIF values for 4x4 and 6x6 meshes with element length 1.0	82
5.2.11	SIF values for 4x4 and 6x6 meshes with element length 1.5	82
5.2.12	Crack length vs. K_I and K_{II} for 8 and 9 noded elements.	84
5.3.1	SIFs for element length 0.4 in a plate with inclined crack.	91
5.3.2	SIFs for element length 0.3 in a plate with inclined crack.	91
5.3.3	SIFs for element length 0.25 in a plate with inclined crack.	92
5.3.4	SIFs for element length 0.2 in a plate with inclined crack.	92
5.3.5	SIFs for element length 0.15 in a plate with inclined crack.	93
5.3.6	SIFs for element length 0.1 in a plate with inclined crack.	93
5.3.7	Mode I and Mode II SIFs for element length 0.25 in 30 elements mesh.	95
5.3.8	Mode I and Mode II SIFs for element length 0.2 in 30 elements mesh.	95
5.3.9	Mode I and Mode II SIFs for element length 0.15 in 30 elements mesh.	96
5.3.10	Mode I and Mode II SIFs for element length 0.1 in 30 elements mesh.	96
5.3.11	Mode I and Mode II SIFs for element length 0.15 in 64 elements mesh.	97
5.3.12	Mode I and Mode II SIFs for element length 0.1 in 64 elements mesh.	98

5.4.1	Stress Intensity factors at various angles of the crack	101
5.4.2	Interpolated values of SIF's at various angles of the crack	102
5.5.1	Stress Intensity factors for curved crack with 8 noded element	108
5.5.2	Stress Intensity factors for curved crack with 9 noded element	108

Symbols and Abbreviations

FE	Finite Element
FEA	Finite Element Analysis
2D	Two Dimensional
3D	Three Dimensional
OOP	Object Oriented Programming
DOF	Degrees of Freedom
[]	Matrix
ν	Poisson's ratio
$\{\sigma\}$	Stress Vector
$\{\varepsilon\}$	Strain Vector
[N]	Matrix of Shape functions
G	Shear Modulus
E	Elasticity Modulus
w_i	Weight functions
[k]	Local element stiffness matrix
[B]	Element Matrix
[D]	Elasticity/Material Matrix
K_I	Mode I Stress Intensity Factor
K_{II}	Mode II Stress Intensity Factor
SIF	Stress Intensity factor

Chapter 1

INTRODUCTION

1.1 Finite Element Method

The finite element method is a numerical procedure for solving differential equations in engineering. The fundamental concept is that any continuous quantity, such as temperature, pressure, displacement etc. can be approximated by a discrete model composed of a set of piecewise continuous functions defined over a finite number of sub-domains. The basic principle of finite element method is that a solution region can be analytically modeled by replacing it with an assemblage of discrete elements. Although various approximate numerical analysis methods have evolved over the years, finite element method works efficiently compared to many other methods. For example finite difference method works well with fairly difficult problems; but for complex, irregular, and intricate geometries which need unusual specification of boundary conditions, it becomes very difficult to use and there comes the finite element method.

The finite element method gives the approximate numerical solution of a boundary value problem described by a differential equation. Finite element analysis consists of various steps, which can be obtained from basic finite element analysis book such as Logan [1].

The procedure consists of following steps;

- Discretization and selection of element types;
- Selection of displacement function such as linear, quadratic or cubic etc.;
- Defining of element stiffness matrix equation;
- Assemblage of element equations to obtain global equations;
- Solving for unknown degrees of freedom;
- Solving for element stresses and strains; and
- Interpretation of results;

The field variables such as temperatures, pressures, displacements etc. possess infinite number of values and the finite element discretization procedures reduce the procedure from infinite unknowns to finite number of unknown variables in terms of assumed approximating function with in each element. These approximating functions are called as interpolation functions and they are defined in terms of nodal values or nodal points. Whatever the type of element is considered, it has nodal points and these nodal points help in connecting with the adjacent elements. If a node is connected to two elements then the value of the field variable for both the elements is same at that point. The field variables within the element are completely described by the interpolation functions and the nodal values of field variables.

The first step in FE method is, proper selection of an element with required properties inorder to get an accurate solution depending on the type of problem. The

nature of solution depends on the type, size, number of elements and also on the interpolation functions used. The interpolation functions are chosen such that they are compatible and continuous at the adjoining element boundaries. If a problem in stress analysis is being solved then stiffness matrix for each element is calculated and then each stiffness matrix is assembled to a global matrix.

Each local stiffness matrix will describe the behaviour of that particular element and the global stiffness matrix will describe the behaviour of the entire structure being analyzed. Solving of the equations is done after incorporating the boundary conditions. Interpretation of the results is the final step in the analysis and in that the values that are obtained after solving are interpreted and if needed some additional computations are performed in order to get the required forms of the values of field variables.

1.1.1 h and p-version FEM

There are 3 types of approaches for solving the finite element equations

- 1) h-version
- 2) p-version
- 3) h-p version

In h-type or standard method the convergence is obtained by increasing the mesh density/refining of the mesh. In h-version the number of shape functions N_i is fixed for

each element. The degree of polynomial will be low, generally it is 1 for linear and 2 for quadratic and the error of approximation is controlled by the mesh refinement.

The symbol ‘*h*’ is used to represent the size of finite elements and when the size of the largest element, *i.e.*, the element maximum length h_{max} , is progressively reduced, convergence occurs. Since the accuracy is controlled by the number of elements used, the local effects of stress singularities near the crack tips, notches etc. can be captured more efficiently using *h*-version finite element method. The *h*-type element is shown in figure 1.1.

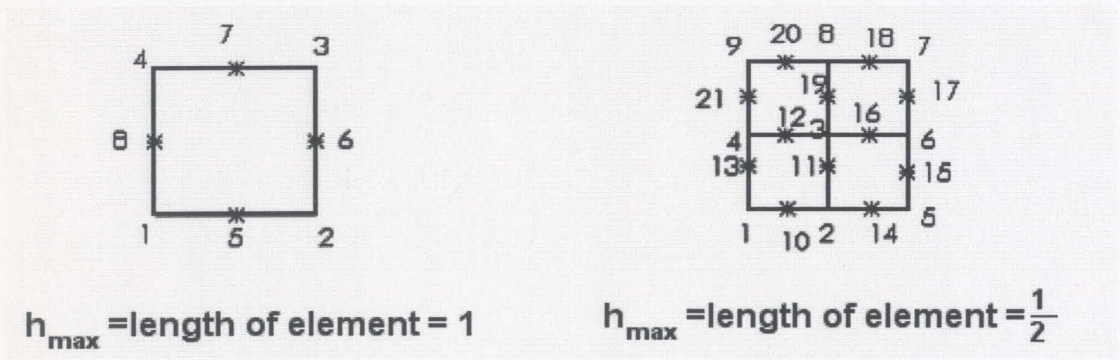


Figure 1.1 *h* type element

In *p*-type method, convergence is reached by increasing the order of the polynomial. The symbol ‘*p*’ is used to represent the polynomial degree and the convergence occurs when the degree of polynomial is progressively increased. This method has some advantages like faster convergence rate, solution accuracy information, reduced sensitivity to mesh complexity etc. Because of the usage of higher order polynomials, smooth functions can be approximated in *p*-version and this is being used in most of the latest software packages developed in the recent years. The disadvantages of

this method are it needs more solution time for the same number of degrees of freedom as in h-type and more computation cost.

The computation cost was a matter to be considered in olden days but during recent times, the computer power and memory are so large and improved that computation costs are minimal for the normal to medium complexity problems.

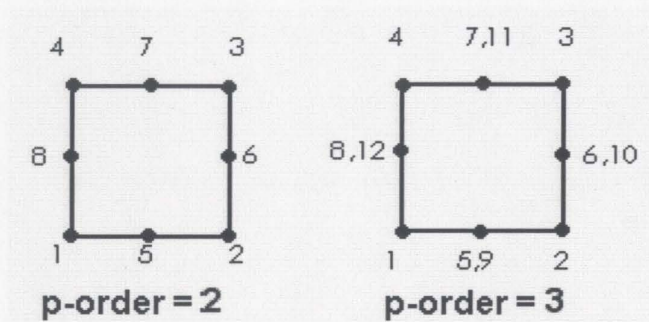


Figure 1.2 p type element

In h-p version, convergence is obtained by mesh refinement as well as increase in the order of polynomial. Since both are being varied there will be faster convergence of the solution compared to the above two methods. The p-type element and h-p type element are shown in figure's 1.2 and 1.3 respectively.

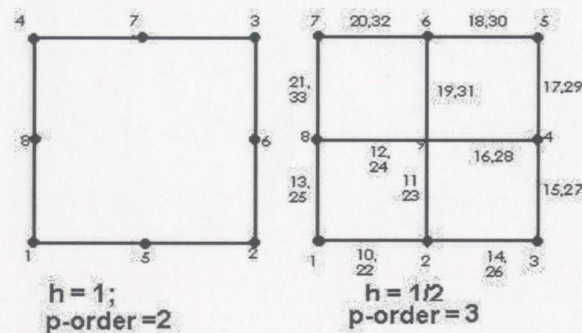


Figure 1.3 h-p type element

1.1.2 Fracture Mechanics

Fracture Mechanics has paved the way for modern engineering design to predict and prevent failure of materials. When severe stress concentrations arise from cracks, conventional engineering design based on strength and stiffness consideration leads to fallacious results. Recognition of the fact that structures contain inherent discontinuities and these grow into cracks with the application of loads, helps in incorporating various changes in the design phase itself. Quantitatively the allowable stress level has to be established for inspection requirements, so that fractures cannot occur. In addition to that, fracture mechanics is used to analyze the growth of small cracks to critical size.

The process of fracture can be considered to be made up of three components, crack initiation, crack propagation and final failure. Many cracks may not lead to fracture, but essentially those cracks that are situated in highly strained regions should be regarded as potential fracture initiators. Crack growth depends on the loading and environmental conditions. Loading conditions include many distinct types, static, dynamic, load controlled, grip controlled etc. Fracture toughness is a new material property that aids the designer in selecting materials to resist failures. It can also be defined as the critical value that makes the crack to propagate to fracture. The fracture mechanics procedures and theory was given by Ranganathan et.al [2].

1.1.3 Linear Elastic Fracture Mechanics

Linear Elastic Fracture Mechanics technology is based on analytical procedure that relates the stress field magnitude and distribution in the vicinity of the crack tip to the nominal stress applied to the structure, the size, shape and orientation of the crack or crack-tip discontinuity, and to material properties. The presence of the crack dominates the stress field in the vicinity of the crack tip.

Crack surface displacement is a fundamental concept in the fracture mechanics. When load is applied to the cracked body, there are three possible modes of crack surface displacements based on the load applied. These are Mode I opening mode, Mode II sliding mode and Mode III tearing mode.

When Mode I crack of length $2a$ is considered in an infinite plate, which is subjected to tensile stress σ at ends then an element $dx dy$ of the plate at the distance 'r' from the crack tip at an angle θ with respect to crack plane, experiences normal stresses σ_x, σ_y and shear stress τ_{xy} in x and y directions .

The stress components for a three dimensional body and the coordinates r and θ are shown in the figure 1.4 and $\sigma_x, \sigma_y, \sigma_z$ are the normal stresses in x, y and z directions.

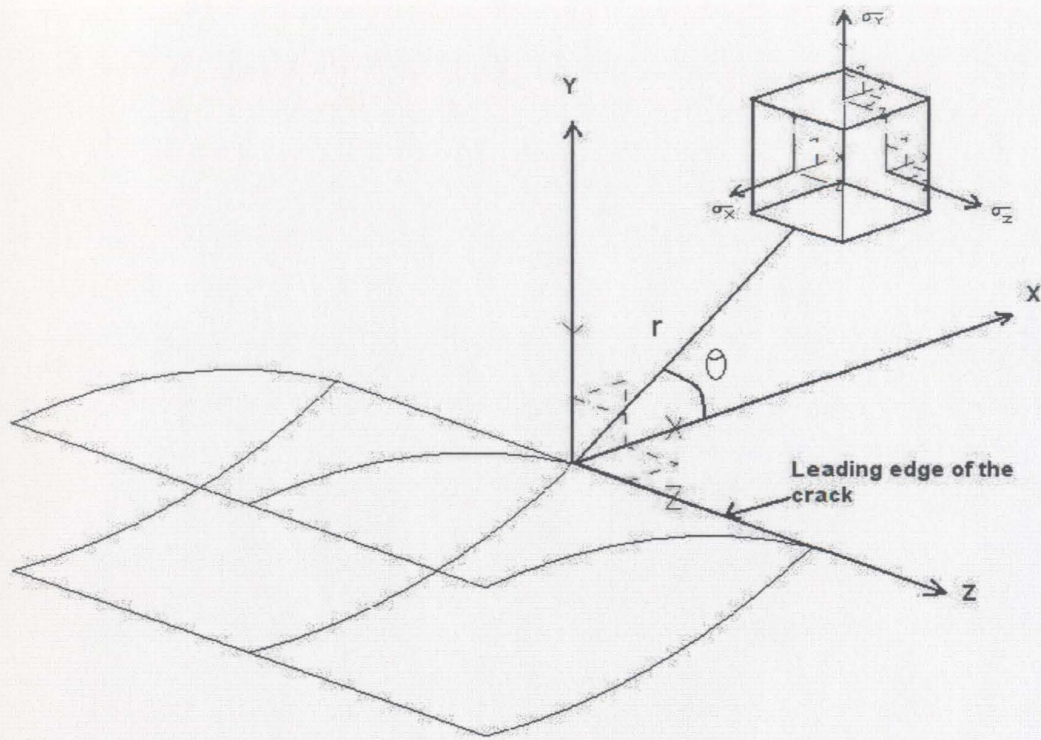


Figure 1.4 Stress components ahead of the crack tip

These stresses for a two dimensional case can be given as

$$\sigma_x = \sigma \sqrt{\frac{a}{2r}} \cos \frac{\theta}{2} \left[1 - \sin \frac{\theta}{2} \sin \frac{3\theta}{2} \right] \quad (1.1.1)$$

$$\sigma_y = \sigma \sqrt{\frac{a}{2r}} \cos \frac{\theta}{2} \left[1 + \sin \frac{\theta}{2} \sin \frac{3\theta}{2} \right] \quad (1.1.2)$$

$$\tau_{xy} = \sigma \sqrt{\frac{a}{2r}} \sin \frac{\theta}{2} \cos \frac{\theta}{2} \cos \frac{3\theta}{2} \quad (1.1.3)$$

1.1.4 Stress Intensity Factors

Stress Intensity factor is a unique parameter which represents the magnitude of stress field severity near a crack tip. From mathematical viewpoint, stress intensity factor gives a measure of the strength of the singularity controlling large stresses at the crack tip. Stress intensity factors for mode I and mode II are calculated using two different approaches,

- a) Direct methods
- b) Indirect methods

Specialized crack tip elements or singularity elements at the crack tip with K_I and K_{II} as unknowns are used to model the crack tip regions in direct methods. In this method the elements near the crack tip are specialized/singularity crack tip elements and conventional elements are used for the remaining or adjacent to these elements.

In indirect methods the stress intensity factors are determined as a function of distance from the crack tip and then the functions are extrapolated to the crack tip to obtain approximate values of K_I and K_{II} . The displacements and stresses obtained are fitted to the singular solution obtained in the vicinity of the crack tip.

1.1.5 Modes of Deformation

The three modes of deformation are shown in the figure 1.5 below.

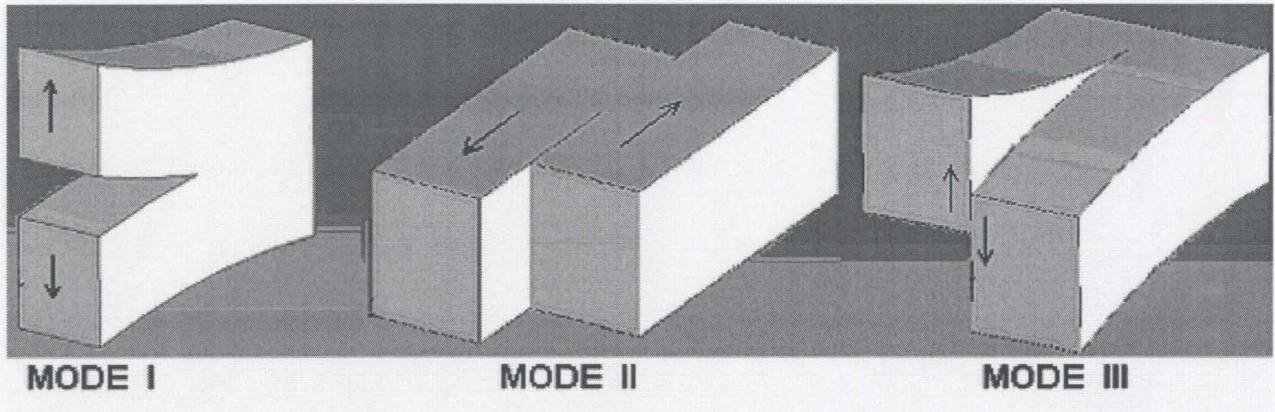


Figure 1.5 Basic Modes of Crack Surface Displacement

The stress and displacement fields in the vicinity of the crack tip subjected to three modes of deformation are given by

Mode - I

$$\sigma_x = \frac{K_I}{\sqrt{2\pi r}} \cos \frac{\theta}{2} \left[1 - \sin \frac{\theta}{2} \sin \frac{3\theta}{2} \right]$$

$$\sigma_y = \frac{K_I}{\sqrt{2\pi r}} \cos \frac{\theta}{2} \left[1 + \sin \frac{\theta}{2} \sin \frac{3\theta}{2} \right]$$

$$\tau_{xy} = \frac{K_I}{\sqrt{2\pi r}} \sin \frac{\theta}{2} \cos \frac{\theta}{2} \cos \frac{3\theta}{2}$$

$$\sigma_z = \nu(\sigma_x + \sigma_y)$$

$$\tau_{xy} = \tau_{yz} = 0$$

$$u = \frac{K_I}{G} \sqrt{\frac{r}{2\pi}} \cos \frac{\theta}{2} \left[1 - 2\nu + \sin^2 \frac{\theta}{2} \right]$$

$$v = \frac{K_I}{G} \sqrt{\frac{r}{2\pi}} \sin \frac{\theta}{2} \left[2 - 2\nu - \cos^2 \frac{\theta}{2} \right]$$

$$w = 0$$

(1.1.4)

Mode – II

$$\begin{aligned}\sigma_x &= \frac{-K_{II}}{\sqrt{2\pi r}} \sin \frac{\theta}{2} \left[2 + \cos \frac{\theta}{2} \cos \frac{3\theta}{2} \right] \\ \sigma_y &= \frac{K_{II}}{\sqrt{2\pi r}} \sin \frac{\theta}{2} \cos \frac{\theta}{2} \cos \frac{3\theta}{2} \\ \tau_{xy} &= \frac{K_{II}}{\sqrt{2\pi r}} \cos \frac{\theta}{2} \left[1 - \sin \frac{\theta}{2} \sin \frac{3\theta}{2} \right] \\ \sigma_z &= \nu(\sigma_x + \sigma_y) \\ \tau_{xz} &= \tau_{yz} = 0 \\ u &= \frac{K_{II}}{G} \sqrt{\frac{r}{2\pi}} \sin \frac{\theta}{2} \left[2 - 2\nu + \cos^2 \frac{\theta}{2} \right] \\ v &= \frac{K_{II}}{G} \sqrt{\frac{r}{2\pi}} \cos \frac{\theta}{2} \left[-1 + 2\nu + \sin^2 \frac{\theta}{2} \right] \\ w &= 0\end{aligned}\tag{1.1.5}$$

Mode – III

$$\begin{aligned}\tau_{xz} &= \frac{-K_{III}}{\sqrt{2\pi r}} \sin \frac{\theta}{2} \\ \tau_{yz} &= \frac{K_{III}}{\sqrt{2\pi r}} \cos \frac{\theta}{2} \\ \sigma_x &= \sigma_y = \sigma_z = \tau_{xy} = 0 \\ w &= \frac{K_{III}}{G} \sqrt{\frac{2r}{\pi}} \sin \frac{\theta}{2} \\ u &= v = 0\end{aligned}\tag{1.1.6}$$

1.1.6 Crack Propagation

The direction of crack propagation is determined by the maximum principal stress criterion. According to maximum principal stress criterion the crack will

propagate in the direction perpendicular to the maximum principal stress and in the direction in which $K_{II} = 0$.

The above condition can be written in an equation form as

$$K_I \sin \theta + K_{II} (3 \cos \theta - 1) = 0 \quad (1.1.7)$$

There are different varieties of approaches used in FE crack growth analysis

- a) Direct application of standard elements.
- b) Singular crack tip elements.
- c) Enriched elements.

The first method is a direct method and to get singular stress fields it requires high degree of mesh refinement at the crack tip. In singular crack tip elements approach mesh refinement is not required but still accuracy can be achieved. In the third method of enriched elements, the finite elements are enriched by including near crack tip fields and thereby calculating the stress intensity factors as part of the solution.

1.2 Scope of Thesis

From the literature review which is given in the next chapter it is obvious that there are numerous advantages of p-version over the h-version. Lot of research is going on over the polynomial approximation (p-version). In the present study hierarchical 2D formulation is given and the method is implemented by applying to real time problems to demonstrate the accuracy, efficiency etc.

For the efficient solving of algebraic linear equations, block conjugate gradient method is developed in Java programming language to suit the current needs and the advantages with object oriented programming are utilized in solving the equations. Numerical examples are also presented by comparing with the solved problems in order to show the accuracy.

1.3 Objectives of Research

The objective of this work is to,

1. Develop a finite element method for solving of crack problems using enriched crack tip elements developed before.
2. Adopting a p-version analysis for crack tip problems which eases the crack propagation analysis to be carried as required.
3. To compare the eight and nine noded quadratic isoparametric elements to validate the distinctive advantages.
4. To utilize the object oriented approach in developing the code which is effective in solving complex engineering equations.
5. Use the iterative schemes such as conjugate gradient method to solve the equations in order to get faster converged results.

In order to achieve these objectives the code is written in Object oriented programming language like Java and incorporating isoparametric formulation, enriched

crack tip elements, conjugate gradient method, finite difference methods etc. to make the analysis more easy, accurate, versatile and computationally efficient.

1.4 Outline of Thesis

The remaining portion of the thesis is divided into five chapters and chapter two reviews the literature published on h-version and p-version finite element methods, calculation of stress intensity factors, crack growth, utilization of enriched finite elements, singularity etc. The singularity is found near the crack tip and use of normal elements leads to errors; so enriched singularity elements are used near the crack tip. The various types of elements used by people in the past are also discussed in the review.

Conventional finite element formulation and enriched finite element formulation are discussed in chapter three. Java programming language is used to develop the Finite element code and detailed discussions about the program, its organization, advantages of Object Oriented Programming (OOP) concept are given in chapter four. In chapter five the numerical implementations and the numerical results are given followed by the conclusions drawn from this thesis investigation and the recommendations for further study are given in chapter six.

Chapter 2

BACKGROUND AND SCOPE OF WORK

2.1 Literature Review

Finite element method represents a powerful and general class of numerical technique for solving the differential equations in the fields of engineering, physics etc. The use of this method is extending to various other areas in engineering because of its ease and accuracy. As discussed in the previous chapter this method consists of important steps like discretization, selection of displacement functions, defining of element stiffness matrices, assemblage of stiffness matrices, solving of equations and interpretation of results.

Most of the fundamentals were given in various books like Zienkiewicz and Taylor [3], Segerland [4]. The normal procedure for solving the problems using finite element method is by using the h-version and later on developments have taken place to solve the problems using p-version and these methods are extended to crack problems also. In this chapter the pertinent literature review in this area of research has been presented.

2.1.1 p-version FEM

Finite element method has unparalleled success in various fields of engineering as it has numerous advantages. In spite of that, research is still going on for finding new methods to improve the performance, accuracy, efficiency etc.

Peano [5] proposed a finite element computer program which permits the user to exercise control over both the number of finite elements and order of approximation over each element. New hierarchies of C^0 and C^1 interpolations over triangles were presented and the main characteristics of this type of finite element is that the shape functions corresponding to an interpolation of order p constitute the subset of higher order interpolation functions ($p+1$) and greater. Hence the stiffness matrix of the element of order p , forms the subset of stiffness matrices of higher order ($p+1$) and greater. This development gives rise to new families of finite elements, which are computationally efficient. The Gaussian quadrature formulas for triangles were used in the calculation of stiffness matrix was given by Cowper [6].

In finite element method, best performances are attained by properly designing the meshes. Initial mesh design is based on certain assumptions and the error is the difference in value between the exact solution and the assumed solution. According to Szabo [7], the error is minimized by performing certain extensions, which are systematic changes of discretization by which the number of degrees of freedom is increased in each change. If the extension is by mesh refinement it is an h -extension or if it is by increase in

degree of polynomial it is a p-extension or when both are used it is an h-p extension. Szabo showed that in the structures with many singularities it is not necessary to refine the mesh in every singular point. The piecewise polynomial approximation, degree 'p' is increased progressively until the desired level of approximation is reached. Babuska et al. [8] showed that the rate of convergence of p-version is twice that of h-version.

The algorithm developed by the Morris et al. [9] branches dynamically to either direct or iterative solution methods. In iterative solution method the substructure of the finite element equation set is used to generate a lower order pre-conditioner for preconditioned conjugate gradient method. This strategy has also been used/implemented in a p-version finite element code. The combination of direct and iterative methods has the advantage of using the robustness of the direct method and the efficiency of iterative solver method. The values obtained from one p-level are passed on to the next as they serve as excellent values for iterative solution at higher polynomial order and solution converges rapidly.

Hierarchical concept for finite element shape functions Zienkiewicz et al. [10] has many advantages such as improved conditioning, ease of introducing error indicators if successive refinement is sought and to construct a range of error estimates that are ideally suited for adaptive refinements of analysis. Generation of hierarchic functions is easier if p-type refinement is used; so the authors advocated that strongly. With the hierarchical

degrees of freedom it is ensured that there is improved conditioning of the stiffness matrix and faster rates of convergence compared to non-hierarchical forms.

The number of linear equations grows enormously and solving of the equations becomes a difficult task, where as the use of proper iterative schemes helps in solving the equations. Wiberg and Petermoller [11] present a general hierarchical formulation applicable to both elliptic and hyperbolic problems. The use of hierarchical basis helps in developing error indicators for determining the areas where refinement gives the best improvement. They performed finite element weighted residual and least squares time integration in conjunction with hierarchical basis functions in time. Four solution algorithms were developed since the hierarchical formulation yields a sequence of nested equation systems, which were intended to outline the properties for electrostatic problems. When m hierarchical spaces are introduced then hierarchical finite element formulation of static elastic problems gives rise to $m+1$ linear equation systems. These linear equation systems are solved using efficient solution algorithms like preconditioned conjugate gradient methods. The solution algorithms yielded the shortest times and the authors showed the results to be very accurate and stable when hierarchical formulation in time domain is combined with exact integration.

The p-version FEM turned out to be superior when compared with h-version in many fields of practical importance as long as computational domain is discretized into a small number of elements. Duster and Rank [12] applied p-version

finite element method to deformation theory of plasticity and compared the results with adaptive h-version. The authors considered numerical problems and compared with the benchmark solution and found that p-version turned out to be significantly more accurate than h-version even when compared to an adaptive h-refinement. The p-version hybrid/mixed finite element formulation is presented by Liu and Busby [13] assuming the shape functions to be hierarchical for displacement variables. Geometry mapping of each element is also performed using an 8-node parametric mapping.

The performance of the solver based on the iterative methods depends on the proper selection of the shape function. Babuska et al. [14] showed the condensation approach to be a very effective tool for keeping the condition number under control and is advantageous for the conjugate gradient method.

Benzeley [15] presented various schemes comparing the features such as minimization by the degrees of freedom, which are necessary for the accurate solution conformable to insure monotone convergence and arbitrary shaped element at the crack tip and ability to handle yielding at the crack tip. He developed a general arbitrary quadrilateral finite element with a singular corner node by incorporating global-local finite element concept, singular enrichment and obtained an excellent comparison between the finite element and other solution with an exception of extreme cracks.

2.1.2 Computational Fracture Mechanics

Finite element method was implemented in fracture mechanics with refinement of mesh at the crack tip that has produced appreciable results. Due to the inability of the finite elements to represent singular near tip deformation, the use of conventional type of elements is not so satisfactory. Tracey [16] introduced a new finite element, which when used near the crack tip allows very accurate determination of K_I . A triangular singularity element is used at the crack tip and these are joined with quadrilateral isoparametric elements. He obtained results with 5% of collocation solution as compared with the results of Chan et al. [17] with coarse mesh.

Chan et al. [17] established the usefulness of finite element method with the comparison of change in stress intensity factors with the variation mesh size, element size etc. It has been demonstrated that crack tip stress intensity factors in various shapes under different loading conditions can be calculated using finite element method, supplemented by special computational procedures. Stress intensity factors are calculated using the displacement method. The results show that greater the element size is decreased near the crack tip the more the curve drawn between K_I and r/W approaches a constant slope. It was demonstrated that the higher degree of accuracy required depends on number of elements needed, which is a limitation with computer storage capacity.

Gifford Jr. and Hilton [18] combined enriched quad12 element in the vicinity of the crack tip and higher order conventional quad12 element elsewhere and made the

corner node to correspond to crack tip. In the element used the displacements varied cubically over the element in its local coordinates. A small displacement discontinuity, which is common to both the conventional and enriched elements, is introduced and the same is also implemented in the present research. The introduction of higher order elements is very beneficial in calculating K_I and K_{II} by using special enriched crack tip finite elements.

The two dimensional conforming singularity elements can be generated from standard conforming elements and the algorithm for converting a standard element to singularity element was presented by Akin [19] for triangular and quadrilateral elements. He stated that these elements significantly reduce the number of degrees of freedom required to obtain accurate results.

Stress intensity factors for a semi-elliptic surface crack is analyzed and the accuracy is verified by Raju and Newman Jr. [20] by increasing the number of degrees of freedom. Models taken consisted of singular elements at crack tip and isoparametric elements elsewhere. The convergence of the solution is studied by increasing the number of degrees of freedom. Stress intensity factors along the crack front are calculated using Nodal force method, which does not require prior assumption of either plane stress or plane strain. The authors showed that by increasing the degrees of freedom near the crack tip the results are in good agreement with the previous results.

Stress intensity factors for an edge cracked plate with two dimensions is studied by using the triangular elements with vertex and mid edge nodes at the crack tip. These allow for linear and quadratic variations along edges which do not intersect the crack edge; they also allow for variations proportional to distance from the crack edge and to the square root of the distance from crack edge and proportional to distance in perpendicular direction and to the square of the distance in this direction for points in the faces containing the crack edge. Blackburn and Hellen [21] presented the results with different gaussian points and with special elements at the crack tip and demonstrated that the accuracy of all these were good.

Approximate stress intensity factors can be calculated using a simple method in cracked plates. The three basic modes of deformation are functions of loading on cracked configuration, size and shape of crack, loading and other geometric boundaries. Usually stress intensity factors are evaluated using finite element methods, boundary element methods. Experimental analysis is also done in order to find K_{Ic} , the fracture toughness of engineering materials for simple cases. Nobile and Nobile [22] employed a new simple method for approximate evaluation of stress intensity factors in cracked plates, which took elastic singularity into account and was derived by the equilibrium condition for internal forces evaluated at the cross section passing through the crack tip. The results obtained by this method were compared with the known solutions for problems such as single edge cracked plate pure bending specimen, single edge cracked plate tension

specimen, 2 cracks emanating from a circular hole etc. and claimed for good approximation for SIF's.

In the finite element method the modeling of moving discontinuities is a difficult process, as the mesh has to be continuously updated according to the new geometry changes. Moes et al. [23] developed a finite element method for the crack growth without remeshing. This model consisted of a standard finite element approach and a crack representation, which was independent of the elements. In one case when crack was aligned with the elements then the finite element space is considered to be consisting of a model without the crack and a discontinuous enrichment. In the case where the crack is not aligned with the elements then discontinuous enrichment for appropriate nodes is used. If the support for the node is cut by the crack into two disjoint pieces then the node itself is enriched.

Stress intensity factors are calculated using quadratic isoparametric elements which embody the inverse square root singularity and the use of these elements has been shown by Barsoum [24] to provide excellent crack tip elements with the subside nodes close to the crack tip at a distance of 25 percent of the element size the element has singularity. This element has also been shown to contain rigid body motion and constant strain modes. Results show that the stiffness is singular for triangular elements when compared to quadrilateral elements if integrated exactly. It has been stated that the

evaluation of stiffness matrix and calculation of stresses very close to crack tip are possible with 9-point gaussian integration.

By choosing the mid-side node points on standard isoparametric elements, singularity occurs at the corner of an element. It is possible to obtain quite accurate results for the problem of determining the stress intensity at the crack tip [25]. Previous research investigations have shown that in order to determine correct stress intensity factors, crack tip elements are required, contrary to that stated by Henshell and Shaw [25] who showed that in order to get accurate results the crack tip elements were not required if the mid-side nodes of the standard elements were moved closer to the crack tip.

Two dimensional crack modeling in linear elasticity was mainly focused during the implementation of extended finite element method by Huang et al. [26]. In their paper they presented numerical solution for stress intensity factors for crack problems and conducted crack growth simulations. For crack modeling, a discontinuous function and two dimensional asymptotic crack tip displacement fields were used to represent the crack with no requirement for re-meshing.

The numerical examples considered included center crack in tension, inclined crack in tension, arc shaped cracks; in the numerical solution, tension domain independence in SIF computation is also studied and presented by them and they also concluded that accurate SIF for mode I were obtained for bench mark solutions. For arc

shaped problems accurate SIF's can be obtained by a good choice of crack representation, crack tip element size and domain size used in domain integral evaluation. Use of path independent form of J integral is required to get domain independence in numerical calculations.

Stress intensity factors at the crack tip are computed using an efficient unified approach and in that stress intensity factors can be obtained directly from the numerical solution without post processing. Partition of unity can be imposed through different methods such as moving least square method, the natural neighbour method or finite element method, in which partition of unity is imposed through finite element method. Finite element method adopts element domain based interpolation and partition of unity adopts nodal cover domain based interpolation. If higher order polynomials are used along with increased degrees of freedom, more accurate results can be obtained. When lower order polynomials ($p \leq 2$) are used in the numerical integration gauss quadrature of (10x10) is used and if the p order is more ($2 < p < 5$) then (20x20) quadrature is used and if it is equal to 5 then (32x32) gauss quadrature points are used. Results obtained by Fan et al. [27] show that the coarse mesh associated with higher order polynomials and larger number of terms of asymptotic function is able to yield very accurate solutions. The formulation used showed that it is not sensitive to the element mesh configuration or distortion, but sometimes higher orders of approximation may be needed.

New techniques are found continuously for modeling the cracks and one such new technique was described by Moes et al. [23] and in their paper they presented a method in which a standard displacement based approximation is enriched near a crack tip by incorporating the discontinuous field and asymptotic fields near the crack tip through partition of unity method. In order to enrich the nodes, which node has to be enriched is a key task and a specific convention is adopted. A node is enriched if its support is cut by the crack into two disjoint pieces. The approximation is the same as the one considered in present research and here also the discontinuity is introduced into a finite element approximation with a local enrichment. Maximum circumferential stress criterion is used for determining the growth direction.

Chapter 3

FINITE ELEMENT FORMULATION

3.1 Conventional Finite Element Formulation

The conventional Finite element formulation consists of 3 steps.

1. Selection of Element type
2. Selection of Displacement Functions
3. Defining of Stress/Strain and Stress/Displacement relationships
4. Derivation of Element stiffness Matrices
5. Assembly and solution

3.1.1 Selection of Element

In Isoparametric formulation same shape/interpolation functions are used to define the geometric shape of the element. The four corner nodes are bounded by +1 and -1 and the edges of the element also correspond to values of r and s of ± 1 . Nodes intermediate to corner nodes r (or s) = 1 correspond to values of r (or s) of $\pm \frac{1}{2}$.

The natural coordinates in terms of r and s are attached to the element with the origin at the center of the element as shown in the figure 3.1.

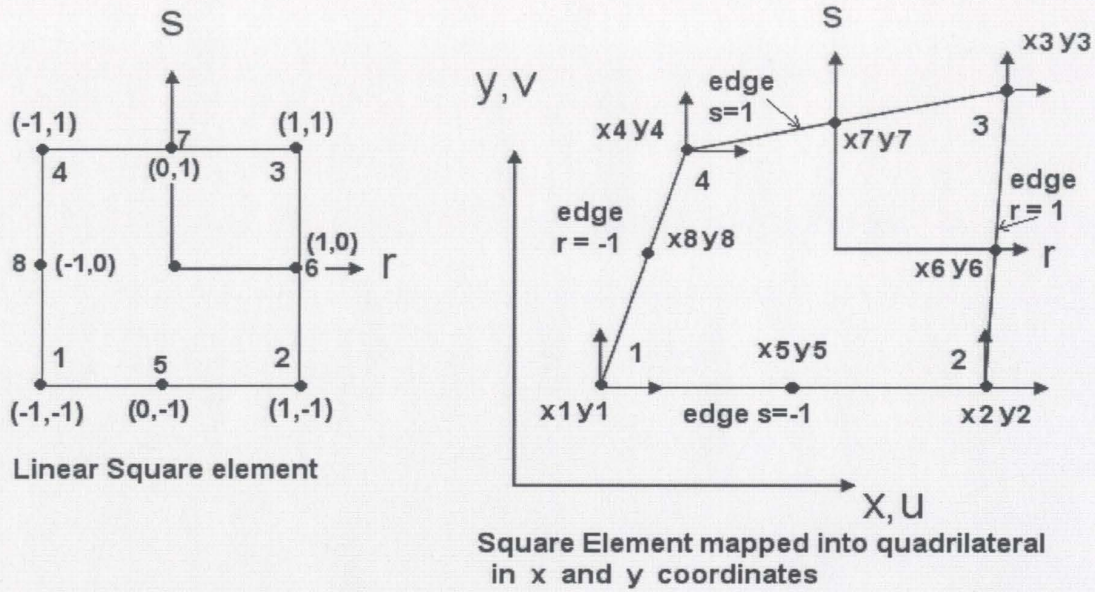


Figure 3.1 Isoparametric Element in Local Coordinates.

The shape functions of the quadratic element are based on the incomplete cubic polynomial such that coordinates x and y are given as

$$x = a_1 + a_2 r + a_3 s + a_4 r s + a_5 r^2 + a_6 s^2 + a_7 r^2 t + a_8 r s^2 \quad (3.1.1)$$

$$y = a_9 + a_{10} r + a_{11} s + a_{12} r s + a_{13} r^2 + a_{14} s^2 + a_{15} r^2 t + a_{16} r s^2 \quad (3.1.2)$$

where

a_1, a_2, \dots, a_{16} are constants to be determined.

3.1.2 Selection of Displacement Functions

The unknown constants in equations 3.1.1 and 3.1.2 can be eliminated and the coordinate expressions for x and y can be expressed as

$$x = \sum_{i=1}^8 N_i(r, s) x_i \quad (3.1.3)$$

$$y = \sum_{i=1}^8 N_i(r, s) y_i \quad (3.1.4)$$

and the shape functions are represented as

$$N_1 = \frac{1}{4}(1-r)(1-s)(-r-s-1)$$

$$N_2 = \frac{1}{4}(1+r)(1-s)(r-s-1)$$

$$N_3 = \frac{1}{4}(1+r)(1+s)(r+s-1)$$

$$N_4 = \frac{1}{4}(1-r)(1+s)(-r+s-1)$$

$$N_5 = \frac{1}{2}(1+r)(1-s)(1-r)$$

$$N_6 = \frac{1}{2}(1+r)(1+s)(1-s)$$

$$N_7 = \frac{1}{2}(1+r)(1+s)(1-r)$$

$$N_8 = \frac{1}{2}(1-r)(1+s)(1-s) \quad (3.1.5)$$

Or

they can also be represented in compact notation as

$$N_i = \frac{1}{4}(1 + r r_0)(1 + s s_0)(r r_0 + s s_0 - 1)$$

where

$$r_0 = -1, 1, 1, -1 \quad (i = 1, 2, 3, 4)$$

$$s_0 = -1, -1, 1, 1 \quad (i = 1, 2, 3, 4)$$

for mid-side nodes in index notation are given as

$$N_i = \frac{1}{2}(1 - r^2)(1 + s s_0) \quad s_0 = -1, 1 \quad (i = 5, 7) \quad (3.1.7)$$

$$N_i = \frac{1}{2}(1 + r r_0)(1 - s^2) \quad r_0 = 1, -1 \quad (i = 6, 8) \quad (3.1.8)$$

3.1.3 Defining of Stress/strain relationships

In the process of defining the stress/strain relationships the strain matrix has to be formulated and then the stiffness matrix is evaluated. In order to formulate element stiffness matrix, the same geometric shape functions are used for displacement interpolation; the displacement vector can be written in the matrix form as

$$\begin{aligned} u &= [N_i] \{u_i\} \\ v &= [N_i] \{v_i\} \end{aligned} \quad (3.1.9)$$

where

$$[N_i] = [N_1, N_2, N_3, \dots, N_8]$$

The same shape functions are used to represent the coordinates of the point within the element in terms of the nodal coordinates in isoparametric formulation. So

$$u = N_1u_1 + N_2u_2 + N_3u_3 + \dots + N_8u_8 \quad (3.1.10)$$

$$v = N_1v_1 + N_2v_2 + N_3v_3 + \dots + N_8v_8$$

It becomes a very difficult process to write shape functions in terms of x and y , so derivatives have to be expressed as functions of r and s coordinates, which are previously in x, y coordinates. A function $f = f(x, y)$ can be considered to be an implicit function of r and s as

$$f = f[x(r, s), y(r, s)] \quad (3.1.11)$$

The chain rule of differentiation has to be applied as it is not possible to express r and s in terms of x and y .

So by chain rule of differentiation f can be expressed as a function of x and y and can be written as

$$\frac{\partial f}{\partial r} = \frac{\partial f}{\partial x} \frac{\partial x}{\partial r} + \frac{\partial f}{\partial y} \frac{\partial y}{\partial r} \quad (3.1.12)$$

$$\frac{\partial f}{\partial s} = \frac{\partial f}{\partial x} \frac{\partial x}{\partial s} + \frac{\partial f}{\partial y} \frac{\partial y}{\partial s} \quad (3.1.13)$$

writing in matrix form

$$\begin{bmatrix} \frac{\partial f}{\partial r} \\ \frac{\partial f}{\partial s} \end{bmatrix} = [J] \begin{bmatrix} \frac{\partial f}{\partial x} \\ \frac{\partial f}{\partial y} \end{bmatrix}$$

where (3.1.14)

$$[J] = \text{jacobian matrix} = \begin{bmatrix} \frac{\partial x}{\partial r} & \frac{\partial y}{\partial r} \\ \frac{\partial x}{\partial s} & \frac{\partial y}{\partial s} \end{bmatrix}$$

the above equation can be inverted as

$$\begin{bmatrix} \frac{\partial f}{\partial x} \\ \frac{\partial f}{\partial y} \end{bmatrix} = [J]^{-1} \begin{bmatrix} \frac{\partial f}{\partial r} \\ \frac{\partial f}{\partial s} \end{bmatrix} \quad (3.1.15)$$

$$dx dy = \det [J] dr ds \quad (3.1.16)$$

Normal and shear strains ϵ_x , ϵ_y and γ_{xy} are as follows

$$\epsilon_x = \frac{\partial u}{\partial x} = \frac{\partial N_1}{\partial x} u_1 + \frac{\partial N_2}{\partial x} u_2 + \frac{\partial N_3}{\partial x} u_3 + \dots + \frac{\partial N_8}{\partial x} u_8 \quad (3.1.17)$$

similarly

$$\epsilon_y = \frac{\partial v}{\partial y} = \frac{\partial N_1}{\partial y} v_1 + \frac{\partial N_2}{\partial y} v_2 + \frac{\partial N_3}{\partial y} v_3 + \dots + \frac{\partial N_8}{\partial y} v_8 \quad (3.1.18)$$

$$\gamma_{xy} = \frac{\partial u}{\partial y} + \frac{\partial v}{\partial x} = \frac{\partial N_1}{\partial y} u_1 + \frac{\partial N_1}{\partial x} v_1 + \frac{\partial N_2}{\partial y} u_2 + \frac{\partial N_2}{\partial x} v_2 + \dots + \frac{\partial N_8}{\partial y} u_8 + \frac{\partial N_8}{\partial x} v_8 \quad (3.1.19)$$

The equations (3.1.17) to (3.1.19) can be written in matrix notation as

$$\begin{Bmatrix} \varepsilon_x \\ \varepsilon_y \\ \gamma_{xy} \end{Bmatrix} = \begin{bmatrix} \frac{\partial N_1}{\partial x} & 0 & \frac{\partial N_2}{\partial x} & 0 & \dots & \dots & \frac{\partial N_8}{\partial x} & 0 \\ 0 & \frac{\partial N_1}{\partial y} & 0 & \frac{\partial N_2}{\partial y} & \dots & \dots & 0 & \frac{\partial N_8}{\partial y} \\ \frac{\partial N_1}{\partial y} & \frac{\partial N_1}{\partial x} & \frac{\partial N_2}{\partial y} & \frac{\partial N_2}{\partial x} & \dots & \dots & \frac{\partial N_8}{\partial y} & \frac{\partial N_8}{\partial x} \end{bmatrix} \begin{Bmatrix} u_1 \\ v_1 \\ u_2 \\ v_2 \\ \dots \\ \dots \\ u_8 \\ v_8 \end{Bmatrix} \quad (3.1.20)$$

$$\{\varepsilon\} = [B]\{u\}$$

where $\{\varepsilon\}$ = strain vector (3.1.21)
 $[B]$ = strain displacement relationship matrix
 $\{u\}$ = displacement vector

Stress Strain Relationship

The stress and strain vectors are related through elasticity matrix $[D]$ and it is in terms of modulus of elasticity E and poisson's ratio ν . According to Hooke's law, the stress and strain are directly proportional to each other within the elastic limits, so the elastic matrix for plane stress and plane strain are given below

for Plane Strain :

$$\begin{Bmatrix} \sigma_x \\ \sigma_y \\ \sigma_{xy} \end{Bmatrix} = \frac{E}{(1+\nu)(1-2\nu)} \begin{bmatrix} (1-\nu) & \nu & 0 \\ \nu & (1-\nu) & 0 \\ 0 & 0 & \left(\frac{1-2\nu}{2}\right) \end{bmatrix} \begin{Bmatrix} \varepsilon_x \\ \varepsilon_y \\ \gamma_{xy} \end{Bmatrix}$$

and

(3.1.22)

$$\sigma_z = \nu(\sigma_x + \sigma_y)$$

for Plane stress:

$$\begin{Bmatrix} \sigma_x \\ \sigma_y \\ \sigma_{xy} \end{Bmatrix} = \frac{E}{(1-\nu^2)} \begin{bmatrix} 1 & \nu & 0 \\ \nu & 1 & 0 \\ 0 & 0 & \left(\frac{1-\nu}{2}\right) \end{bmatrix} \begin{Bmatrix} \varepsilon_x \\ \varepsilon_y \\ \gamma_{xy} \end{Bmatrix}$$

and

(3.1.23)

$$\sigma_z = 0$$

The elemental matrix $[B]$ consists of derivatives of shape functions as the terms and D is the material matrix.

$$[k] = \iint_A [B]^T D [B] h \, dx dy$$

$$\text{where } [B] = \frac{\partial [N]}{\partial x} = \text{element matrix in terms of } r, s \quad (3.1.24)$$

h = thickness

$$[k] = \iint_A [B]^T D [B] h \, \det J \, dr ds \quad (3.1.25)$$

3.1.4 Derivation of stiffness matrix and Numerical Integration

The integration of the equation (3.1.25) is generally done numerically and let us consider the problem of numerically evaluating a one-dimensional integral of the form

$$I = \int_{-1}^1 f(r) dr \quad (3.1.26)$$

The gaussian quadrature approach of evaluating I for n point approximation is given as

$$I = \int_{-1}^1 f(r) dr \cong w_1 f(r_1) + w_2 f(r_2) + \dots + w_n f(r_n) \quad (3.1.27)$$

where

w_1, w_2, \dots, w_n = weights

r_1, r_2, \dots, r_n = sampling points or gauss points

In two dimensions

$$I = \sum_{i=1}^n \sum_{j=1}^n w_i w_j f(r_i, s_j) \quad (3.1.28)$$

Now the stiffness matrix is evaluated by numerical integration and given as

$$[k] = \iint_A [B]^T D [B] |J| w_i w_j \quad (3.1.29)$$

3.1.5 Assembly and Solution

The stiffness matrices calculated are then assembled into a global stiffness matrix and then it is solved using pre conjugate gradient method which is explained in chapter 4. The solution consists of initially assuming a likely solution and then using iterative solver the true solution is achieved.

3.2 h and p adaptivity

In the h version finite element method, in order to obtain more accurate results the size of the element length is decreased so that a denser mesh can be obtained and this is called as h-adaptivity.

In p-adaptivity, contrary to h-adaptivity, the size of the element remains same but the order of approximation is increased, i.e. the shape functions are enriched by adding higher order polynomials.

3.3 Hierarchical Shape functions:

The hierarchical shape functions were first introduced by Zienkiewicz et al. [10], but Peano [5] and Babuska et al. [14] were the first to put them to use. New shape functions are added to the existing shape functions i.e. for example if an eight noded quadrilateral element is taken the shape functions for order 2 will not be changed if new functions of order 3 are added. A brief review of hierarchical shape functions is presented here.

If one dimensional shape functions are considered for displacements or nodal variables then the shape functions for the end nodes can be given as

$$N_1 = \frac{1}{2}(1-r) \quad \text{and} \quad N_2 = \frac{1}{2}(1+r) \quad (3.3.1)$$

so hierarchical shape functions of mid-nodes for different orders of p can be written as

$$\begin{aligned}
 \text{for } p=2 \quad N_h^2 &= \frac{1}{2!}(r^2 - 1) \\
 \text{for } p=3 \quad N_h^3 &= \frac{1}{3!}(r^3 - r) \\
 \text{for } p=4 \quad N_h^4 &= \frac{1}{4!}(r^4 - 1) \\
 \text{for } p=5 \quad N_h^5 &= \frac{1}{5!}(r^5 - r)
 \end{aligned} \tag{3.3.2}$$

and they can be represented in simple notation as

$$\begin{aligned}
 N_h^p &= \frac{1}{p!}(r^p - 1) \quad \text{for } p=2,4,6,\dots \\
 N_h^p &= \frac{1}{p!}(r^p - r) \quad \text{for } p=3,5,7,\dots
 \end{aligned} \tag{3.3.3}$$

The shape functions obtained above are hierarchical in nature and are given for one dimensional case as

$$u = N_1 u_1 + N_2 u_2 + N_h^2 \frac{\partial^2 u_m}{\partial x_m^2} + N_h^3 \frac{\partial^3 u_m}{\partial x_m^3} + N_h^4 \frac{\partial^4 u_m}{\partial x_m^4} + \dots$$

or in simple notation as

$$u = \sum [N][u_i] + \sum_{p=2}^n N_h^p \left. \frac{\partial^p u}{\partial x} \right|_m \tag{3.3.4}$$

where u_i are nodal displacement variables at end nodes and

$\left. \frac{\partial^p u}{\partial x} \right|_m$ are the hierarchical displacement variables for order p at the mid node

Similarly for a two dimensional element also the shape functions can be written as tensor product of simple one-dimensional shape functions. If a 9-noded plane element is considered as shown in the figure 3.3 the first order p shape functions correspond to corner nodes or h nodes and second order p shape functions correspond to mid side nodes or p-nodes.

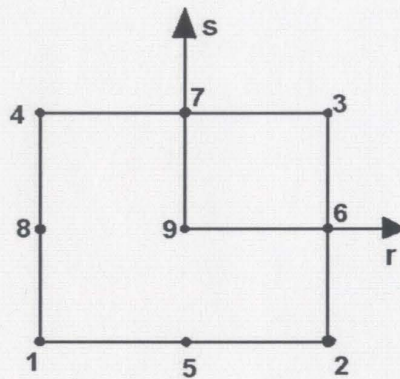


Figure 3.2 Nine Noded Element

The hierarchical displacement equations are given as

$$u = \sum_{i=1}^4 N_i u_i + \sum_{p=2}^n \sum_{i=5}^8 N_{hi}^p u_i^{p'} + \sum_{p=2}^n N_{h9}^p u_9^{p'}$$

Where $u_i^{p'} = \frac{\partial^p u}{\partial r^p}$ or $\frac{\partial^p u}{\partial s^p}$ at node i depending on which edge the node lies.

$$u_i^{p''} = \frac{\partial^p u}{\partial r^p \partial s^p} \text{ at central node.}$$

similarly the displacement functions for v can be written.

The shape functions for 2 D element can be given as below

$$\begin{aligned}
N_h^i &= \frac{1}{4}(1+r r_i)(1+s s_i) \quad \text{for corner nodes } i=1,2,3,4. \\
N_{hi}^2 &= \frac{1}{4}(r^2-1)(1+s s_i) \quad \text{for mid-side nodes } i=5,7. \\
N_{hi}^2 &= \frac{1}{4}(1+r r_i)(s^2-1) \quad \text{for mid-side nodes } i=6,8.
\end{aligned} \tag{3.3.5}$$

similarly the higher order hierarchical shape functions can be written as

for odd orders

$$\begin{aligned}
N_{hi}^p &= \frac{1}{2}(r^p-r)(1+s s_i) \frac{1}{p!} \quad \text{for nodes } i=5,7. \\
N_{hi}^p &= \frac{1}{2}(1+r r_i)(s^p-s) \frac{1}{p!} \quad \text{for nodes } i=6,8. \\
N_{hi}^p &= (r^p-r)(s^p-s) \frac{1}{p!p!} \quad \text{for node } i=9.
\end{aligned}$$

for even orders

$$\begin{aligned}
N_{hi}^p &= \frac{1}{2}(r^p-1)(1+s s_i) \frac{1}{p!} \quad \text{for nodes } i=5,7. \\
N_{hi}^p &= \frac{1}{2}(1+r r_i)(s^p-1) \frac{1}{p!} \quad \text{for nodes } i=6,8. \\
N_{hi}^p &= (r^p-1)(s^p-1) \frac{1}{p!p!} \quad \text{for node } i=9.
\end{aligned} \tag{3.3.6}$$

In the finite element formulation it is given as

$$\begin{aligned}
u &= [N][x] \\
u &= \sum_{i=1}^n N_i x^n
\end{aligned} \tag{3.3.7}$$

and the stiffness equation for finding the stiffness matrix is given as

$$K_n x^n = f^n \quad (3.3.8)$$

where K_n = stiffness matrix involving the derivatives of the shape functions N

f = force vector.

When the density of the mesh is increased then the mesh becomes denser and the number of elements increases which, results in more degrees of freedom. Here Zienkiewicz et al. [10] says that an identical discretization process as in FEM results in algebraic equation

$$K_{n+m} x^{n+m} = f^{n+m} \quad (3.3.9)$$

If refinement is made hierarchically then original stiffness coefficients reappear and the above equation can be written as

$$\begin{bmatrix} K_n & K_{n,m} \\ K_{m,n} & K_m \end{bmatrix} \begin{Bmatrix} a^n \\ a^m \end{Bmatrix} = \begin{Bmatrix} f^n \\ f^m \end{Bmatrix} \quad (3.3.10)$$

Zienkiewicz et al. [10] claims in his paper that the K_n is preserved, possibly saving some coefficients computations and taking the values of a^n as starting values in an iterative solution and first approximation as

$$a^m = K_m^{-1} (f^m - K_{m,n} a^n) \quad (3.3.11)$$

substituting the value of a^m from the equation (3.3.11)

$$a^m = K_m^{-1} \{ f^m - K_{m,n} (K_n^{-1} f^n) \} \quad (3.3.12)$$

3.4 Enriched Element formulation

Singular terms are obtained when the displacement equations near the crack tip are differentiated to yield strain field. The effects of singularities are included in the element by enriching an element displacement assumption. The singularity is obtained at the node because of this enrichment and is represented in terms of stress intensity factors, which is given by

$$u = a_1 + a_2 r + a_3 s + a_4 r s + a_5 r^2 + a_6 s^2 + a_7 r^2 t + a_8 r s^2 + U_s \quad (3.4.1)$$

$$v = a_9 + a_{10} r + a_{11} s + a_{12} r s + a_{13} r^2 + a_{14} s^2 + a_{15} r^2 t + a_{16} r s^2 + V_s \quad (3.4.2)$$

and

$$U_s = K_I f_1(R, \theta) + K_{II} g_1(R, \theta) \quad (3.4.3)$$

$$V_s = K_I f_2(R, \theta) + K_{II} g_2(R, \theta) \quad (3.4.4)$$

where

$$f_1 = \frac{1}{4G} \sqrt{\frac{r}{2\pi}} \left[\cos \phi \left\{ (2\gamma - 1) \cos \frac{\theta}{2} - \cos \frac{3\theta}{2} \right\} - \sin \phi \left\{ (2\gamma + 1) \sin \frac{\theta}{2} - \sin \frac{3\theta}{2} \right\} \right] \quad (3.4.5)$$

$$g_1 = \frac{1}{4G} \sqrt{\frac{r}{2\pi}} \left[\cos \phi \left\{ (2\gamma + 3) \sin \frac{\theta}{2} + \sin \frac{3\theta}{2} \right\} + \sin \phi \left\{ (2\gamma - 3) \cos \frac{\theta}{2} + \cos \frac{3\theta}{2} \right\} \right] \quad (3.4.6)$$

$$f_2 = \frac{1}{4G} \sqrt{\frac{r}{2\pi}} \left[\sin \phi \left\{ (2\gamma - 1) \cos \frac{\theta}{2} - \cos \frac{3\theta}{2} \right\} + \cos \phi \left\{ (2\gamma + 1) \sin \frac{\theta}{2} - \sin \frac{3\theta}{2} \right\} \right] \quad (3.4.7)$$

$$g_2 = \frac{1}{4G} \sqrt{\frac{r}{2\pi}} \left[\sin \phi \left\{ (2\gamma + 3) \sin \frac{\theta}{2} + \sin \frac{3\theta}{2} \right\} - \cos \phi \left\{ (2\gamma - 3) \cos \frac{\theta}{2} + \cos \frac{3\theta}{2} \right\} \right] \quad (3.4.8)$$

In the above equations, R and θ are polar coordinates around the crack tip and ϕ is the angle of the crack tip measured counter clockwise from the x axis as shown in the fig 3.3

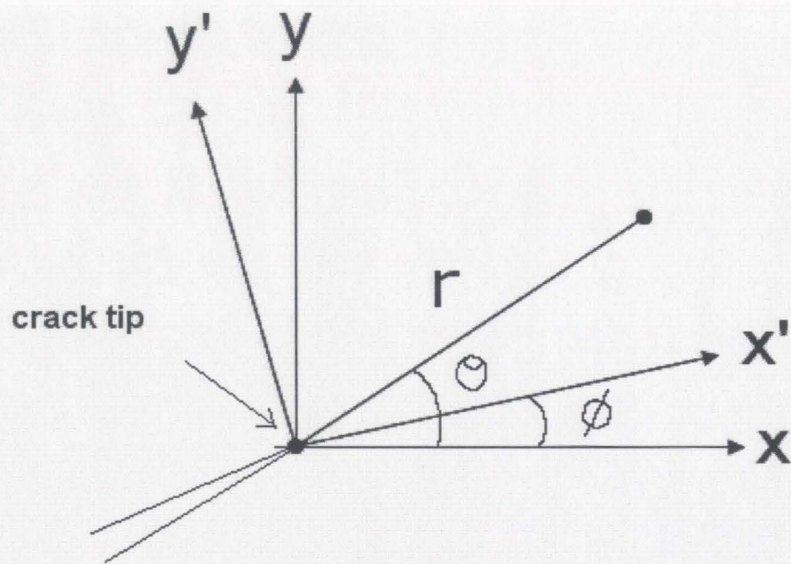


Figure 3.3 Local coordinate system at the crack tip

G is the shear modulus of elasticity and γ is the constant which depends on the value of Poisson's ratio ν and is given by

$$\gamma = \begin{cases} 3-4\nu & (\text{plain strain or axisymmetric}) \\ \frac{3-\nu}{1+\nu} & (\text{plain stress}). \end{cases} \quad (3.4.9)$$

and

Modulus of rigidity G is given by

$$G = \frac{E}{2(1+\nu)} \quad (3.4.10)$$

In the above equations (3.4.1) to (3.4.8) the a_i 's and K_I and K_{II} are undetermined constants.

Now the displacements can be written as

$$u = a_1 + a_2 r + a_3 s + a_4 r s + a_5 r^2 + a_6 s^2 + a_7 r^2 t + a_8 r s^2 + \dots + K_I f_1 + K_{II} g_1$$

$$v = a_9 + a_{10} r + a_{11} s + a_{12} r s + a_{13} r^2 + a_{14} s^2 + a_{15} r^2 t + a_{16} r s^2 + \dots + K_I f_2 + K_{II} g_2$$

The above equations can be written as

$$[u] = [P]\{a\} + K_I f_1 + K_{II} g_1 \quad (3.4.11)$$

$$[v] = [P]\{a\} + K_I f_2 + K_{II} g_2 \quad (3.4.12)$$

In the above equations the unknowns are $[u]$, $[v]$ and $[a]$. Solving equations (3.4.11) and (3.4.12) to obtain $[a]$ and it is represented as

$$\begin{aligned} [a] &= [P]^{-1} \{u\} - K_I [P]^{-1} f_1 - K_{II} [P]^{-1} g_1 \\ [a] &= [P]^{-1} \{v\} - K_I [P]^{-1} f_2 - K_{II} [P]^{-1} g_2 \end{aligned} \quad (3.4.13)$$

Substituting the above equations in u and v , so the enriched displacements can be given as

$$u_s = [N]\{u\} + K_I \left(f_1 - \sum_{i=1}^4 N_i f_{1i} - \sum_{p=2}^P \sum_{j=5}^8 N_j^p f_{1j}^p \right) + K_{II} \left(g_1 - \sum_{i=1}^4 N_i g_{1i} - \sum_{p=2}^P \sum_{j=5}^8 N_j^p g_{1j}^p \right) \quad (3.4.14)$$

$$v_s = [N]\{v\} + K_I \left(f_2 - \sum_{i=1}^4 N_i f_{2i} - \sum_{p=2}^P \sum_{j=5}^8 N_j^p f_{2j}^p \right) + K_{II} \left(g_2 - \sum_{i=1}^4 N_i g_{2i} - \sum_{p=2}^P \sum_{j=5}^8 N_j^p g_{2j}^p \right) \quad (3.4.15)$$

Where

$$f_{ij}^p = \frac{\partial^p f_1}{\partial r^p} \quad \text{or} \quad \frac{\partial^p f_1}{\partial s^p}$$

$$\text{and} \quad g_{ij}^p = \frac{\partial^p g_1}{\partial r^p} \quad \text{or} \quad \frac{\partial^p g_1}{\partial s^p} \quad \text{calculated at node } j$$

Chapter 4

COMPUTER IMPLEMENTATION

4.1 Java as programming language

Most of the programs that were developed in the past were written in FORTRAN, which lacks many of the new features present in the present day computer languages. Object oriented programming has brought some new frontiers in the field of computer programming. The modern day computer programming languages uses object-oriented approach that has great many advantages compared to other programming languages and the programming techniques can be obtained from various books such as Lewis and Loftus [28] and Slack [29].

Java is one such language, which utilizes object-oriented concept. As far as the knowledge of the author is concerned there are quite a few people who used this object-oriented concept. Since Java has many advantages for dealing with sophisticated projects it is used as programming tool in my research. It is used as the main programming language in developing the program for FEA.

Java has several advantages compared to all other languages. Some of them are

1) Platform Independent/Architecture neutral

Java compiler generates a byte code, which is architecture-neutral object file format, which can be executed in any processor. These byte code instructions developed by the java compiler works on well with today's most common computer compiler instructions.

2) Encapsulation

Encapsulation means all the data and implementation code for an object will be hidden in an interface and in java program the object and the properties of the object are hidden within the class. As long as the interface remains consistent, the application can interact with the objects. By encapsulation the object can be accessed but the object hides all its variables. The older programs, which are not encapsulated, suffered from the values of variables getting changed / reused.

3) Inheritance and polymorphism

Inheritance is the ability of the class to use the methods and properties of another class in addition to its own properties. Inheritance helps the subclasses to have specialized behaviours and functions along with common elements provided by super class. Inheritance provides a powerful and natural mechanism for organizing and structuring software programs. Polymorphism as the greek name

says, “having multiple forms” is the property of being able to assign different meaning or usage to something in different contexts.

4) Data Abstraction

If the most generalized items are taken from a given problem and leaving behind the utmost details of data it is called as data abstraction. It can also be explained as keeping the data in groups so that it can be manipulated as a unit. Data abstraction gives advantage in terms of storing the data and reading the data.

5) Multithreading

A thread executes a series of statements and if there is a single set of program statements then it is a single thread and if multiple sets of statements are run in parallel then it is multithreading. The thread may be alive for the entire execution time or for a few milliseconds, which again depends on the program code.

Usually when programs are written for solving FEM problems the input to the computer is cumbersome and most of the errors are caused due to the error in input. The input of the crack problem that is being solved consists of initially giving the total number of nodes, elements, corner nodes, mid side nodes, and the order of the problem. Based on the order given it reads the coordinates, boundary conditions and crack problem is implemented by giving an additional parameter for crack elements in the elemental

connectivity. For the crack elements specific number greater than zero is assigned which distinguishes from normal element since zero is assigned for normal element.

The program is organized in various steps

- 1) Main program
- 2) Input
- 3) Calculation of jacobian and shape functions
- 4) Creation of stiffness matrix
- 5) Assembly of stiffness matrices
- 6) Solving of the global stiffness matrix

The program code in the main file coordinates with other parts of the program, while input file reads the input parameters such as the order of polynomial, type of element, the total number of nodes and elements etc. and allocates memory. Some of the parameters read are stored in the matrices for easy manipulation of data. The main function of this file is to create the objects of each file and using those objects it accesses the file to perform required operations. It creates an input object and that object reads the total nodes, total elements, corner nodes, mid-side nodes and constants like Young's modulus of elasticity, poisson's ratio etc. Then it starts reading the nodal coordinates, boundary conditions, nodal connectivity etc. Nodal coordinates are the coordinates in x and y direction at those specific nodal points. The flow chart of the complete program organization is given in figure 4.1.

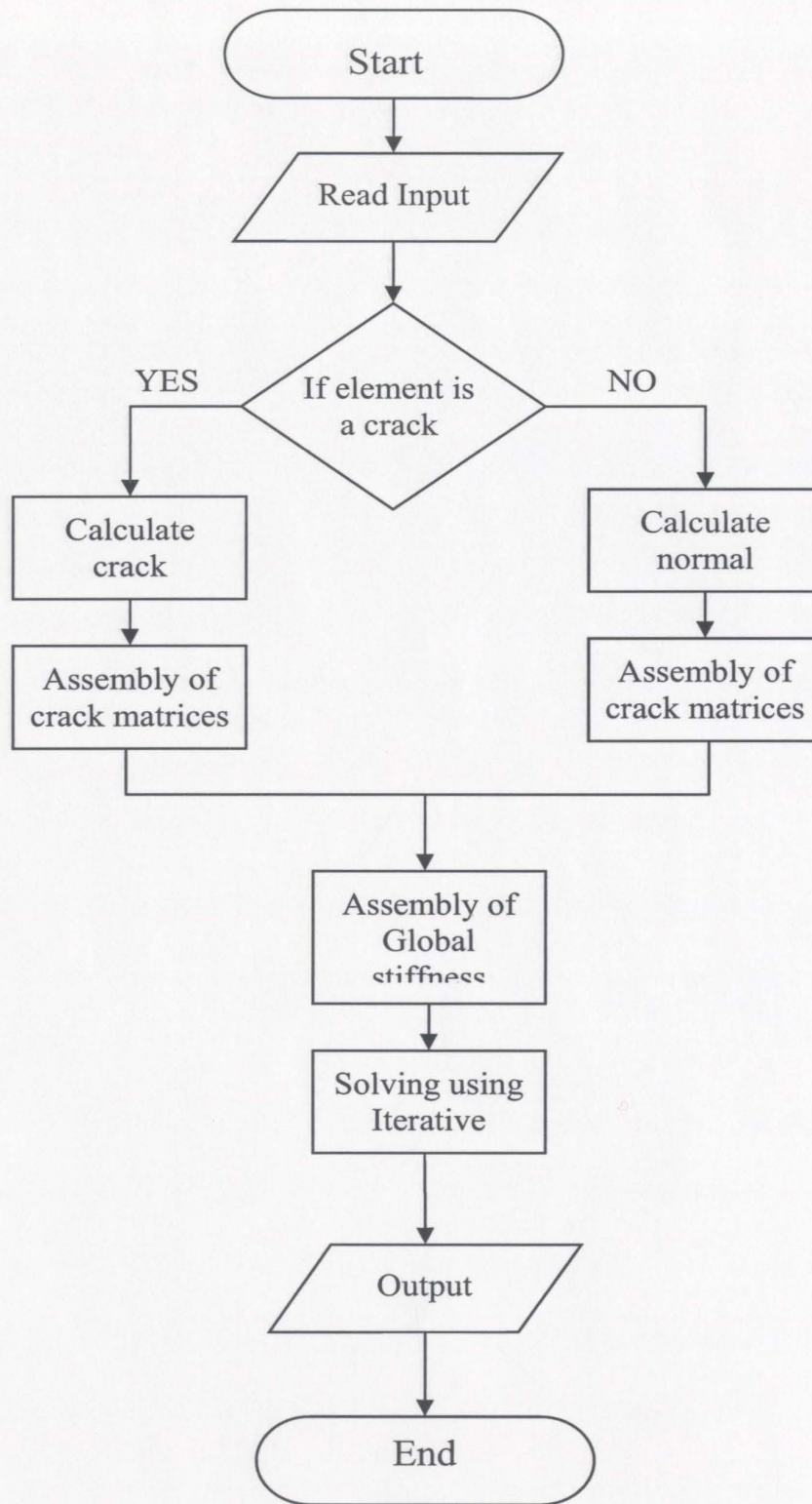
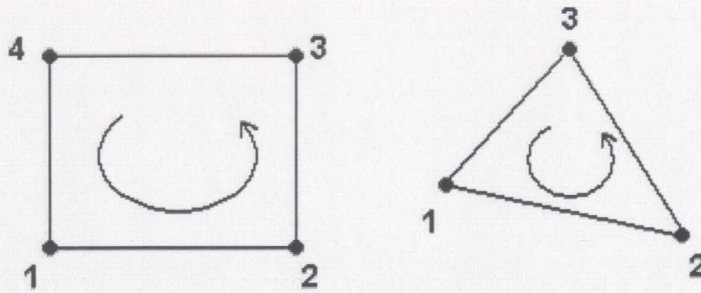


Figure 4.1 Organization of the computer program

4.1.1 Nodal connectivity and nodal coordinates

The finite element model is a geometric replica of a prototype and each node should have an identification number and it is called as node number. Nodal numbering is done in order to obtain a local stiffness matrix and assigning of node numbers is done in a systematic fashion keeping the bandwidth, computer memory allocation etc, as low as possible. It is a normal practice to follow one particular order while numbering the nodes. The right hand screw rule is used for the nodal connectivity, otherwise element stiffness will become singular and hence counter clock wise numbering is used as shown in the figure 4.2.

For either quadrilateral 4-noded element or triangular element, mid-side nodes are assigned for greater accuracy. The more the nodes in an element the more the element behavioural characteristics can be calculated. Usually in an element the corner nodes are numbered first and mid-side nodes are numbered second. Each element has also an identifier called element number and the array of nodal connectivity consists of all the node numbers of that particular element. In the nodal connectivity array there is one more additional parameter known as element type, which distinguishes the regular element from crack element as well the crack tip number if there are more than one crack tip.



Counter clockwise nodal numbering

Figure 4.2 Nodal numbering

4.1.2 Shape Function Derivatives:

The derivatives of the shape functions are done in the starting of the analysis and for convenience the code for the calculation of the derivatives is written in a separate file. The computations that are carried out in that file are the shape functions derivatives, hierarchical shape functions and weights. The input to the methods in this file are the polynomial order and element type. Based on the element used in the analysis it calculates the shape functions, shape function derivatives and hierarchical shape functions. The values of the derivatives and shape functions are stored in arrays and they are returned to the program for the calculation of the local stiffness matrices.

Local stiffness matrices are calculated by using the results obtained from various files and then each matrix is assembled into a global stiffness matrix and it is then solved

using one of the solver methods to get the desired results. If proper care is taken while numbering of nodes bandwidth can be reduced and equations can be solved easily with minimal computer processing power.

4.2 Convergence

Convergence of the results is obtained up to some extent by making the size 'h' smaller or increasing the polynomial degree but when the problem size increases then the number of linear equations to be solved increases enormously. For any type of problem convergence of the solution is the key factor and in order to get the exact answer to the problem how good should be the approximation and convergence should be is the question.

From the equation $u = \sum_{i=1}^n N_i u_i$ it is understood that if the number of parameters u_i

is increased then convergence or more exact solution can be reached. Fourier series is known to represent any function with desired accuracy if the number of terms is increased and here it can be said that convergence is also an approximation to the true solution when the number of terms increases. Convergence of a given element type as its size is reduced referred as h convergence and convergence obtained by increasing order of the polynomial is referred as p convergence.

4.2.1 Iterative techniques used for convergence:

Sometimes convergence cited above by decreasing the size or increasing the polynomial also needs lot of computational time although the best computer processors are used. If iterative techniques are used for convergence when there are lots of equations to be solved then a substantial amount of time and cost are saved. An iterative method refers to large number of techniques that use successive approximations in order to obtain a more accurate solution.

There are many iterative techniques, which have advantages over others. Iterative techniques are classified as

- a) Stationary iterative methods
- b) Non-stationary iterative methods.

Stationary iterative methods perform the same operations on current iterative vectors/approximations and some of the methods used in this category are Jacobi method, Gauss-Seidal method, successive over relaxation method, symmetric successive over relaxation method etc.

Non-stationary methods use the transformation matrix that is referred as preconditioner and perform operations on iterative vector and this method may even fail to converge without preconditioner. Some of the common examples of this category are

Conjugate Gradient method (CG), Conjugate gradient on normal equations, generalized Minimal residual (GMRES), Bi-conjugate gradient method (BiCG), Conjugate gradient squared method (CGS), Preconditioned conjugate gradient method (PCG) etc.

4.2.1.1 Preconditioned Conjugate Gradient Method:

The iterative method used in the present solution is preconditioned Conjugate gradient method. In this method the preconditioned matrix $M = \begin{bmatrix} k_{11} & 0 \\ 0 & k_{22} \end{bmatrix}$ is used. The preconditioner is a transformation matrix, which transforms the coefficient matrix into one of the favourable spectrum on which the convergence rate depends. In the Conjugate gradient method successive vector sequences or successive approximations are generated and residuals corresponding to iterates are used in updating the iterates. The main concept is to find the search direction vectors p^i for $i=1,2,3\dots n$ which satisfies the condition $(p^i)^T M(p^j) = 0$ when $i \neq j$ and as efficiency is concerned, only small number of approximations are stored in the memory which increases the performance of the computer.

The linear system that has to be solved is represented as $Ax = B$. Usually 'A' has a large condition number when used in conjugate gradient method and so it is preconditioned. Preconditioning essentials means to replace the system with an equivalent system $B Ax = B b$

The Preconditioned conjugate gradient method consists of essentially 5 steps:

1. Initialization
2. Begin Iteration
3. Perform Updates
4. Check for Convergence
5. Prepare for next CG update

1. Initialization:

The Preconditioned conjugate gradient method starts with an initial guess X^0 of the results and then it is multiplied by the preconditioned conjugate gradient matrix. Even though the matrices A and B are symmetric it is not necessary that BA be a symmetric matrix. A good preconditioner is the starting point in the PCG method, which should satisfy two criteria

- a) It should be able to contract the Eigen spectrum of the original system.
- b) It should be easy to factorize relative to the original system.
- c) It should be cheap for storage and fast to evaluate.

2. Begin Iteration:

The maximum number of iterations that are required is defined and usually this would be less because this method converges rapidly. The iteration starts and the method

generates successive approximations to the solutions. The residuals are calculated corresponding to the iterates.

3. Performing Updates:

The iterates X^i are calculated for each iteration and after end of each iteration it is updated by a multiple α^i times search direction vector

$$x^i = x^{i-1} + \alpha_i p^i \quad (4.1)$$

In a similar way the residuals are also updated as

$$r^i = r^{i-1} - \alpha_i q^i \quad (4.2)$$

and the search direction vectors p^i are updated using residuals

$$p^i = z^{i-1} + \beta_{i-1} p^{i-1} \quad (4.3)$$

4. Checking for Convergence:

Although maximum number of iterations is predetermined in the program if the results are converged then the iterations should not continue further; so, in order to do this the convergence has to be checked after every iteration and if it is less than the tolerance limit the iterations have to be stopped.

$$\text{if } \|r^{i+1}\| < \textit{tolerance}$$

then

stop iterations

5. Prepare for next CG updates:

Once the convergence checking is done and if the solution is not yet converged then the search direction vectors, iterates and the residuals are updated for the next

iterations. Updating is done till the proper converged solution or the maximum number of iterations is achieved, whichever ever come first.

Preconditioned Conjugate Gradient Method

compute

$$r^0 = b - Ax^0 \quad \text{for some initial guess } x^0$$

for $i = 1, 2, 3, \dots$

Solve

$$Mz^{i-1} = r^{i-1} \quad \text{where } M \text{ is a preconditioned matrix}$$

$$\rho_{i-1} = r^{(i-1)T} z^{i-1}$$

if $i = 1$

$$p^1 = z^0$$

else

$$\beta_{i-1} = \rho_{i-1} / \rho_{i-2}$$

$$p^i = z^{i-1} + \beta_{i-1} p^{i-1}$$

endif

$$q^i = Ap^i$$

$$\alpha_i = \rho_{i-1} / (p^i)^T q^i$$

$$x^i = x^{i-1} + \alpha_i p^i$$

$$r^i = r^{i-1} - \alpha_i q^i$$

check convergence and continue if necessary

(4.4)

Figure 4.3 Pre-conditioned Conjugate Gradient Method.

A psuedo code for preconditioned conjugate gradient method is given in figure 4.3.

4.3 Evaluation of higher order derivatives of crack tip displacement function

In engineering it is known that many processes follow one form of differential equation or other and exact solution for those methods is almost not possible. So it becomes necessary to find numerical methods for approximating the solution to these equations. There are various solution techniques like finite element methods, finite difference methods, finite volume methods, collocation methods etc. for finding the approximate solutions.

In the numerical integration, calculation of the derivatives with respect to R and θ are required and manual calculation is easy for second degree functions but when the order of polynomial is increased the degree of equations also increases and manual calculation becomes very cumbersome. So in this analysis Maple, a mathematical software is used for calculating the derivatives of the functions. In order to reduce the complexity the constants are separated out of the equation and then the computation is performed. Maple has an integrated server for converting the calculated equations into the user specified form and the computed equations are converted to Java compatible functions.

$$\begin{aligned}
\frac{dr}{dx} &= \cos(\theta + \phi); \\
\frac{dt}{dx} &= \frac{-\sin(\theta + \phi)}{R}; \\
\frac{dr}{dy} &= \sin(\theta + \phi); \\
\frac{dt}{dy} &= \frac{\cos(\theta + \phi)}{R}
\end{aligned}
\tag{4.3.1}$$

$$f_1 = \sqrt{R} \left\{ (\cos(\phi)((\gamma-1)\cos(\frac{\theta}{2}) - \cos(\frac{3\theta}{2})) - \sin(\phi)((\gamma+1)\sin(\frac{\theta}{2}) - \sin(\frac{3\theta}{2})) \right\};$$

$$f_1 = f(F1, F2, F3, F4)$$

where

$$F1 = \sqrt{R} \cos(\phi)(\gamma-1)\cos(\frac{\theta}{2}) \tag{4.3.2}$$

$$F2 = \sqrt{R} \cos(\phi)\cos(\frac{3\theta}{2})$$

$$F3 = \sqrt{R} \sin(\phi)(\gamma+1)\sin(\frac{\theta}{2})$$

$$F4 = \sqrt{R} \sin(\phi)\sin(\frac{3\theta}{2})$$

As shown in the above equation (4.3.2) the function f_1 can be written as a function of $F1$,

$F2$, $F3$, $F4$. In order to find the value of $\frac{\partial f_1}{\partial x}$ the derivatives of the functions

$\frac{\partial F1}{\partial x}$, $\frac{\partial F2}{\partial x}$, $\frac{\partial F3}{\partial x}$, $\frac{\partial F4}{\partial x}$ are calculated separately and then they are summed up.

The value of $\frac{\partial F1}{\partial x}$ and $\frac{\partial F1}{\partial y}$ is obtained by

$$\frac{\partial F1}{\partial x} = \frac{\partial F1}{\partial R} \frac{dr}{dx} + \frac{\partial F1}{\partial \theta} \frac{d\theta}{dx}$$

$$\frac{\partial F1}{\partial y} = \frac{\partial F1}{\partial R} \frac{dr}{dy} + \frac{\partial F1}{\partial \theta} \frac{d\theta}{dy}$$

Similarly for the remaining functions $\frac{\partial F2}{\partial x}, \frac{\partial F2}{\partial y}, \frac{\partial F3}{\partial x}, \frac{\partial F3}{\partial y}, \frac{\partial F4}{\partial x}, \frac{\partial F4}{\partial y}$ are calculated.

By separating the equations in this form the computation of the functions is easy to process in Maple. The same procedure is followed for the remaining functions such as g_1, f_2, g_2 .

The double derivatives of the functions with respect to r and s are calculated using the equation (4.3.3) as shown below.

$$\frac{\partial^2 f_1}{\partial r^2} = \frac{\partial f_1}{\partial x^2} \left(\frac{dx}{dr} \right) \left(\frac{dx}{dr} \right) + 2 \frac{\partial f_1}{\partial x \partial y} \left(\frac{dx}{dr} \right) \left(\frac{dy}{dr} \right) + \frac{\partial f_1}{\partial y^2} \left(\frac{dy}{dr} \right) \left(\frac{dy}{dr} \right) \quad (4.3.3)$$

In order to calculate $\frac{\partial^2 f_1}{\partial r^2}$ the expressions $\frac{\partial^2 f_1}{\partial x^2}, \frac{\partial^2 f_1}{\partial y^2}, \frac{\partial^2 f_1}{\partial xy}$ have to be calculated first following a similar procedure used for calculating $\frac{\partial f_1}{\partial x}$ and $\frac{\partial f_1}{\partial y}$. The same process has to be repeated for calculating the derivatives with respect to s also. This computation is easy for 2nd order but as the order of the polynomial increases then the computation becomes difficult which can be performed easily using Maple software.

Chapter 5

NUMERICAL STUDIES AND DISCUSSIONS

The finite element analysis is used in many of the engineering fields and it has been researched and developed to such an extent that very accurate results can be obtained. Although traditional finite element method is very efficient in most of the fields but it is not so efficient when it is applied to crack tip problems. Still research is going on in this field and new methods are being developed. In this chapter the formulation presented in the previous chapters has been applied to various numerical problems. The yard-stick for these numerical problems is the accuracy of the stress intensity factors (SIFs). The results obtained are compared with the bench-mark solution which is considered by many authors as described in literature review.

During the computational process, gauss quadrature was adopted for each element separately. If the polynomial degree is 'p' then, the Gaussian points taken are $(p+1)(p+1)$. The material is assumed to be isotropic with an elastic modulus of $30e6$ psi and Poisson's ratio of 0.3.

In order to demonstrate the accuracy and the advantages of the present analysis, various examples were considered. The results were compared with the bench mark results obtained by various authors to prove the accuracy of the method. To demonstrate

the size and density of the meshes, various figures are shown below which are plotted from the exact values taken from the input file. The values from the input files are taken and then converted to drawing exchange file format and then plotted in the drawing software. In order to demonstrate the versatility of the methods various types of problems are taken for analysis and they were

- 1) A plate with an edge crack loaded in tension.
- 2) A plate with an edge crack loaded in shear.
- 3) A plate with a 45 degrees inclined edge crack loaded in tension
- 4) A plate with a centered angle crack in tension
- 5) Curved crack plate subjected to biaxial stresses.

In this section several numerical examples of cracks and crack growth are presented.

Example 1: A plate with an edge crack loaded in tension.

As the first example, a plate with an edge crack subjected to tension load is considered. The model geometry is shown in figure 5.1.1. The material is assumed to be isotropic and the modulus of elasticity is $30e6$ psi and Poisson's ratio of 0.3.

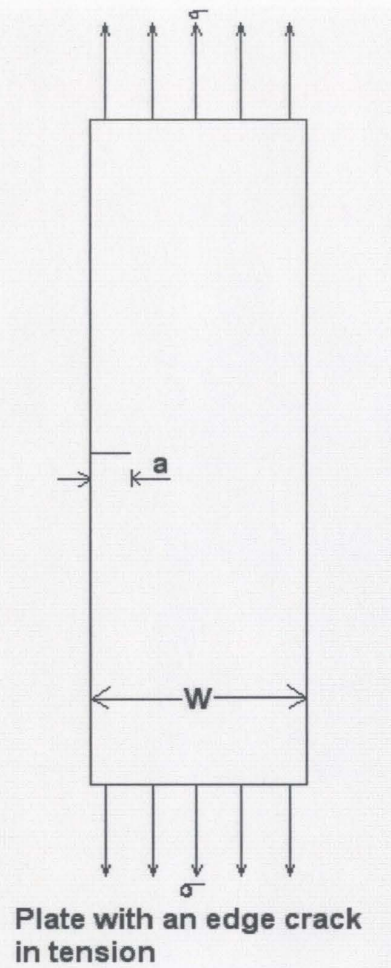


Figure 5.1.1 Geometry of Edge crack problem.

Consider the geometry shown in the figure 5.1.1, the crack configuration gives the picture of how the loads are applied and the basic dimensions of the plate. The plate is of width ' W ' and length ' L ' with an edge crack of length ' a '. The geometrical parameters are as follows: $a/W = 1/2$; $L/W = 16/7$ and $W = 7$. The plate is loaded in tension along the perpendicular direction to the crack plane. With respect to the above configuration various aspects are analyzed. The mode I stress intensity factor K_I and mode II stress intensity factor K_{II} for different sizes of the mesh and different orders of the polynomial are calculated.

The exact solution for the problem is given Ewalds and Wanhill [30] and [23].

$$K_I = C\sigma\sqrt{\pi a}$$

where

C=finite geometry correction factor

$$= 1.12 - 0.231\left(\frac{a}{W}\right) + 10.55\left(\frac{a}{W}\right)^2 - 21.72\left(\frac{a}{W}\right)^3 + 30.39\left(\frac{a}{W}\right)^4 \quad (5.1.1)$$

a=half crack length

W=width of plate

Bench mark Solution:

Considering the plate of width W=7 inches, height L=16 inches and crack of length 2a= 7inches, then $\left(\frac{a}{W}\right) = \frac{1}{2}$ and $\left(\frac{L}{W}\right) = \frac{16}{7}$. Substituting the above values of

$\left(\frac{a}{W}\right)$ the finite geometry correction factor is obtained as C=2.826375. Substituting the

above value of C in the equation 5.1.1, gives the value of $K_I=9.375 \text{ psi}\sqrt{\text{in}}$ and this is taken as the bench mark value.

The mesh considered is of very less density and although the aspect ratio seems to be high still the results are close to the analytical value. Various lengths of the element are considered to see the variation in the obtained value. The crack length 'a' is 3.5 and the various sizes of the element lengths at the crack tip taken are from as high as 1.5 to lowest value of 0.005. The stress intensity factors are obtained for 4x4 mesh and 6x6 meshes. The results are tabulated for various crack element lengths in tables 5.1.1 to

5.1.12. The table 5.1.1 shows the global degrees of freedom for different meshes and various p-orders. Also the results are presented in figures 5.1.2 and 5.1.8.

The global degrees of freedom for these meshes are given in table 5.1.1

p-order	2	3	4	5	6	7
4x4 mesh (8 noded element)	138	222	306	390	474	558
4x4 mesh (9 noded element)	170	286	402	518	634	750
6x6 mesh (8 noded element)	278	452	626	800	974	1148
6x6 mesh (9 noded element)	350	596	842	1088	1334	1580

Table 5.1.1: Degrees of freedom for different meshes and orders

p-order	Element length (inches)	Anal. Sol K_I ($psi\sqrt{in}$)	8 Noded Element		9 Noded Element	
			K_I		K_I	
			4x4 mesh	6x6 mesh	4x4 mesh	6x6 mesh
2	1.5	9.375	9.55	9.61	9.45	9.64
3	1.5	9.375	9.69	9.46	9.52	9.56
4	1.5	9.375	9.75	9.57	9.66	9.59
5	1.5	9.375	9.74	9.55	9.64	9.58
6	1.5	9.375	9.791	9.50	9.62	9.63
7	1.5	9.375	9.795	9.54	9.59	9.63

Table 5.1.2: SIFs for element length 1.5 in crack plate with tension load.

p-order	Element length (inches)	Anal. Sol $(psi\sqrt{in})$	8 Noded Element		9 Noded Element	
			K_I		K_I	
			4x4 mesh	6x6 mesh	4x4 mesh	6x6 mesh
2	1.0	9.375	9.36	9.55	9.2	9.56
3	1.0	9.375	9.69	9.41	9.45	9.49
4	1.0	9.375	9.773	9.45	9.64	9.52
5	1.0	9.375	9.764	9.49	9.61	9.51
6	1.0	9.375	9.818	9.49	9.56	9.57
7	1.0	9.375	9.824	9.47	9.53	9.57

Table 5.1.3: SIFs for element length 1.0 in crack plate with tension load.

p-order	Element length (inches)	Anal. Sol $(psi\sqrt{in})$	8 Noded Element		9 Noded Element	
			K_I		K_I	
			4x4 mesh	6x6 mesh	4x4 mesh	6x6 mesh
2	0.75	9.375	9.203	9.47	8.97	9.46
3	0.75	9.375	9.705	9.37	9.4	9.45
4	0.75	9.375	9.803	9.48	9.62	9.48
5	0.75	9.375	9.79	9.46	9.60	9.47
6	0.75	9.375	9.85	9.45	9.55	9.53
7	0.75	9.375	9.86	9.40	9.53	9.53

Table 5.1.4: SIFs for element length 0.75 in crack plate with tension load.

p-order	Element length (inches)	Anal. Sol K_I ($psi\sqrt{in}$)	8 Noded Element		9 Noded Element	
			K_I		K_I	
			4x4 mesh	6x6 mesh	4x4 mesh	6x6 mesh
2	0.5	9.375	8.91	9.28	8.59	9.26
3	0.5	9.375	9.7	9.31	9.3	9.38
4	0.5	9.375	9.86	9.44	9.596	9.43
5	0.5	9.375	9.86	9.42	9.590	9.42
6	0.5	9.375	9.926	9.37	9.578	9.49
7	0.5	9.375	9.927	9.36	9.557	9.49

Table 5.1.5: SIFs for element length 0.5 in crack plate with tension load.

p-order	Element length (inches)	Anal. Sol K_I ($psi\sqrt{in}$)	8 Noded Element		9 Noded Element	
			K_I		K_I	
			4x4 mesh	6x6 mesh	4x4 mesh	6x6 mesh
2	0.25	9.375	8.24	8.75	7.78	8.75
3	0.25	9.375	9.58	9.17	9.03	9.26
4	0.25	9.375	9.96	9.38	9.49	9.37
5	0.25	9.375	10.01	9.37	9.52	9.37
6	0.25	9.375	10.07	9.35	9.68	9.44
7	0.25	9.375	10.06	9.34	9.77	9.45

Table 5.1.6: SIFs for element length 0.25 in crack plate with tension load.

p-order	Element length (inches)	Anal. Sol $(psi\sqrt{in})$	8 Noded Element		9 Noded Element	
			K_I		K_I	
			4x4 mesh	6x6 mesh	4x4 mesh	6x6 mesh
2	0.2	9.375	7.97	8.53	7.487	8.55
3	0.2	9.375	9.496	9.11	8.913	9.22
4	0.2	9.375	9.986	9.35	9.447	9.37
5	0.2	9.375	10.078	9.34	9.505	9.37
6	0.2	9.375	10.15	9.45	9.740	9.43
7	0.2	9.375	10.14	9.45	9.86	9.43

Table 5.1.7: SIFs for element length 0.2 in crack plate with tension load.

p-order	Element length (inches)	Anal. Sol $(psi\sqrt{in})$	8 Noded Element		9 Noded Element	
			K_I		K_I	
			4x4 mesh	6x6 mesh	4x4 mesh	6x6 mesh
2	0.15	9.375	7.063	8.26	7.571	8.21
3	0.15	9.375	8.709	9.16	9.337	9.01
4	0.15	9.375	9.364	9.37	9.997	9.31
5	0.15	9.375	9.477	9.38	10.164	9.31
6	0.15	9.375	9.893	9.43	10.268	9.55
7	0.15	9.375	10.024	9.42	10.261	9.67

Table 5.1.8: SIFs for element length 0.15 in crack plate with tension load.

p-order	Element length (inches)	Anal. Sol K_I ($psi\sqrt{in}$)	8 Noded Element		9 Noded Element	
			K_I		K_I	
			4x4 mesh	6x6 mesh	4x4 mesh	6x6 mesh
2	0.1	9.375	6.403	7.79	6.924	7.7
3	0.1	9.375	9.3224	9.02	8.995	8.63
4	0.1	9.375	9.18136	9.41	9.940	9.25
5	0.1	9.375	9.41815	9.45	10.274	9.28
6	0.1	9.375	10.1299	9.53	10.403	9.74
7	0.1	9.375	10.4533	9.49	10.450	10.08

Table 5.1.9: SIFs for element length 0.1 in crack plate with tension load.

p-order	Element length (inches)	Anal. Sol K_I ($psi\sqrt{in}$)	8 Noded Element		9 Noded Element	
			K_I		K_I	
			4x4 mesh	6x6 mesh	4x4 mesh	6x6 mesh
2	0.05	9.375	5.176	7.79	5.66	7.7
3	0.05	9.375	7.348	9.02	8.04	8.83
4	0.05	9.375	8.584	9.41	9.51	9.25
5	0.05	9.375	9.152	9.45	10.29	9.28
6	0.05	9.375	10.562	9.53	10.564	9.74
7	0.05	9.375	11.074	9.49	10.802	10.08

Table 5.1.10: SIFs for element length 0.05 in crack plate with tension load.

p-order	Element length (inches)	Anal. Sol K_I ($psi\sqrt{in}$)	8 Noded Element		9 Noded Element	
			K_I		K_I	
			4x4 mesh	6x6 mesh	4x4 mesh	6x6 mesh
2	0.01	9.375	2.66	3.9	2.953	3.76
3	0.01	9.375	4.31	6.01	4.820	5.62
4	0.01	9.375	5.713	7.8	6.613	7.08
5	0.01	9.375	6.883	9.17	8.30	8.09
6	0.01	9.375	11.79	9.74	9.128	13.01
7	0.01	9.375	9.431	10.26	10.072	11.85

Table 5.1.11: SIFs for element length 0.01 in crack plate with tension load.

p-order	Element length (inches)	Anal. Sol K_I ($psi\sqrt{in}$)	8 Noded Element		9 Noded Element	
			K_I		K_I	
			4x4 mesh	6x6 mesh	4x4 mesh	6x6 mesh
2	0.005	9.375	1.92	2.89	2.136	2.76
3	0.005	9.375	3.18	4.65	3.577	4.31
4	0.005	9.375	4.327	6.38	5.053	5.68
5	0.005	9.375	5.438	8.01	6.711	6.85
6	0.005	9.375	9.83	8.74	7.585	13.4
7	0.005	9.375	5.549	9.71	8.754	9.55

Table 5.1.12: SIFs for element length 0.005 in crack plate with tension load.

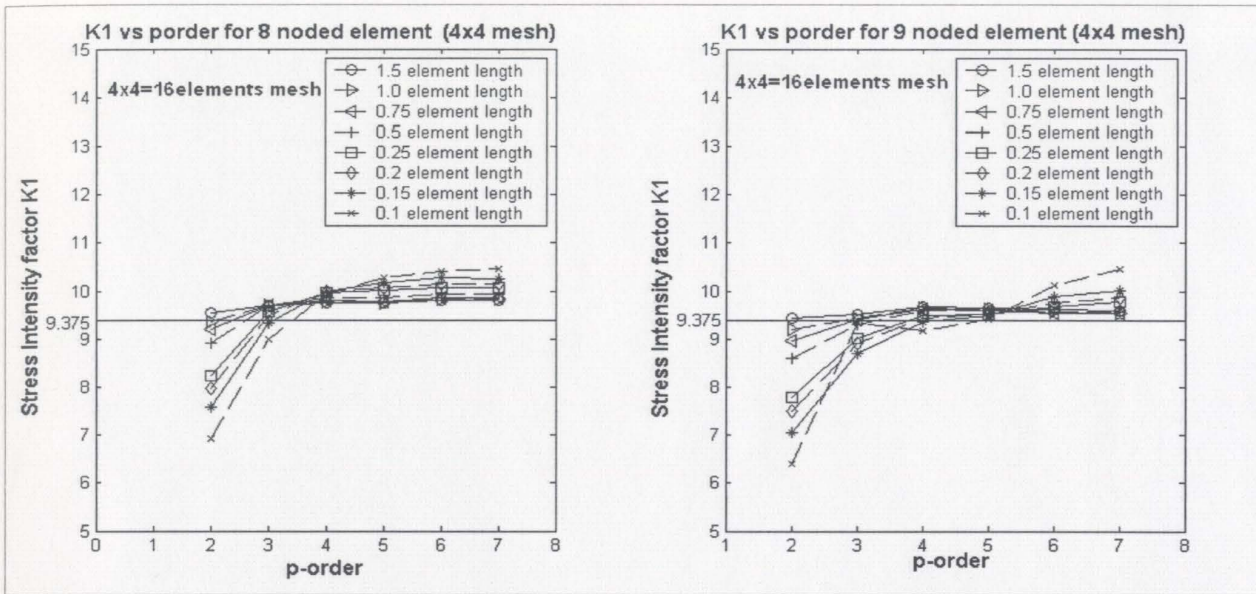


Figure 5.1.2 : K_I vs. p-order comparison for 8 noded and 9 noded 4x4 meshes.

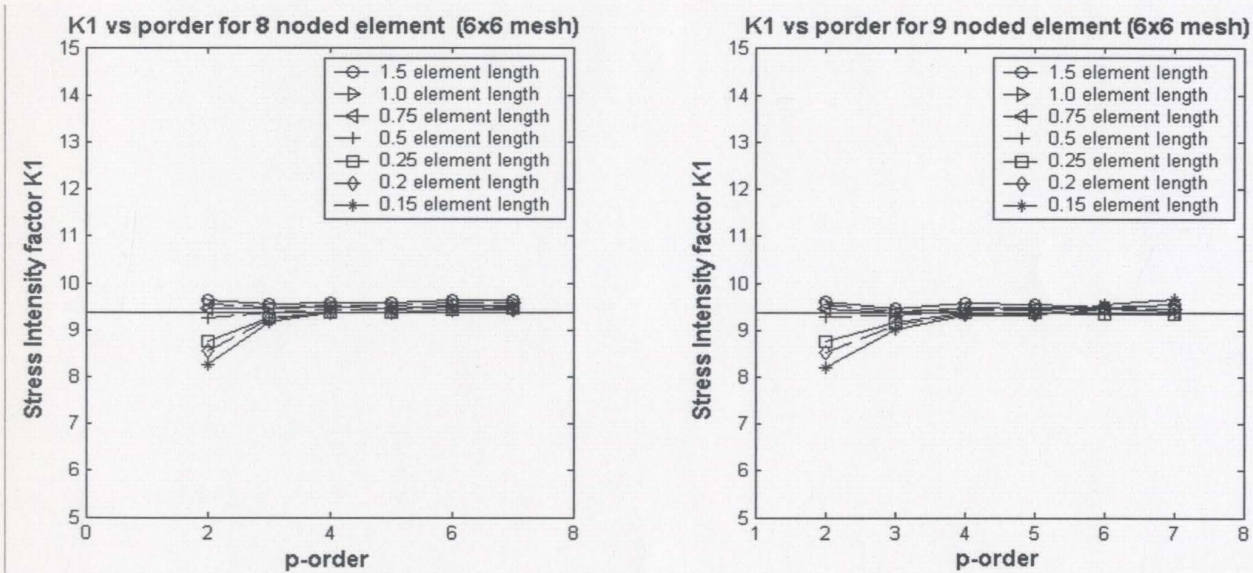


Figure 5.1.3: K_I vs. p-order comparison for 8 noded and 9 noded 6x6 meshes.

Sl	Crack length 'a'	Element length (inches)	8 Noded Element		9 Noded Element	
			$K_I(\text{psi}\sqrt{\text{in}})$	$K_I(\text{psi}\sqrt{\text{in}})$	$K_I(\text{psi}\sqrt{\text{in}})$	$K_I(\text{psi}\sqrt{\text{in}})$
			4x4 Mesh	6x6 mesh	4x4 mesh	6x6 mesh
1	0.5	0.2	1.35	1.378	1.37	1.374
2	1	0.2	2.11	2.118	2.15	2.126
3	1.5	0.2	2.96	2.933	3.04	2.939
4	2.0	0.2	3.98	3.929	4.13	3.925
5	2.5	0.2	5.29	5.21	5.55	5.19
6	3.0	0.2	7.06	6.922	7.44	6.882
7	3.5	0.2	9.51	9.372	10.07	9.348
8	4.0	0.2	13.08	12.877	13.90	12.836
9	4.5	0.2	18.60	12.94	19.77	12.92

Table 5.1.13: Stress intensity factors for varying crack lengths.

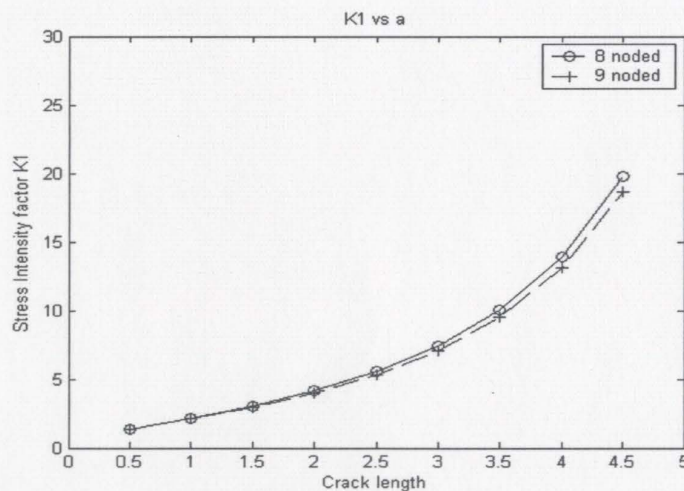


Figure: 5.1.4 K_I vs. crack length 'a' for element length of 0.2 at crack tip for 4x4 mesh

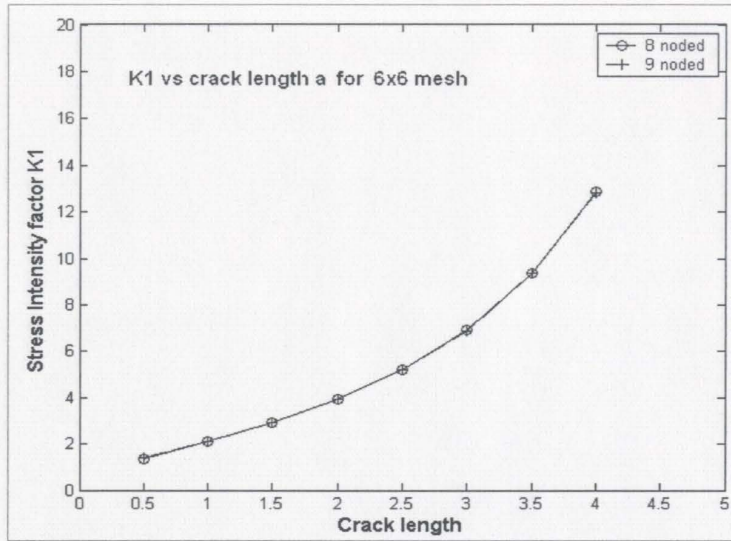


Figure 5.1.5 K_I vs. crack length 'a' for element length of 0.2 at crack tip for 6x6 mesh

The table 5.1.12 gives the values of the stress intensity factors for a constant element length of 0.2 and crack length varying from 0.5 to 4.5 and the graph is plotted in the figure 5.1.5 for various values of crack length 'a' and stress intensity factor K_I using 8 noded and 9 noded element.

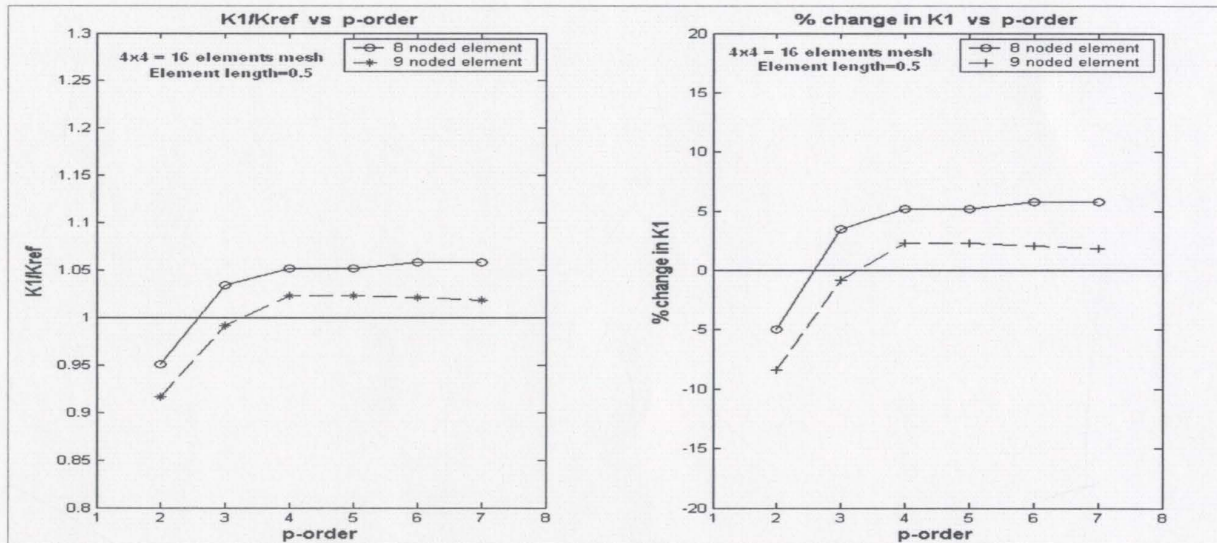


Figure: 5.1.6 Comparison of K_I / K_{ref} vs. p-order and percent change in K_I vs. p-order for 4x4 mesh for 8 noded and 9 noded element.

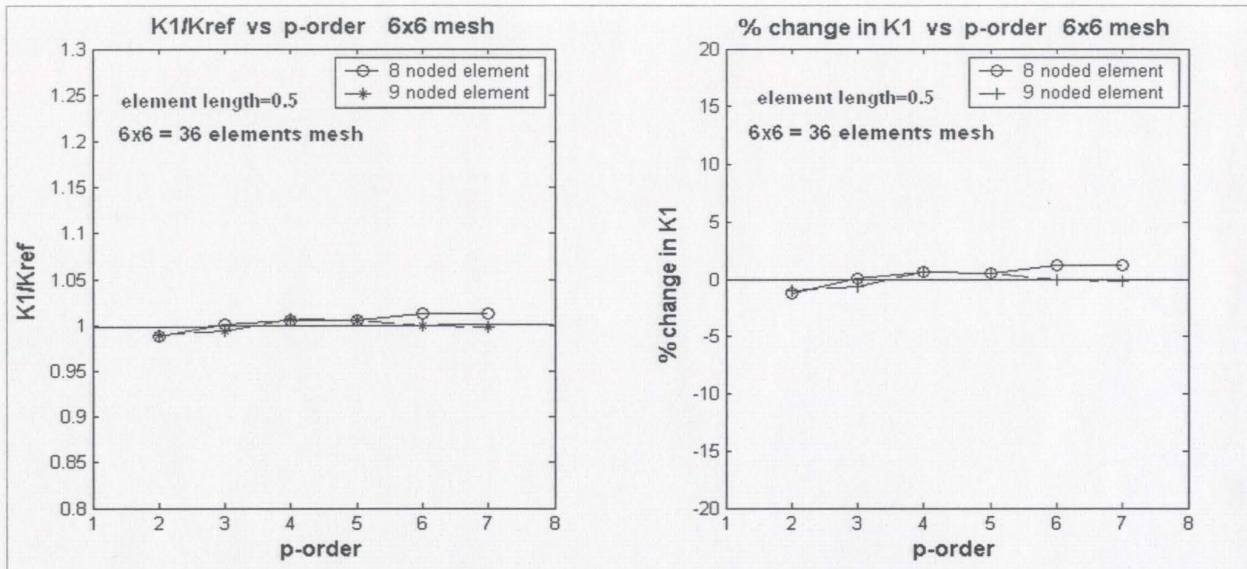


Figure: 5.1.7 Comparison of K_I/K_{ref} vs. p-order and % change in K_I vs. p-order for 6x6 mesh for 8-noded and 9-noded element.

Discussions:

The results obtained in the present analyses are presented in tables 5.1.1 to 5.1.12 for various crack lengths, crack tip, element lengths, orders etc. It is found that the results obtained by using 9 noded elements were closer to the analytical value and percentage change in the value of K_I is less than 1 % with 9 noded elements and less than 2% with 8 noded elements. The number of elements used in this analyses were 16 elements for 4x4 mesh and 36 elements for 6x6 mesh. The mesh density is very small when compared with Huang et al. [26], for the same type of problem with 50x100=5000 elements for structured mesh and Moes et al. [23] where they have used 2501 to 2541 degrees of freedom. As it can be seen from the figure 5.1.2 and 5.1.3 the curves plotted for K_I vs. p-order tends to converge more for a 6x6 mesh compared to 4x4 mesh indicating that a very little denser mesh gives very accurate results.

Example 2: A plate with an edge crack subjected to shear load:

As a second example, a plate with a crack under shear loads is modeled. The modal geometry is shown in the figure 5.2.1 One end of the plate is constrained and the other end is loaded with shear load as shown in figure. The material is assumed to be isotropic and the dimensions of the plate are height L , width $2W$ and crack length of $2a$. The modulus of elasticity for the plate is 30×10^6 psi. and the Poisson's ratio of 0.3.

Stress intensity factors are calculated for the problem and then compared with the bench mark values given by Moes et al. [23] of $K_I=34$ and $K_{II}= 4.55$. Figure 5.2.2 and 5.2.3 gives the mesh discretization used in the present analyses and the mesh used by Moes et al.

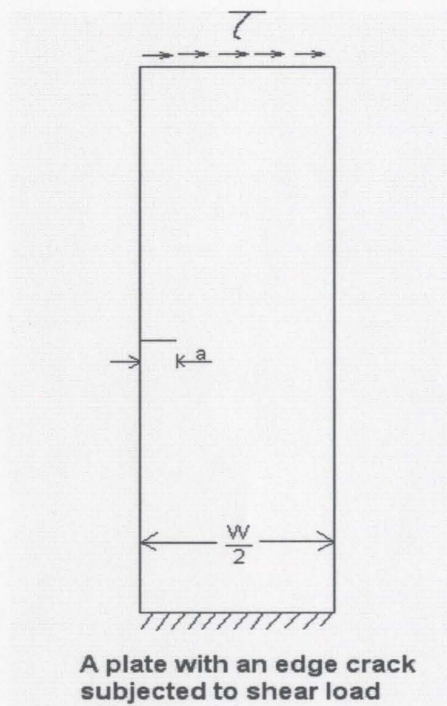


Figure 5.2.1: A plate with an edge crack in shear plate in shear

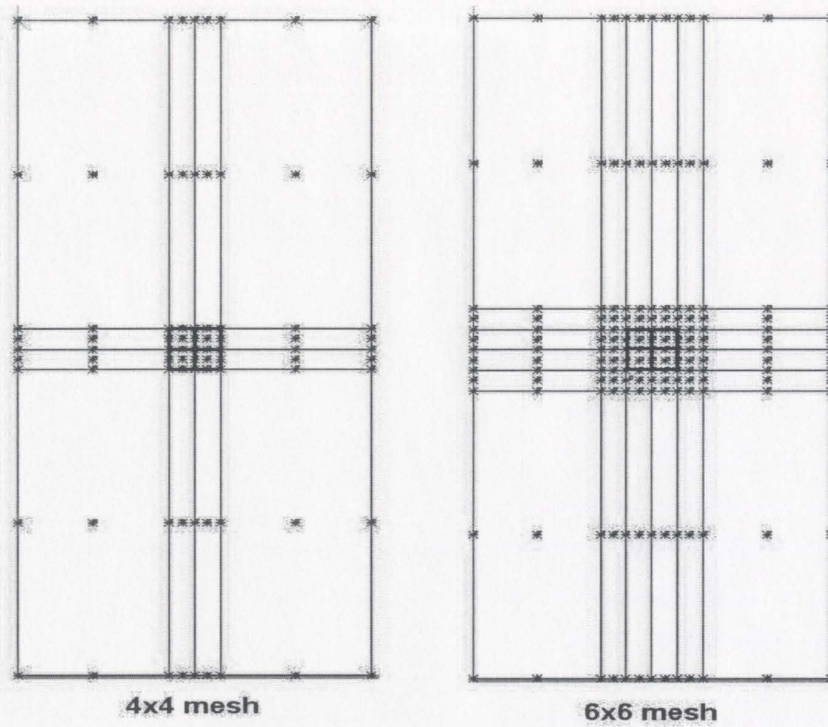


Figure 5.2.2 Mesh discretization used in the present analysis.

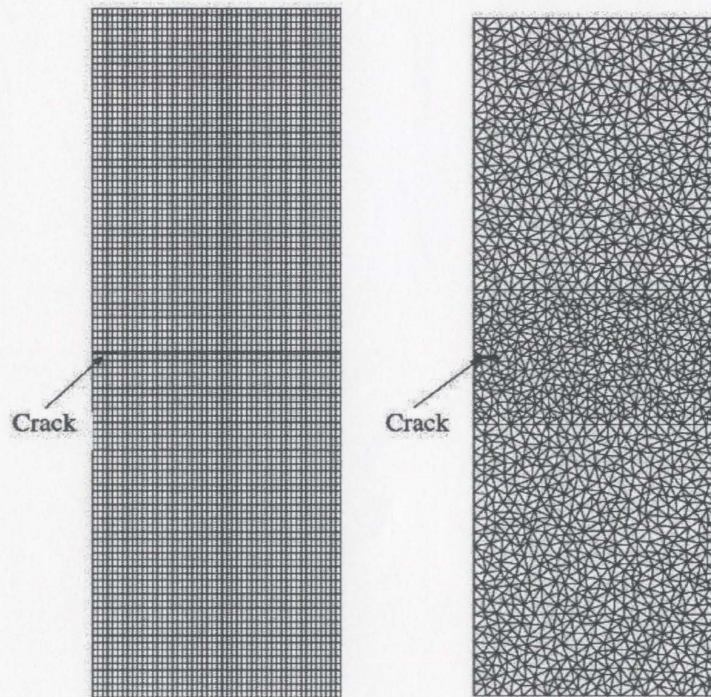


Figure 5.2.3 Mesh discretization used by Moes et al. [23]

The number of elements used [23] are nearly $24 \times 48 = 1152$ elements for structured mesh and $25 \times 49 = 1225$ elements for unstructured mesh as shown in figure 5.2.3 and in the present analyses only $4 \times 4 = 16$ elements and $6 \times 6 = 36$ elements were used and the results are obtained with less than 1 % error for polynomial order 4.

Table's 5.2.2 to 5.2.11 gives the values obtained for the two mesh discretizations for various crack element lengths used in this example.

p-order	Element length (inches)	8 Noded Element ($psi\sqrt{in}$)				9 Noded Element ($psi\sqrt{in}$)			
		K_I 4x4 mesh	K_{II} 4x4 mesh	K_I 6x6 mesh	K_{II} 6x6 mesh	K_I 4x4 mesh	K_{II} 4x4 mesh	K_I 6x6 mesh	K_{II} 6x6 mesh
2	0.005	7.64	0.755	10.43	1.01	6.83	1.31	9.88	1.81
3	0.005	12.42	1.728	16.58	2.25	10.76	1.70	15.35	2.51
4	0.005	14.98	1.745	19.78	2.25	9.53	1.72	12.95	2.50
5	0.005	17.74	1.684	23.39	2.30	14.26	1.94	21.32	3.12
6	0.005	24.22	2.063	29.86	2.69	4.35	0.72	5.55	1.03
7	0.005	28.21	2.269	32.83	2.97	12.37	1.43	15.06	2.23

Table 5.2.1 SIF values for 4x4 and 6x6 meshes with element length 0.005

p-order	Element length (inches)	8 Noded Element ($psi\sqrt{in}$)				9 Noded Element ($psi\sqrt{in}$)			
		K_I 4x4 mesh	K_{II} 4x4 mesh	K_I 6x6 mesh	K_{II} 6x6 mesh	K_I 4x4 mesh	K_{II} 4x4 mesh	K_I 6x6 mesh	K_{II} 6x6 mesh
2	0.01	10.64	1.035	14.18	1.39	9.5	1.76	13.47	2.34
3	0.01	17.24	2.147	22.03	2.75	15.41	2.31	20.78	3.29
4	0.01	20.46	2.130	25.29	2.70	14.17	2.41	19.81	3.52
5	0.01	24.26	2.115	30.00	3.15	22.34	2.76	29.76	3.96
6	0.01	30.92	2.459	35.47	3.47	6.439	1.03	8.19	1.46
7	0.01	34.02	2.725	36.05	3.5	17.24	2.10	21.53	3.28

Table 5.2.2 SIF values for 4x4 and 6x6 meshes with element length 0.01

p-order	Element length (inches)	8 Noded Element ($psi\sqrt{in}$)				9 Noded Element ($psi\sqrt{in}$)			
		K_I 4x4 mesh	K_{II} 4x4 mesh	K_I 6x6 mesh	K_{II} 6x6 mesh	K_I 4x4 mesh	K_{II} 4x4 mesh	K_I 6x6 mesh	K_{II} 6x6 mesh
2	0.05	20.52	2.07	28.10	3.16	18.56	2.95	27.64	3.7
3	0.05	29.77	3.16	33.15	4.16	27.17	3.709	32.43	4.68
4	0.05	33.07	3.07	34.5	4.23	34.06	4.31	33.44	4.72
5	0.05	36.63	3.32	34.67	4.31	34.23	3.77	33.83	4.824
6	0.05	38.76	3.57	34.85	4.37	19.57	2.81	29.06	4.927
7	0.05	39.09	3.72	34.81	4.37	31.78	4.29	32.63	5.347

Table 5.2.3 SIF values for 4x4 and 6x6 meshes with element length 0.05

p-order	Element length (inches)	8 Noded Element ($psi\sqrt{in}$)				9 Noded Element ($psi\sqrt{in}$)			
		K_I 4x4 mesh	K_{II} 4x4 mesh	K_I 6x6 mesh	K_{II} 6x6 mesh	K_I 4x4 mesh	K_{II} 4x4 mesh	K_I 6x6 mesh	K_{II} 6x6 mesh
2	0.1	25.07	2.64	28.11	3.16	22.97	3.34	27.64	3.7
3	0.1	33.2	3.63	33.15	4.16	30.68	4.10	32.43	4.68
4	0.1	36.14	3.63	34.5	4.23	33.68	4.06	33.44	4.72
5	0.1	37.95	3.86	34.67	4.31	34.07	4.15	33.83	4.82
6	0.1	38.26	4.01	34.85	4.37	29.02	4.24	29.06	4.92
7	0.1	38.07	4.03	34.81	4.37	33.23	4.72	32.64	5.34

Table 5.2.4 SIF values for 4x4 and 6x6 meshes with element length 0.1

p-order	Element length (inches)	8 Noded Element ($psi\sqrt{in}$)				9 Noded Element ($psi\sqrt{in}$)			
		K_I 4x4 mesh	K_{II} 4x4 mesh	K_I 6x6 mesh	K_{II} 6x6 mesh	K_I 4x4 mesh	K_{II} 4x4 mesh	K_I 6x6 mesh	K_{II} 6x6 mesh
2	0.15	27.38	2.98	29.79	3.48	25.33	3.52	29.49	3.87
3	0.15	34.4	3.88	33.56	4.35	32.03	4.27	33.01	4.75
4	0.15	36.8	3.87	34.23	4.37	33.75	4.28	33.75	4.83
5	0.15	37.21	4.11	34.43	4.45	34.53	4.43	35.9	4.88
6	0.15	37.61	4.15	34.55	4.51	31.09	4.66	29.98	5.13
7	0.15	37.6	4.22	34.52	4.50	33.34	4.81	31.80	5.17

Table 5.2.5 SIF values for 4x4 and 6x6 meshes with element length 0.15

p-order	Element length (inches)	8 Noded Element ($\psi\sqrt{in}$)				9 Noded Element ($\psi\sqrt{in}$)			
		K_I 4x4 mesh	K_{II} 4x4 mesh	K_I 6x6 mesh	K_{II} 6x6 mesh	K_I 4x4 mesh	K_{II} 4x4 mesh	K_I 6x6 mesh	K_{II} 6x6 mesh
2	0.2	28.82	3.2	30.84	3.71	26.86	3.64	30.64	4.0
3	0.2	34.95	4.05	33.76	4.46	32.72	4.38	33.31	4.79
4	0.2	36.7	4.09	34.25	4.51	34.2	4.47	33.95	4.86
5	0.2	37.02	4.22	34.34	4.52	34.74	4.57	34.01	4.91
6	0.2	37.2	4.29	34.51	4.58	31.87	4.88	30.14	5.15
7	0.2	37.25	4.31	34.55	4.55	33.19	4.87	31.92	5.16

Table 5.2.6 SIF values for 4x4 and 6x6 meshes with element length 0.2

p-order	Element length (inches)	8 Noded Element ($\psi\sqrt{in}$)				9 Noded Element ($\psi\sqrt{in}$)			
		K_I 4x4 mesh	K_{II} 4x4 mesh	K_I 6x6 mesh	K_{II} 6x6 mesh	K_I 4x4 mesh	K_{II} 4x4 mesh	K_I 6x6 mesh	K_{II} 6x6 mesh
2	0.25	29.81	3.39	31.58	3.88	27.95	3.73	31.45	4.10
3	0.25	35.24	4.16	33.89	4.54	33.13	4.45	33.49	4.80
4	0.25	36.44	4.23	34.3	4.58	34.47	4.57	34.11	4.87
5	0.25	36.8	4.31	34.3	4.60	34.8	4.66	34.131	4.91
6	0.25	36.97	4.39	34.53	4.62	32.17	5.01	31.22	5.27
7	0.25	37.0	4.38	34.54	4.6	33.10	4.91	32.41	5.21

Table 5.2.7 SIF values for 4x4 and 6x6 meshes with element length 0.25

p-order	Element length (inches)	8 Noded Element ($\psi\sqrt{in}$)				9 Noded Element ($\psi\sqrt{in}$)			
		K_I 4x4 mesh	K_{II} 4x4 mesh	K_I 6x6 mesh	K_{II} 6x6 mesh	K_I 4x4 mesh	K_{II} 4x4 mesh	K_I 6x6 mesh	K_{II} 6x6 mesh
2	0.5	32.32	3.92	33.59	4.34	30.89	4.05	33.51	4.41
3	0.5	35.67	4.46	34.33	4.69	34.01	4.657	33.98	4.8
4	0.5	36.27	4.5	34.55	4.72	34.99	4.75	34.49	4.87
5	0.5	36.28	4.57	34.53	4.72	35.04	4.80	34.45	4.89
6	0.5	36.47	4.57	34.75	4.74	32.49	5.01	32.49	5.1
7	0.5	36.48	4.57	34.77	4.75	33.45	5.0	33.09	5.04

Table 5.2.8 SIF values for 4x4 and 6x6 meshes with element length 0.5

p-order	Element length (inches)	8 Noded Element ($\psi\sqrt{in}$)				9 Noded Element ($\psi\sqrt{in}$)			
		K_I 4x4 mesh	K_{II} 4x4 mesh	K_I 6x6 mesh	K_{II} 6x6 mesh	K_I 4x4 mesh	K_{II} 4x4 mesh	K_I 6x6 mesh	K_{II} 6x6 mesh
2	0.75	33.5	4.21	34.49	4.49	32.38	4.24	34.34	4.53
3	0.75	35.26	4.59	34.65	4.72	34.8	4.72	34.27	4.78
4	0.75	36.14	4.639	34.82	4.75	35.21	4.79	34.77	4.85
5	0.75	36.14	4.659	34.79	4.78	35.22	4.82	34.73	4.87
6	0.75	36.32	4.672	34.99	4.77	33.42	5.05	34.23	5.06
7	0.75	36.34	4.673	35.01	4.77	34.01	4.98	34.54	4.94

Table 5.2.9 SIF values for 4x4 and 6x6 meshes with element length 0.75

p-order	Element length (inches)	8 Noded Element ($psi\sqrt{in}$)				9 Noded Element ($psi\sqrt{in}$)			
		K _I 4x4 mesh	K _{II} 4x4 mesh	K _I 6x6 mesh	K _{II} 6x6 mesh	K _I 4x4 mesh	K _{II} 4x4 mesh	K _I 6x6 mesh	K _{II} 6x6 mesh
2	1	34.25	4.4	34.99	4.54	33.28	4.36	34.74	4.58
3	1	35.84	4.67	34.96	4.72	34.63	4.74	34.5	4.76
4	1	36.14	4.72	35.09	4.76	35.28	4.80	34.99	4.85
5	1	36.13	4.73	35.06	4.76	35.36	4.82	34.97	4.86
6	1	36.29	4.75	35.25	4.78	34.27	4.95	34.65	4.95
7	1	36.33	4.75	35.25	4.78	34.78	4.91	34.83	4.93

Table 5.2.10 SIF values for 4x4 and 6x6 meshes with element length 1.0

p-order	Element length (inches)	8 Noded Element ($psi\sqrt{in}$)				9 Noded Element ($psi\sqrt{in}$)			
		K _I 4x4 mesh	K _{II} 4x4 mesh	K _I 6x6 mesh	K _{II} 6x6 mesh	K _I 4x4 mesh	K _{II} 4x4 mesh	K _I 6x6 mesh	K _{II} 6x6 mesh
2	1.5	35.20	4.61	35.5	4.56	34.41	4.48	35.10	4.59
3	1.5	36.06	4.77	35.48	4.71	35.11	4.71	34.96	4.79
4	1.5	36.3	4.86	35.63	4.78	35.72	4.8	35.49	4.83
5	1.5	36.29	4.85	35.63	4.78	35.72	4.81	35.46	4.85
6	1.5	36.43	4.86	35.77	4.78	35.34	4.87	35	4.91
7	1.5	36.45	4.87	35.78	4.78	35.32	4.87	35.22	4.91

Table 5.2.11 SIF values for 4x4 and 6x6 meshes with element length 1.5

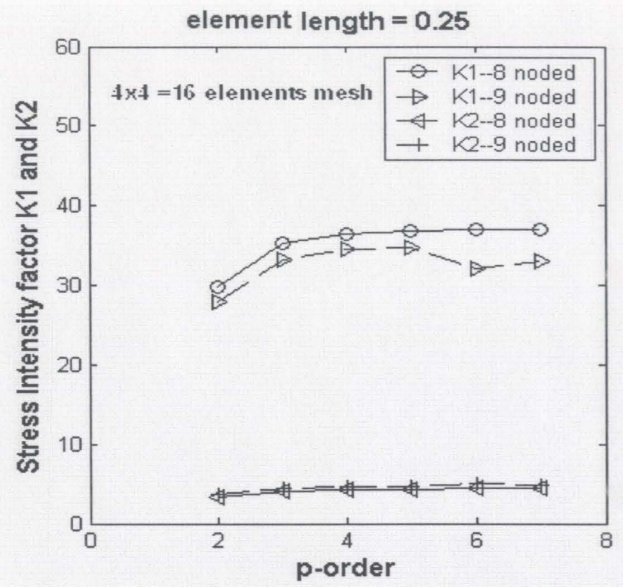
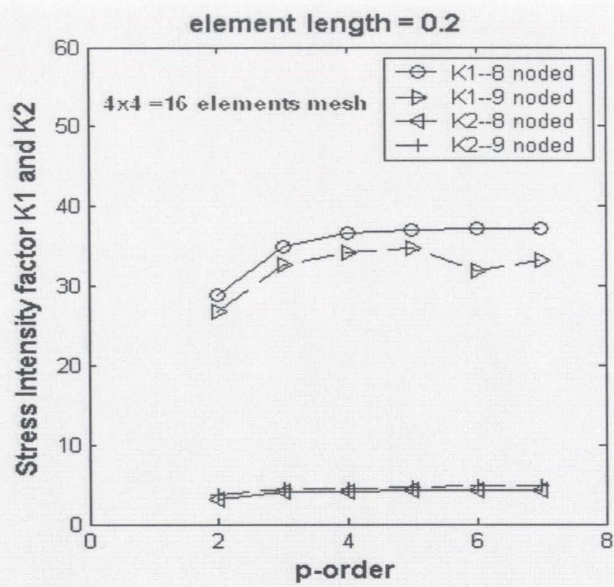


Figure 5.2.4: K_I , K_{II} vs. p-order for element length at crack tip 0.2 and 0.25 (4x4 mesh)

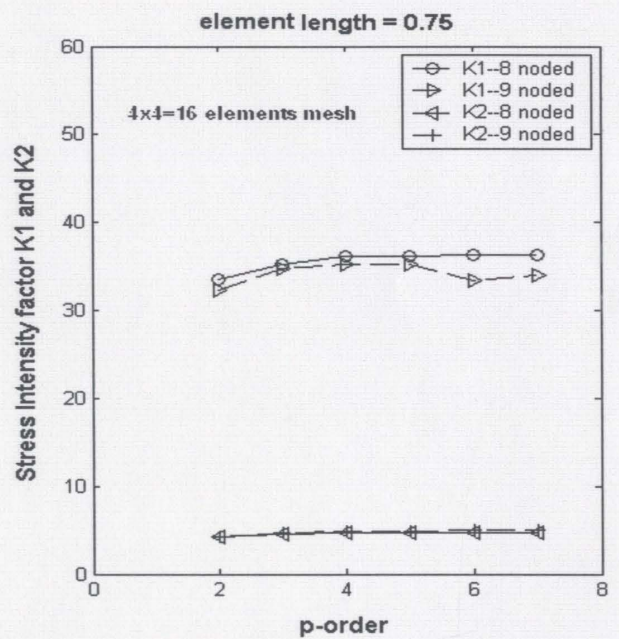
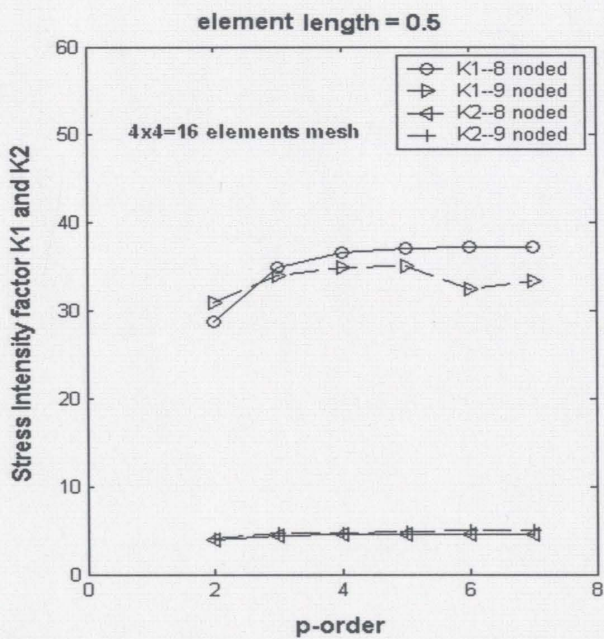


Figure 5.2.5: K_I , K_{II} vs. p-order for element length at crack tip 0.5 and 0.75 (4x4 mesh)

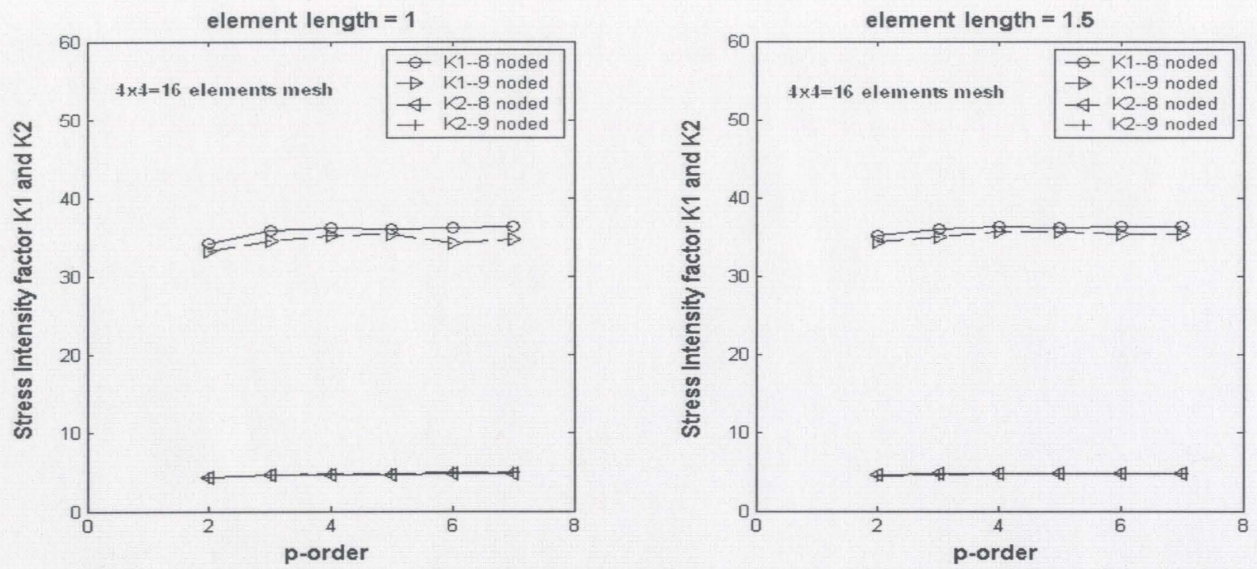


Figure 5.2.6: K_I , K_{II} vs. p-order for element length at crack tip 1 and 1.5 (4x4 mesh)

Sl	Crack length a	Element length (inches)	8 Noded Element ($psi\sqrt{in}$)				9 Noded Element ($psi\sqrt{in}$)			
			K_I	K_{II}	K_I	K_{II}	K_I	K_{II}	K_I	K_{II}
1	1	0.2	12.28	0.35	--	--	9.4	1.07	--	--
2	1.5	0.2	15.7	0.92	10.6	0.98	15.99	1.88	12.15	0.7
3	2.0	0.2	19.51	1.64	14.7	1.65	18.32	2.28	15.25	1.3
4	2.5	0.2	24.02	2.47	18.9	2.75	22.38	2.91	18.77	2.04
5	3.0	0.2	29.53	3.28	27.1	3.32	27.49	3.63	22.6	2.84
6	3.5	0.2	36.7	4.09	33.9	4.04	34.2	4.47	27.48	3.64
7	4.0	0.2	46.58	5.02	43	4.86	43.76	5.31	34.25	4.52
8	4.5	0.2	61.05	6.00	43.9	5.73	57.7	6.16	43.42	5.4

Table. 5.2.12: Crack length vs. K_I and K_{II} for 8 and 9 noded elements.

The element length of 0.2 at the crack tip was taken and the crack length is varied to see the behaviour of results for 4x4 mesh density and they are given in table 5.2.12

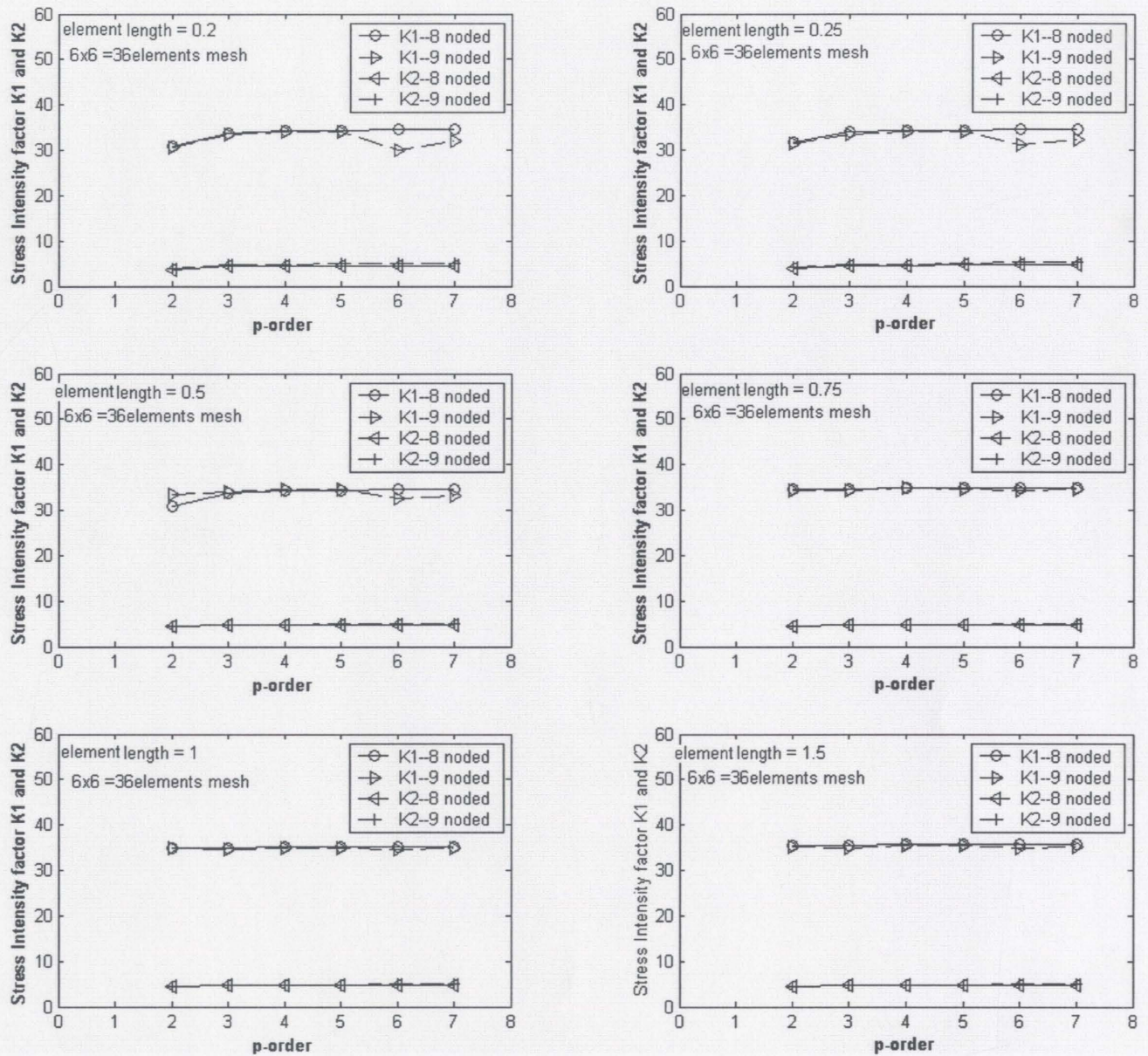


Figure 5.2.7: K_I , K_{II} vs. p-order for element length at crack tip varying from 0.2 to 1.5 for(6x6 mesh)

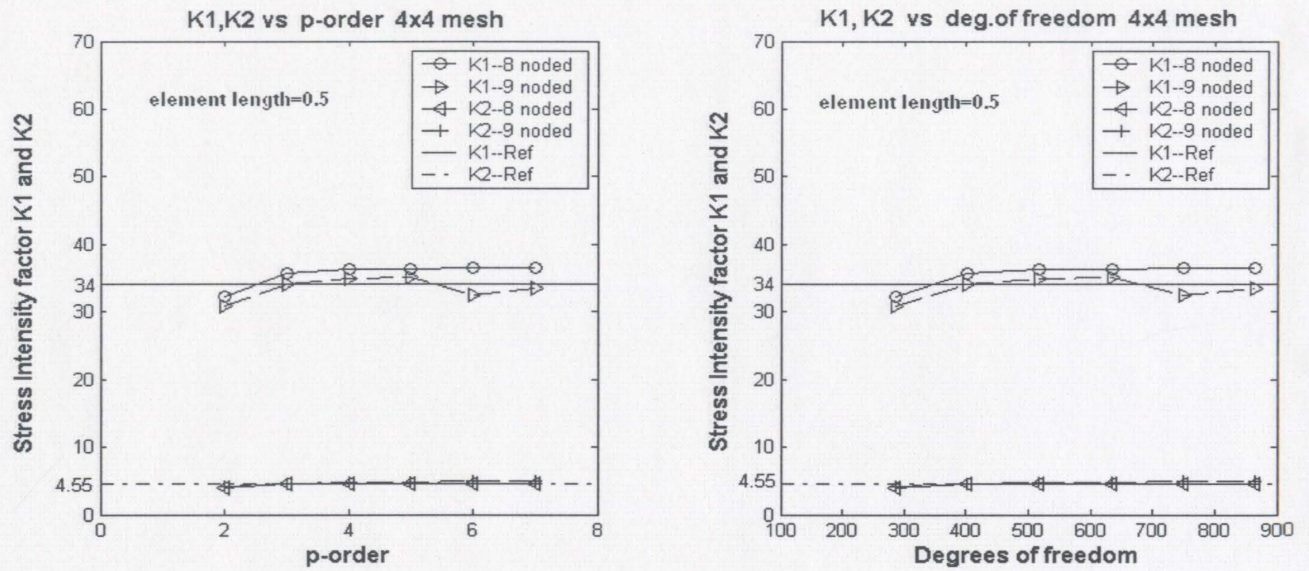


Figure 5.2.8 K_I , K_{II} vs. p-order and degrees of freedom (4x4 mesh)

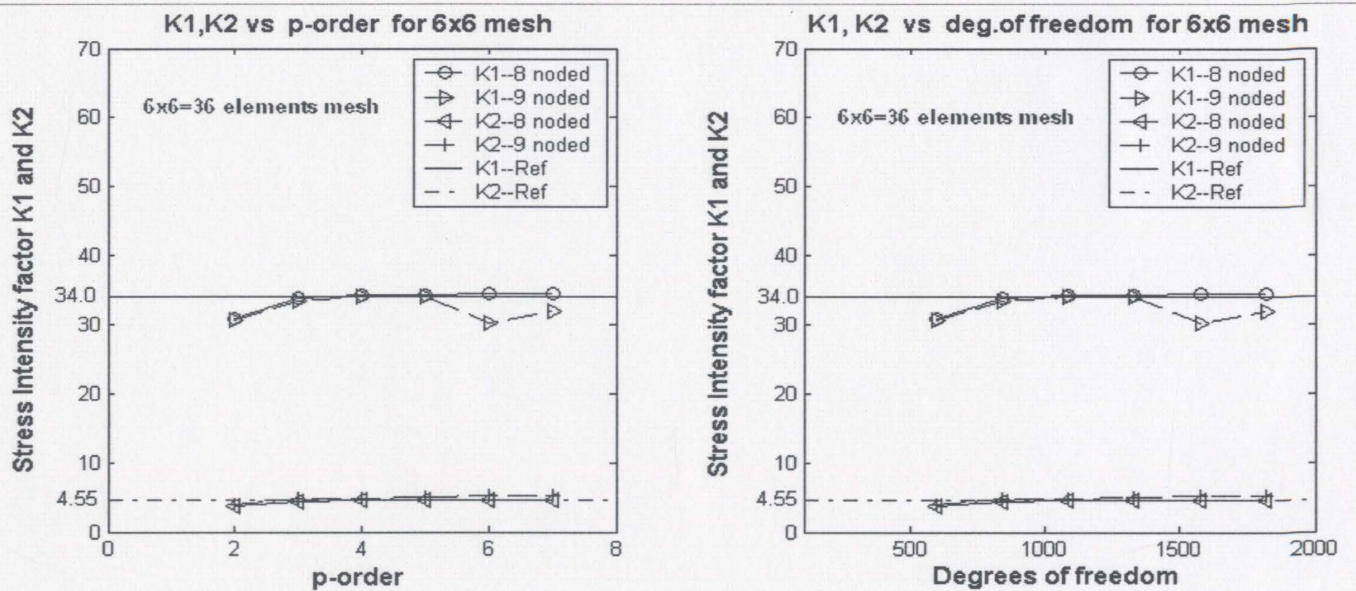


Figure. 5.2.9 K_I , K_{II} vs. p-order and degrees of freedom (6x6 mesh)

The figure 5.2.10 shows the relation between K_I and K_{II} vs. different crack lengths for 8 noded and 9 noded elements and as the crack length is increasing the stress intensity factors are also increasing.

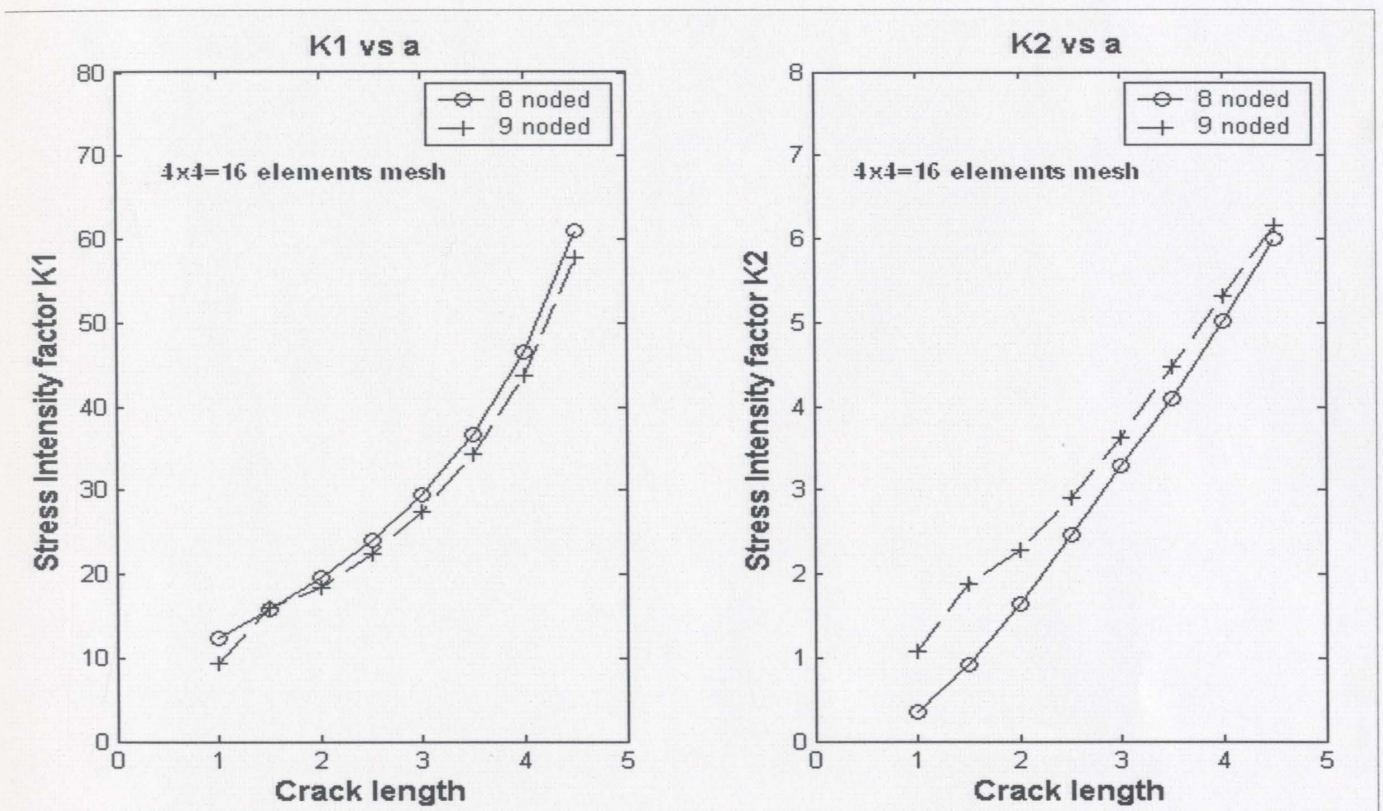


Figure 5.2.10: K_I , K_{II} vs. crack length (4x4 mesh)

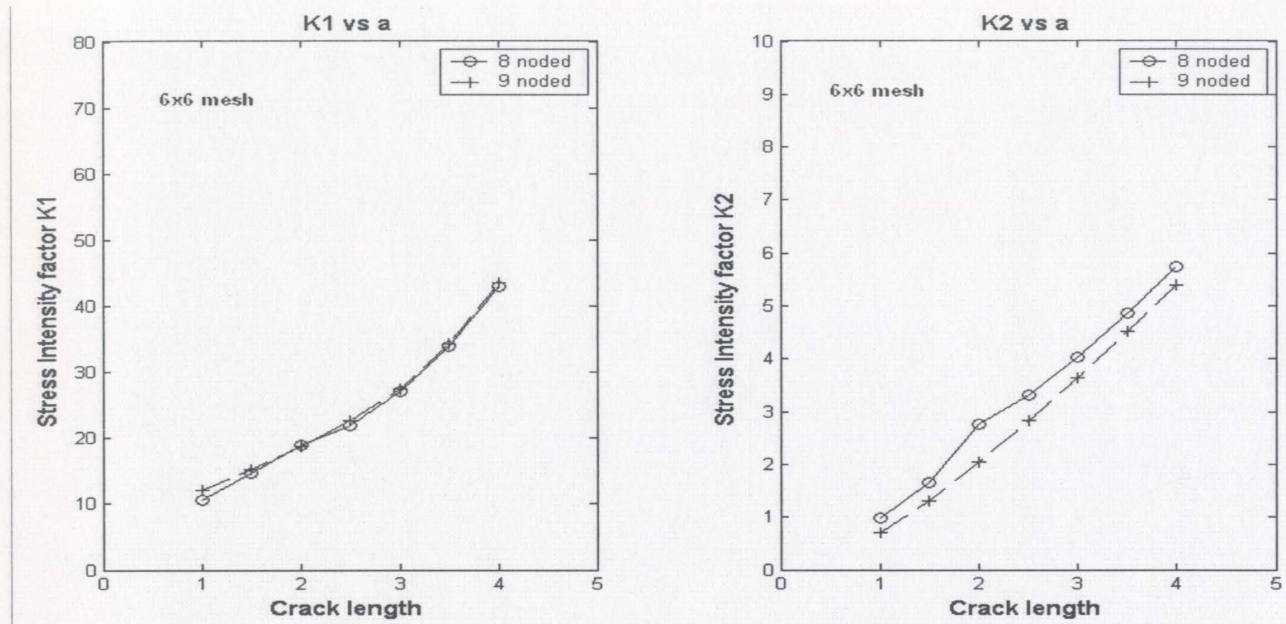


Figure 5.2.11: K_I , K_{II} vs. crack length (6x6 mesh)

Discussion:

The results for the edge shear crack indicate that they are in perfect comparison with the bench mark values and also the accuracy increases with a very small increase in the mesh discretization. The number of elements used by Moes et al. [23] were 1152 for structured mesh and 1225 for the unstructured mesh. The elements used in this analysis are 16 and 36, but the results obtained are accurate for 5th order polynomial itself. The results indicate that the results of significant accuracy can be obtained by increasing the polynomial and which can be done with a lot more convenience than increasing the mesh size or remeshing etc.

Example 3: Plate with Inclined crack in tension

The stress intensity factors are calculated for the plate with a 45 degrees inclined crack in tension and as shown in the figure 5.3.1 it is subjected to uniaxial stress. The geometry of the problem and different finite element idealizations with corresponding results are shown in the subsequent paragraphs. The reference values for the problem are taken from the values provided by Gifford and Hilton [18] and they considered for various idealizations taking a reference value of $K_1=1.86$ and $K_2=0.88$. The plate is considered to be isotropic and the values of Young's modulus of elasticity and Poisson's ratio are 30×10^6 and 0.3 respectively.

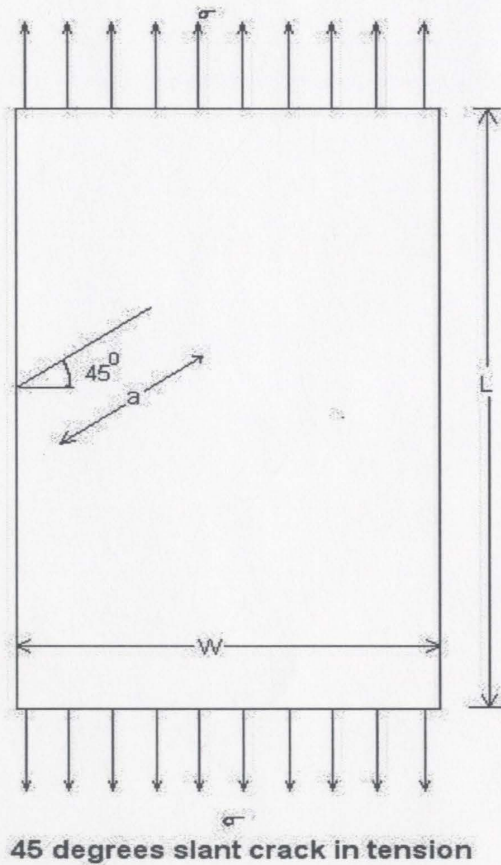


Figure 5.3.1 Plate with inclined crack in tension.

The plate is of width 'W', height 'h' and the length of the crack 'a' with an inclined angle of 45 degrees to the vertical edge of the plate. Although this program can be applied to any angle crack, it is only considered for an angle of 45 degrees to compare with previously published results. The width of 2.5 in and height of 5 in plate is taken for analysis. Different sizes of elements and mesh densities are shown in the figure Crack tip elements are marked in the figure 5.3.2. The numerical results obtained for various mesh descriptions and different lengths of crack tip elements are presented in tables 5.3.1 to 5.3.12 and in figures 5.3.3 to 5.3.6.

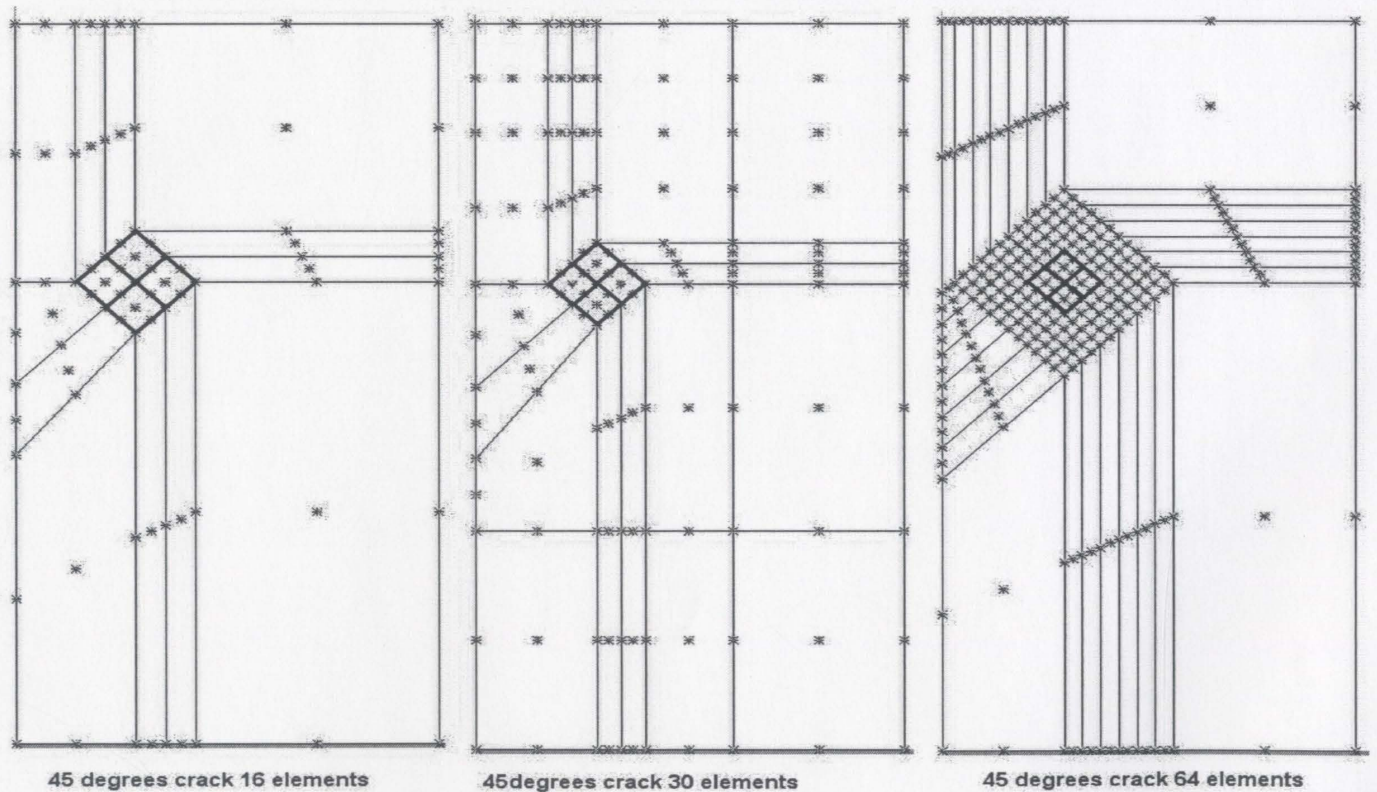


Figure:5.3.2 : Types of meshes used in the analysis.

p-order	Element length (inches)	No. of Elements	8 Noded Element		9 Noded Element	
			K_I ($psi\sqrt{in}$)	K_{II} ($psi\sqrt{in}$)	K_I ($psi\sqrt{in}$)	K_{II} ($psi\sqrt{in}$)
2	0.4	16	1.815	0.74	1.72	0.772
3	0.4	16	1.908	0.73	1.82	0.75
4	0.4	16	1.938	0.769	1.885	0.806
5	0.4	16	1.937	0.776	1.886	0.815
6	0.4	16	1.950	0.769	1.847	0.811
7	0.4	16	1.952	0.769	1.853	0.814

Table 5.3.1: SIFs for element length 0.4 in a plate with inclined crack.

p-order	Element length (inches)	No. of Elements	8 Noded Element		9 Noded Element	
			K_I ($psi\sqrt{in}$)	K_{II} ($psi\sqrt{in}$)	K_I ($psi\sqrt{in}$)	K_{II} ($psi\sqrt{in}$)
2	0.3	16	1.781	0.724	1.688	0.752
3	0.3	16	1.899	0.707	1.807	0.713
4	0.3	16	1.93	0.748	1.876	0.771
5	0.3	16	1.93	0.757	1.877	0.782
6	0.3	16	1.946	0.751	1.831	0.778
7	0.3	16	1.947	0.751	1.809	0.774

Table 5.3.2: SIFs for element length 0.3 in a plate with inclined crack.

p-order	Element length (inches)	No. of Elements	8 Noded Element		9 Noded Element	
			K_I ($psi\sqrt{in}$)	K_{II} ($psi\sqrt{in}$)	K_I ($psi\sqrt{in}$)	K_{II} ($psi\sqrt{in}$)
2	0.25	16	1.754	0.712	1.657	0.739
3	0.25	16	1.891	0.696	1.793	0.695
4	0.25	16	1.93	0.737	1.866	0.752
5	0.25	16	1.93	0.747	1.868	0.764
6	0.25	16	1.94	0.741	1.834	0.760
7	0.25	16	1.94	0.743	1.80	0.751

Table 5.3.3: SIFs for element length 0.25 in a plate with inclined crack.

p-order	Element length (inches)	No. of Elements	8 Noded Element		9 Noded Element	
			K_I ($psi\sqrt{in}$)	K_{II} ($psi\sqrt{in}$)	K_I ($psi\sqrt{in}$)	K_{II} ($psi\sqrt{in}$)
2	0.2	16	1.714	0.696	1.613	0.72
3	0.2	16	1.877	0.682	1.770	0.674
4	0.2	16	1.925	0.724	1.851	0.732
5	0.2	16	1.927	0.736	1.856	0.743
6	0.2	16	1.942	0.73	1.820	0.743
7	0.2	16	1.943	0.73	1.808	0.737

Table 5.3.4: SIFs for element length 0.2 in a plate with inclined crack.

p-order	Element length (inches)	No. of Elements	8 Noded Element		9 Noded Element	
			K_I ($psi\sqrt{in}$)	K_{II} ($psi\sqrt{in}$)	K_I ($psi\sqrt{in}$)	K_{II} ($psi\sqrt{in}$)
2	0.15	16	1.65	0.669	1.545	0.689
3	0.15	16	1.849	0.663	1.732	0.647
4	0.15	16	1.91	0.707	1.824	0.706
5	0.15	16	1.92	0.719	1.834	0.716
6	0.15	16	1.937	0.715	1.691	0.703
7	0.15	16	1.937	0.717	1.436	0.667

Table 5.3.5: SIFs for element length 0.15 in a plate with inclined crack.

p-order	Element length (inches)	No. of Elements	8 Noded Element		9 Noded Element	
			K_I ($psi\sqrt{in}$)	K_{II} ($psi\sqrt{in}$)	K_I ($psi\sqrt{in}$)	K_{II} ($psi\sqrt{in}$)
2	0.10	16	1.54	0.62	1.43	0.63
3	0.10	16	1.78	0.630	1.66	0.599
4	0.10	16	1.88	0.68	1.76	0.667
5	0.10	16	1.90	0.69	1.78	0.544
6	0.10	16	1.92	0.69	1.46	0.687
7	0.10	16	1.92	0.69	1.20	0.609

Table 5.3.6: SIFs for element length 0.1 in a plate with inclined crack.

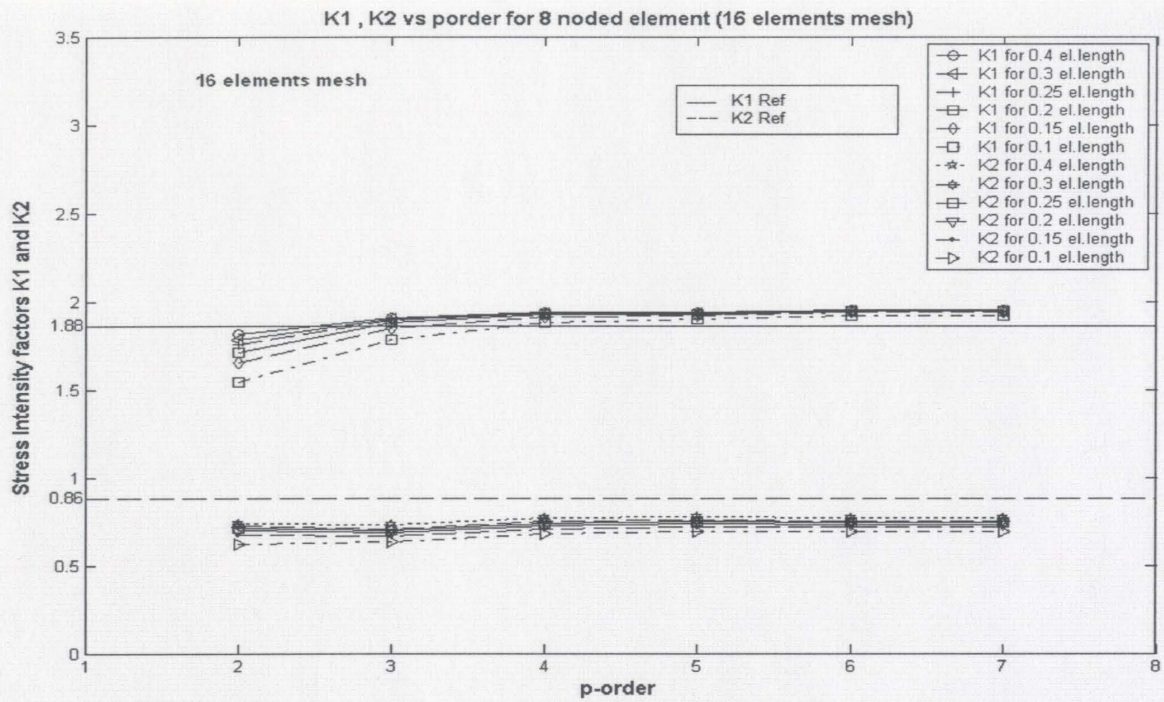


Figure 5.3.3 Stress intensity factors vs. p order for 8 noded elements (16 elements mesh)

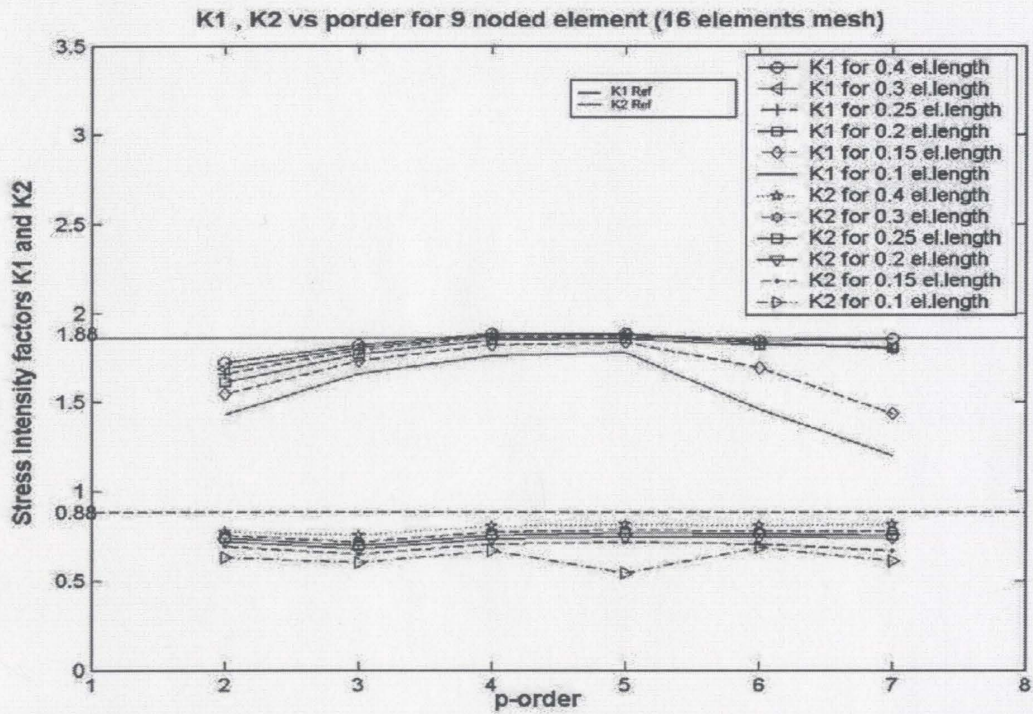


Figure 5.3.4 Stress Intensity factors vs. p order for 9 noded elements (16 elements mesh)

The following tables consist of the results for a 30 element mesh.

p-order	Element length (inches)	No. of Elements	8 Noded Element		9 Noded Element	
			K_I ($psi\sqrt{in}$)	K_{II} ($psi\sqrt{in}$)	K_I ($psi\sqrt{in}$)	K_{II} ($psi\sqrt{in}$)
2	0.25	30	1.882	0.739	1.807	0.762
3	0.25	30	1.915	0.733	1.843	0.765
4	0.25	30	1.933	0.771	1.89	0.790
5	0.25	30	1.930	0.776	1.888	0.797
6	0.25	30	1.944	0.769	1.871	0.794
7	0.25	30	1.944	0.769	1.870	0.791

Table 5.3.7: Mode I and Mode II SIFs for element length 0.25 in 30 elements mesh.

p-order	Element length (inches)	No. of Elements	8 Noded Element		9 Noded Element	
			K_I ($psi\sqrt{in}$)	K_{II} ($psi\sqrt{in}$)	K_I ($psi\sqrt{in}$)	K_{II} ($psi\sqrt{in}$)
2	0.2	30	1.875	0.72	1.792	0.754
3	0.2	30	1.92	0.723	1.838	0.722
4	0.2	30	1.938	0.763	1.884	0.779
5	0.2	30	1.935	0.769	1.882	0.787
6	0.2	30	1.948	0.762	1.895	0.788
7	0.2	30	1.95	0.763	1.886	0.783

Table 5.3.8: Mode I and Mode II SIFs for element length 0.2 in 30 elements mesh.

p-order	Element length (inches)	No. of Elements	8 Noded Element		9 Noded Element	
			K_I ($psi\sqrt{in}$)	K_{II} ($psi\sqrt{in}$)	K_I ($psi\sqrt{in}$)	K_{II} ($psi\sqrt{in}$)
2	0.15	30	1.85	0.721	1.76	0.745
3	0.15	30	1.925	0.712	1.825	0.709
4	0.15	30	1.946	0.752	1.872	0.766
5	0.15	30	1.943	0.760	1.872	0.776
6	0.15	30	1.956	0.754	1.789	0.765
7	0.15	30	1.958	0.756	1.765	0.751

Table 5.3.9: Mode I and Mode II SIFs for element length 0.15 in 30 elements mesh.

p-order	Element length (inches)	No. of Elements	8 Noded Element		9 Noded Element	
			K_I ($psi\sqrt{in}$)	K_{II} ($psi\sqrt{in}$)	K_I ($psi\sqrt{in}$)	K_{II} ($psi\sqrt{in}$)
2	0.1	30	1.80	0.696	1.69	0.724
3	0.1	30	1.92	0.692	1.79	0.688
4	0.1	30	1.955	0.733	1.83	0.748
5	0.1	30	1.953	0.742	1.82	0.748
6	0.1	30	1.969	0.737	1.86	0.375
7	0.1	30	1.973	0.739	1.8	0.65

Table 5.3.10: Mode I and Mode II SIFs for element length 0.1 in 30 elements mesh.

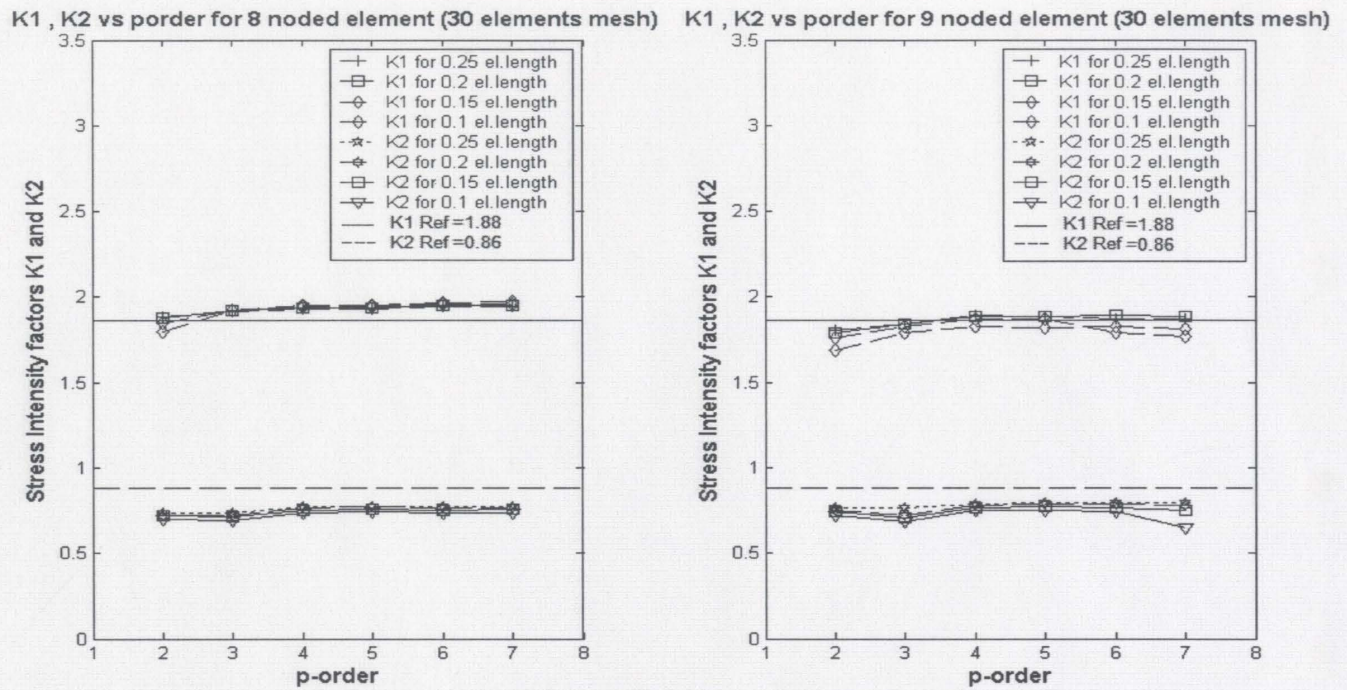


Figure 5.3.5 K_I, K_{II} vs. p-order for 8 and 9 noded elements(30 elements mesh)

p-order	Element length (inches)	No. of Elements	8 Noded Element		9 Noded Element	
			K_I ($psi\sqrt{in}$)	K_{II} ($psi\sqrt{in}$)	K_I ($psi\sqrt{in}$)	K_{II} ($psi\sqrt{in}$)
2	0.15	64	1.84	0.825	1.824	0.853
3	0.15	64	1.88	0.798	1.851	0.808
4	0.15	64	1.905	0.833	1.887	0.857
5	0.15	64	1.904	0.838	1.884	0.864
6	0.15	64	1.919	0.832	1.853	0.858
7	0.15	64	1.920	0.831	1.831	0.845

Table 5.3.11: Mode I and Mode II SIFs for element length 0.15 in 64 elements mesh.

p-order	Element length (inches)	No. of Elements	8 Noded Element		9 Noded Element	
			K_I ($psi\sqrt{in}$)	K_{II} ($psi\sqrt{in}$)	K_I ($psi\sqrt{in}$)	K_{II} ($psi\sqrt{in}$)
2	0.10	64	1.839	0.819	1.822	0.843
3	0.10	64	1.886	0.791	1.848	0.797
4	0.10	64	1.905	0.827	1.886	0.844
5	0.10	64	1.904	0.832	1.885	0.852
6	0.10	64	1.919	0.825	1.849	0.845
7	0.10	64	1.921	0.825	1.827	0.832

Table 5.3.12: Mode I and Mode II SIFs for element length 0.1 in 64 elements mesh.

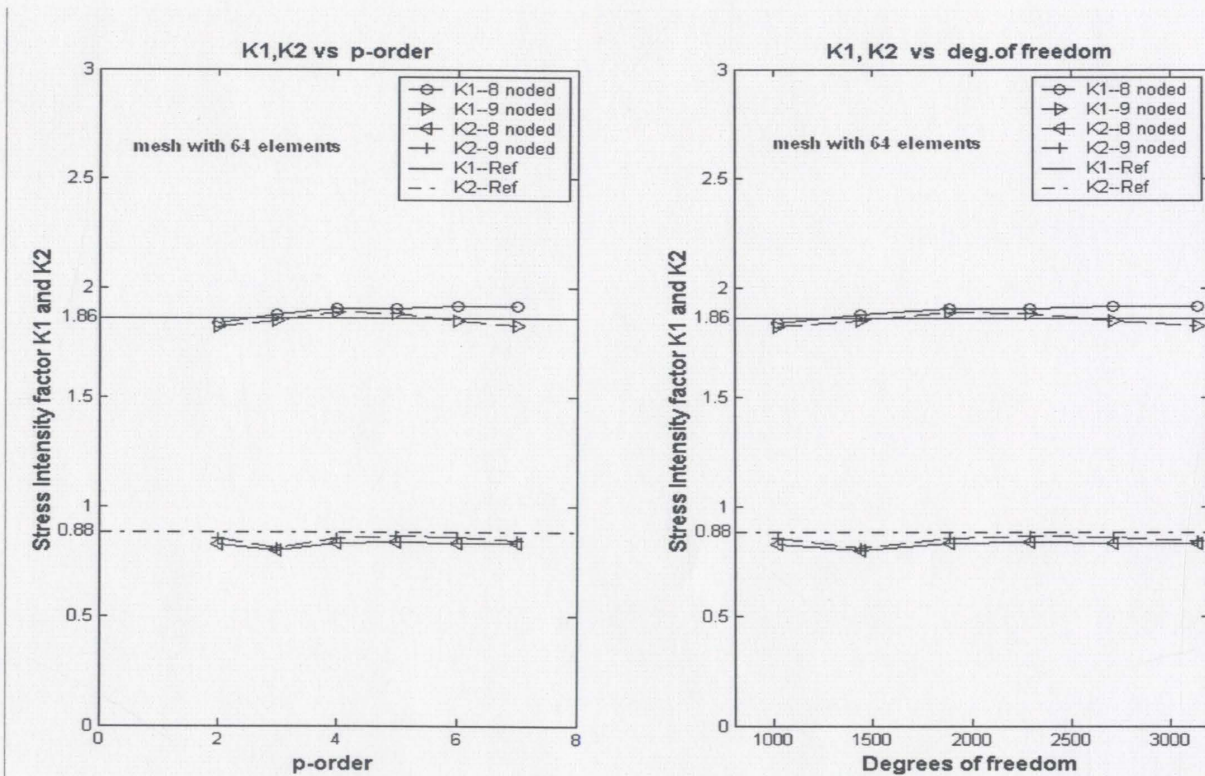


Figure 5.3.6 K_I, K_{II} vs p-order and K_I, K_{II} vs degrees of freedom

Discussion:

The inclined crack is at an angle of 45 degrees and when it is compared with the results obtained for the mesh with 16 elements, 30 elements and 64 elements the values of Mode I stress intensity factors for 64 elements has lesser error compared to the 30 elements and 16 elements. The value of Mode II stress intensity factor is less than the bench mark value in the 16 elements mesh and a little more improved in 30 elements mesh; still it gets more improved and very close to the reference values when 64 elements mesh is used which indicates that the mesh near the crack tip is increased, the results converge to the reference / analytical solution.

Example 4: Plate with an angled center crack

The plate with an angled center crack is also analyzed to illustrate the effectiveness and the versatility of the method and the formulation. The stress intensity factors K_1 and K_2 are calculated for the plate with the center crack with an angle ' β ' to the horizontal as shown in the figure 5.4.1. As a reference solution Moes et al. [23] was taken and results were interpolated.

The material is assumed to be isotropic and the value of $E=30e6$ psi and Poisson's ratio of 0.3 is taken. The dimensions of the plate considered are $W=10$ in width, crack length a of 1in .

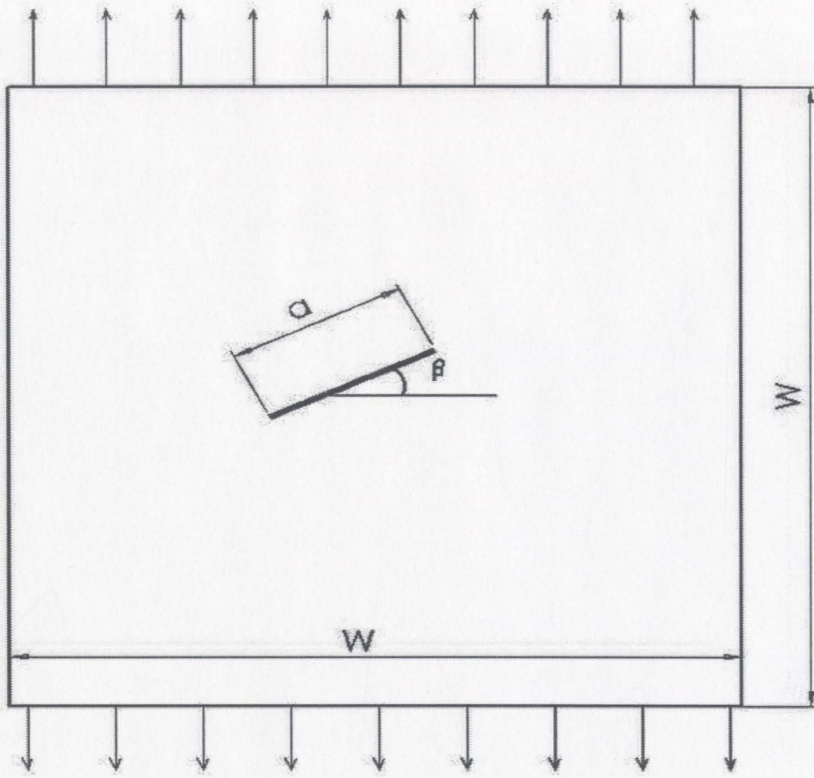


Fig 5.4.1 Plate with center crack at an angle β

Since the crack length 'a' of the plate is very small compared to the dimensions of the plate. The geometry can be considered to be a crack in an infinite plate. The stress intensity factors can be calculated analytically by the using the formulas given below

$$K_I = \sigma \sqrt{\pi a} \cos^2 \beta$$

$$K_{II} = \sigma \sqrt{\pi a} \cos \beta \sin \beta$$

(5.4.1)

where σ =stress/ load applied,
 a = half crack length ,
 β = crack angle with horizontal

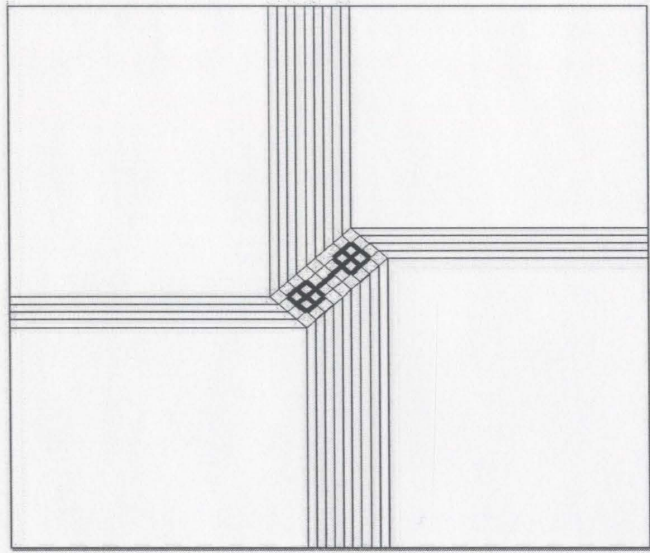


Figure 5.4.2 Discretization mesh used in the analysis

Beta	Analytical value		Obtained Value		Percentage Change	
	K_I ($psi\sqrt{in}$)	K_{II} ($psi\sqrt{in}$)	K_I ($psi\sqrt{in}$)	K_{II} ($psi\sqrt{in}$)	K_I ($psi\sqrt{in}$)	K_{II} ($psi\sqrt{in}$)
10	1.2155	0.2143	1.268	0.191	4.31	-10.8
20	1.1067	0.4028	1.146	0.389	3.55	-3.47
30	0.9399	0.5427	0.963	0.553	2.44	1.89
40	0.7355	0.6171	0.741	0.651	0.77	5.55
45	0.6266	0.6266	0.626	0.667	0.09	5.87
50	0.5178	0.6171	0.512	0.660	-1.12	6.45
60	0.3133	0.5427	0.303	0.575	-3.28	6.0
70	0.1466	0.4028	0.138	0.413	-5.47	2.55
80	0.0378	0.2143	0.031	0.208	17	-2.93

Table:5.4.1 Stress Intensity factors at various angles of the crack.

The analytical values for different values of beta obtained from the above equation 5.4.1 are compared with the numerical results obtained in the present work in table 5.4.1.

The stress intensity factors for various angles to the horizontal, β are calculated. The numerical results obtained from the present analysis are compared with the interpolated results (table 5.4.2) from the graph of Moes et al. [23] and are presented in Figure 5.4.3.

β (degrees)	K_I ($psi\sqrt{in}$)	K_{II} ($psi\sqrt{in}$)
10	1.23	0.22
20	1.12	0.40
30	0.95	0.54
40	0.74	0.62
45	0.63	0.63
50	0.62	0.61
60	0.32	0.55
70	0.15	0.41
80	0.04	0.21

Table:5.4.2 Interpolated values of SIF's at various angles of the crack.

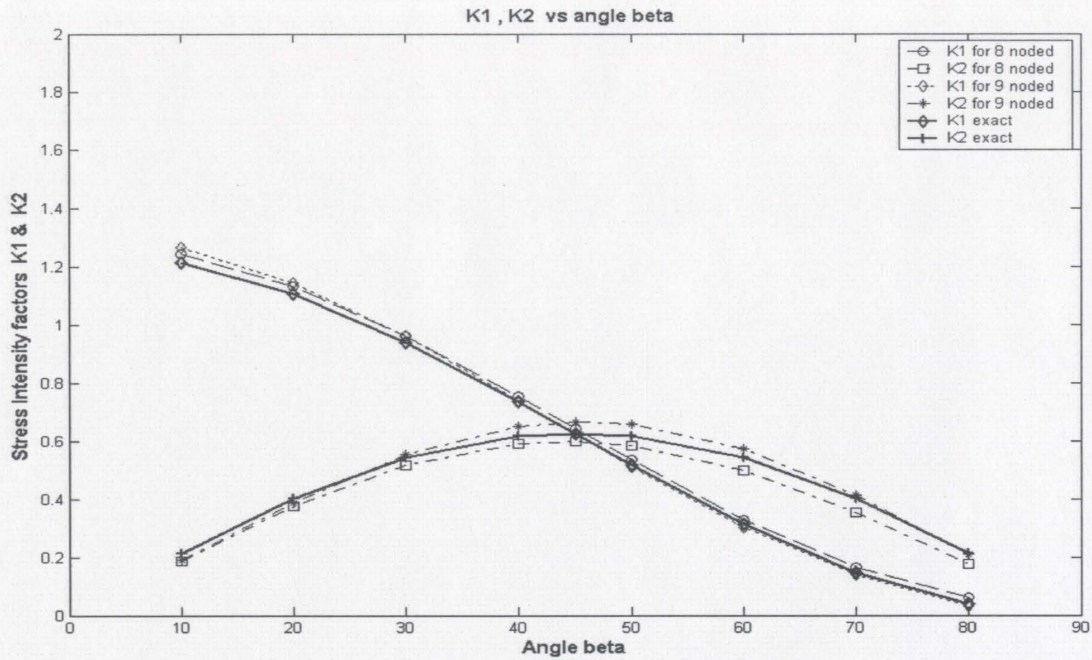


Figure 5.4.3 Stress Intensity factors vs. angle β

Discussion:

A uniform mesh consisting of $11 \times 6 = 66$ elements is taken as shown in the figure 5.4.2 and the mesh near the crack tip is denser than the mesh away from the crack tip. The results are in excellent agreement with the published results of Huang et al. [26] with a mesh density of $100 \times 100 = 10000$ elements which is considerably large number as far as the computational resources are concerned.

The values obtained for 8 noded elements and the 9 noded elements are also shown in the graphs, which indicate that the 9 noded element gives better results than the 8 noded element. The graph also shows the exact values of stress intensity factors obtained for various angles of β calculated using the equation 5.4.1. and the error percentage is less than 5 for most values.

Example 5 : Circular Arc Crack subjected to biaxial stresses:

Consider a circular arc crack in a plate with dimensions of length ' $20r$ ' and width of ' $20r$ ' with an arc crack of radius ' r '. The angle subtended by the circular arc is ' 2β '. The plate and arc are symmetrical about y axis, so only half length of the plate is considered for the analysis.

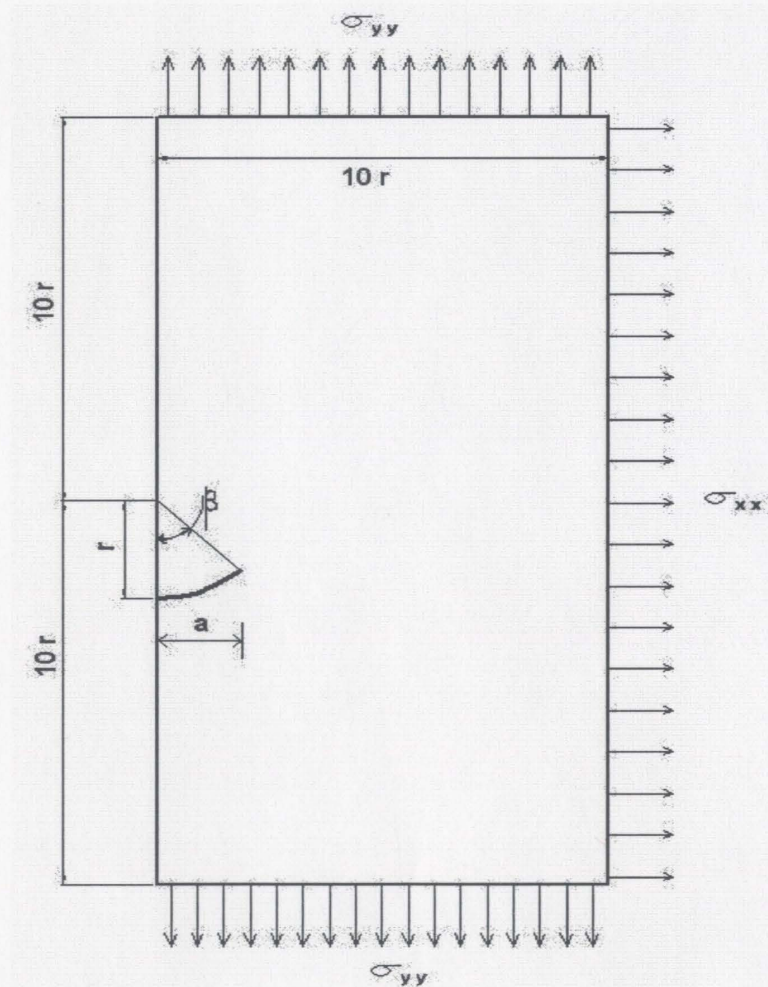


Figure 5.5.1 : Circular arc crack subjected to biaxial stresses.

The length of the crack is very small compared to the dimensions of the plate so, the plate is considered to be an infinite plate which is subjected to bi-axial stresses of σ_{xx} and σ_{yy} with respect to x and y axis respectively and is shown in the figure 5.5.1.

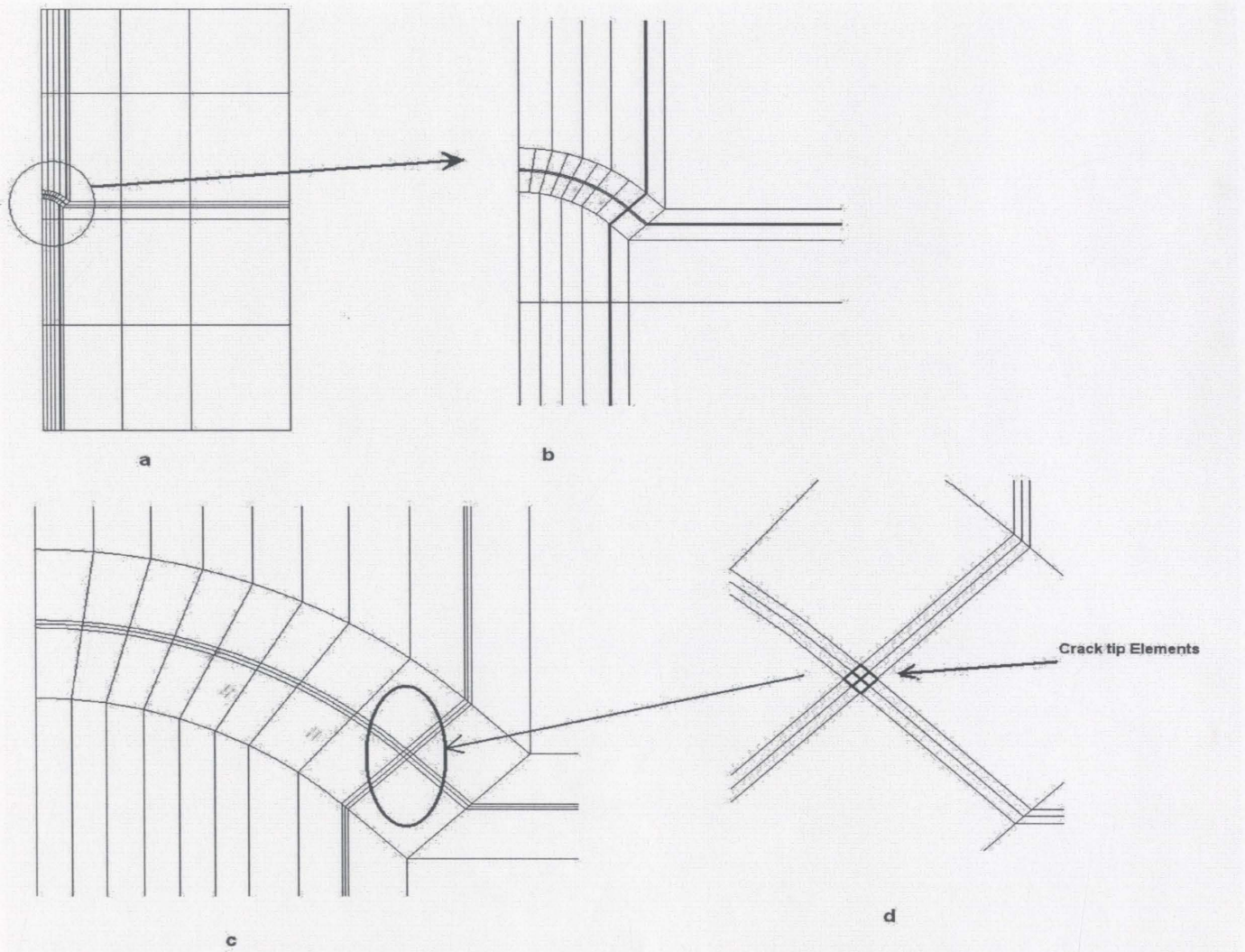


Figure 5.5.2: Curved crack plate discretizations. a) Full view of the meshed curved crack plate b) crack zone c) Closer view of crack zone d) Crack tip elements

The crack is analysed for an element length of 0.01 and in the figure 5.5.2 the crack mesh discretization is shown with a detailed view of the crack zone and closer views of crack tip elements.

The finite element mesh used by Huang et al. [26] is also shown in the figure 5.5.3 and it is obvious from the figures that the number of elements taken in the present discretization when compared with [26] was very less.

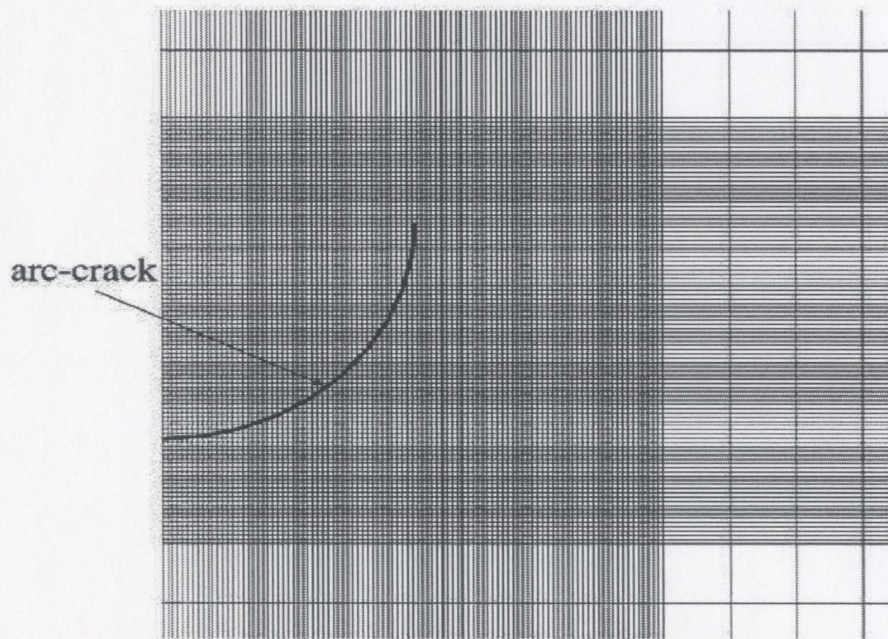


Figure : 5.5.3 Crack mesh used by Huang et al. [26]

The curved crack meshing is different from the center crack, inclined crack etc as finer mesh is required due to the crack curvature. The exact analytical solution for the stress intensity factors are obtained from the solution of Cotterell and Rice [31].

The stress intensity factors K_I and K_{II} for the circular arc crack under uniform biaxial stress field are given by the equation:

$$K_I = \sqrt{\pi a} \left[\left(\frac{\sigma_{yy} + \sigma_{xx}}{2} \right) - \left(\frac{\sigma_{yy} - \sigma_{xx}}{2} \right) \sin^2 \left(\frac{\beta}{2} \right) \cos^2 \left(\frac{\beta}{2} \right) \right] \frac{\cos \left(\frac{\beta}{2} \right)}{1 + \sin^2 \left(\frac{\beta}{2} \right)} + \left[\left(\frac{\sigma_{yy} - \sigma_{xx}}{2} \right) \cos \left(\frac{3\beta}{2} \right) \right] - \sigma_{xy} \left[\sin \left(\frac{3\beta}{2} \right) + \sin^3 \left(\frac{\beta}{2} \right) \right]$$

and

$$K_{II} = \sqrt{\pi a} \left[\left(\frac{\sigma_{yy} + \sigma_{xx}}{2} \right) - \left(\frac{\sigma_{yy} - \sigma_{xx}}{2} \right) \sin^2 \left(\frac{\beta}{2} \right) \cos^2 \left(\frac{\beta}{2} \right) \right] \frac{\sin \left(\frac{\beta}{2} \right)}{1 + \sin^2 \left(\frac{\beta}{2} \right)} + \left[\left(\frac{\sigma_{yy} - \sigma_{xx}}{2} \right) \sin \left(\frac{3\beta}{2} \right) \right] + \sigma_{xy} \left[\cos \left(\frac{3\beta}{2} \right) + \cos \left(\frac{\beta}{2} \right) \sin^2 \left(\frac{\beta}{2} \right) \right]$$

where $a = \text{crack length} = r \cos(\beta)$,
 $\beta = \text{angle subtended by the arc}$
 $\sigma_{xx} = \text{Stress in } x \text{ direction}$
 $\sigma_{yy} = \text{Stress in } y \text{ direction}$

If a uniform stress field of σ is applied then exact stress intensity factors as referred by Huang et al. [23] are given by

$$K_I = \frac{\sigma}{1 + \sin^2 \left(\frac{\beta}{2} \right)} \sqrt{\left[\frac{\pi r \sin \beta (1 + \cos \beta)}{2} \right]}$$

and

$$K_{II} = \frac{\sigma}{1 + \sin^2 \left(\frac{\beta}{2} \right)} \sqrt{\left[\frac{\pi r \sin \beta (1 - \cos \beta)}{2} \right]}$$

where

$r = \text{radius of the arc}$
 $\beta = \text{angle subtended by the arc}$

The element size considered in this analysis is 0.01 at the crack tip and larger sizes away from the crack. The results obtained from analyses are presented below.

p-order	Analytical Solution		Present solution for 8 noded element	
	K_I ($psi\sqrt{in}$)	K_{II} ($psi\sqrt{in}$)	K_I ($psi\sqrt{in}$)	K_{II} ($psi\sqrt{in}$)
2	1.31573	0.54449	1.340	0.3666
3	1.31573	0.54449	1.4099	0.4392
4	1.31573	0.54449	1.444	0.4973
5	1.31573	0.54449	1.443	0.5126
6	1.31573	0.54449	1.449	0.5119
7	1.31573	0.54449	1.4479	0.5124

Table: 5.5.1 Stress intensity factors for curved crack with 8 noded element.

P-order	Analytical Solution		Present solution for 9 noded element	
	K_I ($psi\sqrt{in}$)	K_{II} ($psi\sqrt{in}$)	K_I ($psi\sqrt{in}$)	K_{II} ($psi\sqrt{in}$)
2	1.31573	0.54449	1.259	0.3631
3	1.31573	0.54449	1.326	0.4182
4	1.31573	0.54449	1.366	0.4876
5	1.31573	0.54449	1.366	0.5045
6	1.31573	0.54449	1.594	0.5344
7	1.31573	0.54449	1.629	0.5287

Table: 5.5.2 Stress intensity factors for curved crack with 9 noded element.

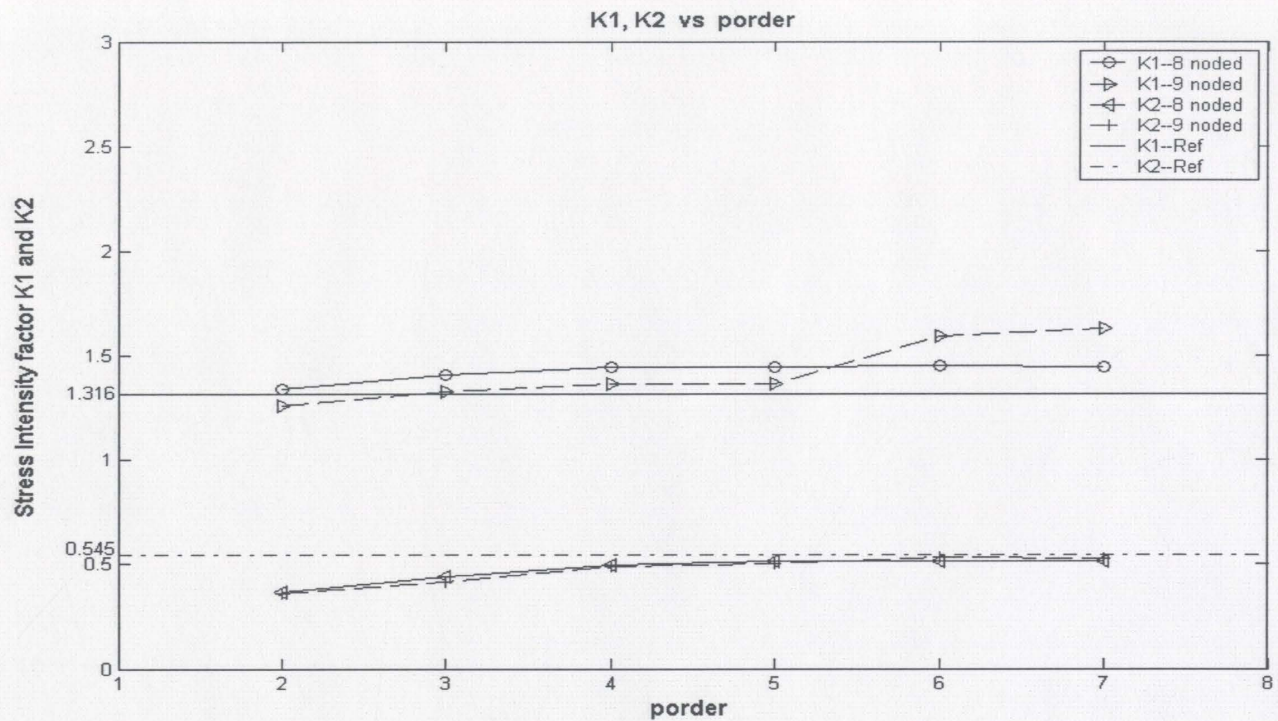


Figure: 5.5.4 Stress Intensity factors vs. p-order for 8 and 9 noded elements

Discussion:

It is known that arc shaped cracked need a very dense mesh since it is a curvature, as shown in the figures 5.5.3, many people considered very dense meshes for getting the accurate results but in this analyses the mesh as shown in the figure 5.5.2 was considered whose density was much less than the others. In the vicinity of the crack tip [23] the element length was considered to be 0.02 and a total of 21390 elements are taken where in the present analysis only 90 elements are considered. The Analytical result is obtained from the equation 5.5.1 and the numerical results obtained from the present analysis are compared in figure 5.5.4. From the tables 5.5.1 and 5.5.2 and from the figure 5.5.4, it can be shown that with a very small number of elements, accurate results are obtained in the present analysis.

Chapter 6

CONCLUSIONS AND RECOMMENDATIONS

6.1 Conclusions

In the crack growth analyses constant re-meshing of the component is required to obtain accurate results with changing geometries. In order to overcome this re-meshing there has to be a way to remove the re-meshing or mesh with very less elements which helps in re-meshing easily. The present formulation helps in obtaining accurate results with fewer elements as presented in the numerical results section. It is observed that if the elements surrounding the crack tip are all of equal size then accurate results can be obtained. This characteristic of finding the stress intensity factors with fewer elements makes this method promising for the fatigue crack growth analyses.

Accurate stress intensity factor computations (mode I and mode II) are obtained for bench mark problems such as symmetrically loaded edge crack in tension, symmetrically loaded edge crack in shear, 45 degrees inclined crack in tension, Center angle crack plate in tension which are subjected to uniaxial stress and in addition to that curved crack plate in tension which is subjected to bi axial stresses is also studied.

The following conclusions are drawn through the study of various numerical examples

1. It is very common problem for any finite element analysis to mesh the component with least aspect ratio. In order to generate a mesh with least aspect ratio large effort is required and one big advantage in this formulation is aspect ratio has very little effect. It is observed that vary large aspect ratio in order of 75:1 also has less significance on the final results. This makes the meshing very easy and by which the number of elements can also be reduced.
2. If p-version singular elements are used for the analysis near the crack tip, higher orders of polynomial gives the better control on the analyses in order to model various stress zones at the crack tip. It is also observed that analysis should be limited to fifth order in most cases beyond which local oscillations takes place [10] and values deviate from the analytical solution.
3. The method can be used for any number of crack tips in a component and this is observed from the numerical solution of angled center crack problem.
4. This method allows the use of larger crack tip elements in normal analysis to get accurate results and in some of the problems like crack in the form of a curvature smaller elements are needed.

5. The advantage with the method is it eliminates the need to mesh the components on regular basis which is a prime requirement for the analysis of crack growth problems. The polynomial orders are changed with out the need to remesh the geometry and computations are performed to obtain accurate results.

6. It is observed from the numerical implementation that the accuracy of the solution grows significantly if an additional row of elements are taken around the crack tip in addition to the 4 crack tip elements.

7. From the analysis of various crack problems it is observed that the 9 noded element gives good results compared to 8 noded element when complex crack geometry is involved.

6.2 Recommendations:

The crack tip elements modeled should be square elements and for curvature problems they need to be very small. Enriched elements at the crack tip require transition elements and due to this the values deteriorate if the element size is reduced after certain length. There should be four crack tip elements around the crack tip. In order to obtain an accurate result one more row of elements , usually 12 elements surrounded by 4 crack tip elements are required.

REFERENCES

- [1] Daryl. L. Logan, "A first course in the Finite Element method", Brooks/Cole Thomson learning (2000).
- [2] S. Ranganath, R. Narasimham and K. R. Y. Simha, "Fracture Mechanics for Engineering Design", *Golden Jubilee Commemoration Workshop*, Indian Institute of Science, (1995).
- [3] O. C. Zienkiewicz and R. L. Taylor, "The finite element method", *Vol I*, McGraw-Hill, UK (1989).
- [4] Larry J. Segerlind, "Applied Finite element Analysis ", John Wiley & Sons, Inc,(1976).
- [5] Alberto Peano, "Hierarchies of conforming finite elements for plane elasticity and plate bending", *Comp. & Maths. With Appls. , 2*, 211-224(1976).
- [6] G. R. Cowper, "Gaussian quadrature formulas for triangles", *Int. J. Num. Methods Eng., 7*, 405-408(1973).
- [7] B. A. Szabo, "Mesh design for the p-version of the finite element method", *Comp. Methods Appl. Mech. Eng., 55*, 181-197(1986).
- [8] I. Babuska, B. A. Szabo and I. N. Katz, "The p-version of finite element method", *SIAM J. Num. Analysis , 18*, 515-543(1981).
- [9] R. B. Morris, Y. Tsuzi and P. Carnevali, "Adaptive Solution strategy for solving large systems of p-type finite element equations", *Int. J. Num. Methods Eng., 33*, 2059-2071(1992).

- [10] O. C. Zienkiewicz, J. P. des R Gagio and D. W. Kelly, "The hierarchical concept in finite element analysis", *Comp. & Struc.*, 16, 53-65(1983).
- [11] N. Wiberg and P. Moller, "Formulation and solution of hierarchical finite element equations", *Int. J. Num. Methods Eng.*, 26, 1213-1233(1988).
- [12] A. Duster and E. Rank, "The p-version of the finite element method compared to an adaptive h-version for the deformation theory of plasticity", *Comp. Methods Appl. Mech. Eng.*, 190, 1925-1935(2001).
- [13] Y. Liu and H. R. Busby, "p-version hybrid/mixed finite element method", *Finite elements in Analysis and Design*, 30, 325-333 (1998).
- [14] I. Babuska, M. Griebel and J. Pitkaranta, "The problem of selecting the shape functions for a p-type finite element", *Int. J. Num. Methods Eng.*, 28, 1891-1908(1989).
- [15] S. E. Benzley, "Representation of singularities with isoparametric finite elements", *Int. J. Num. Methods Eng.*, 8, 537-545(1974).
- [16] D. M. Tracey, "Finite elements for determination of crack tip elastic stress intensity factors", *Engg. Frac. Mech.*, 3, 255-265(1971).
- [17] S. K. Chan, I. S. Tuba and W. K. Wilson, "On the finite element in linear fracture mechanics", *Engg. Frac. Mech.*, 2, 1-17(1970).
- [18] L. N. Gifford Jr. and P. D. Hilton, "Stress Intensity Factors by enriched finite elements", *Engg. Frac. Mech.*, 10, 485-496(1978).
- [19] J. E. Akin, "The generation of elements with singularities", *Int. J. Num. Methods Eng.*, 10, 1249-1259(1976).

- [20] I. S. Raju and J. C. Newman Jr. , “Stress intensity factors for a wide range of semi-elliptical surface cracks in finite thickness plates”, *Engg. Frac. Mech.*,11, 817-829(1979).
- [21] W. S. Blackburn and T. K. Hellen , “Calculation of Stress Intensity factors in 3 dimensions by finite element methods”, *Int. J. Num. Methods Eng.*,11, 211-229(1977).
- [22] L. Nobile and M. Nobile, “An approximate evaluation of the stress intensity factors for cracked plates”, *Key Engineering Materials*, 251-252, 291-296 (2003).
- [23] Nicholas Moes, John Dolbow and Ted Belytschko, “A Finite element method for crack growth without remeshing”, *Int. J. Num. Methods Eng.*, 46, 131-150(1999).
- [24] R. S. Barsoum, “On the use of isoparametric finite elements in linear fracture mechanics”, *Int. J. Num. Methods Eng.*, 10, 25-37(1976).
- [25] R. D. Henshell and K. G. Shaw, “Crack tip finite elements are unnecessary”, *Int. J. Num. Methods Eng.*,9, 495-507(1975).
- [26] R. Huang, N. Sukumar and J. H. Prevost, “Modeling quasi-static crack growth with the extended finite element method Part II : Numerical applications”, *Int. J.of Solids and Structures*, 40, 7539-7552 (2003).
- [27] S. C. Fan, X. Liu and C. K. Lee, “Enriched partition of unity finite element method for stress intensity factors at crack tips”, *Comp & Structures*, 82, 445-461(2004).

- [28] John Lewis and William Loftus, “Java software solutions, Foundations of program Design”, Addison-Wesley (2001).
- [29] James M. Slack, “Programming and problem solving with Java”, Brooks/Cole Thomson learning (2000).
- [30] Ewalds H, Wanhill R., “Fracture Mechanics ”, Edward Arnold:Newyork,(1989).
- [31] Cotterell B and Rice J. R, “ Slightly curved or Kinked cracks”, *International Journal of fracture*, 16, 155-169 (1980).

APPENDIX

SHAPE FUNCTIONS FOR DIFFERENT ELEMENTS

Plane Element – 4 Noded.

$$N_1 = \frac{(1-r)(1-s)}{4}$$

$$N_2 = \frac{(1+r)(1-s)}{4}$$

$$N_3 = \frac{(1+r)(1+s)}{4}$$

$$N_4 = \frac{(1-r)(1+s)}{4}$$

Plane Element—8 Noded

$$N_1 = \frac{(1-r)(1-s)(-r-s-1)}{4}$$

$$N_2 = \frac{(1+r)(1-s)(r-s-1)}{4}$$

$$N_3 = \frac{(1+r)(1+s)(r+s-1)}{4}$$

$$N_4 = \frac{(1-r)(1+s)(-r+s-1)}{4}$$

$$N_5 = \frac{(1+r)(1-s)(1+r)}{2}$$

$$N_6 = \frac{(1+r)(1+s)(1-s)}{2}$$

$$N_7 = \frac{(1+r)(1+s)(1-r)}{2}$$

$$N_8 = \frac{(1-r)(1+s)(1-s)}{2}$$

Plane Element—9 Noded

$$N_1 = \frac{(rs)(1-r)(1-s)}{4}$$

$$N_2 = \frac{(-rs)(1+r)(1-s)}{4}$$

$$N_3 = \frac{(rs)(1+r)(1+s)}{4}$$

$$N_4 = \frac{(-rs)(1-r)(1+s)}{4}$$

$$N_5 = \frac{(-s)(1-r^2)(1-s)}{2}$$

$$N_6 = \frac{(r)(1+r)(1-s^2)}{2}$$

$$N_7 = \frac{(1-r^2)(s)(1+s)}{2}$$

$$N_8 = \frac{(-r)(1-r)(1-s^2)}{2}$$

$$N_9 = (1-r^2)(1-s^2)$$

1870-1871

1872-1873

1874-1875

1876-1877

1878-1879

1880-1881

1882-1883

1884-1885

1886-1887

